MUTAGENIC EFFECTS OF CHROMIUM (IV) ON HUMAN ENDOTHELIAL AND LUNG EPITHELIAL CELLS

A Thesis Presented to

the Faculty of the Department of Chemistry

University of Houston

In Partial Fulfillment

of the Requirement for the Degree

Master of Science

By

Mu Wang

May 2014

MUTAGENIC EFFECTS OF CHROMIUM (IV) ON HUMAN ENDOTHELIAL AND LUNG EPITHELIAL CELLS

Mu Wang

APPROVED:

Dr. Rathindra N. Bose, Chairman

Dr. Scott Gilbertson

Dr. Randolph Thummel

Dr. Yuhong Wang

Dean, College of Natural Sciences and Mathematics

MUTAGENIC EFFECTS OF CHROMIUM (IV) ON HUMAN ENDOTHELIAL AND LUNG EPITHELIAL CELLS

An Abstract of a Thesis

Presented to

the Faculty of the Department of Chemistry

University of Houston

In Partial Fulfillment

of the Requirement for the Degree

Master of Science

By

Mu Wang

May 2014

ABSTRACT

Effects of a chromium (IV) compound, diperoxoaquoethylenediaminechromium (IV) monohydrate (Cr(IV)-DPO), on human umbilical vein endothelial cells (HUVEC) and human bronchial epithelial cells (BEAS-2B) were investigated through morphological, cell viability, gene expression, and cDNA sequencing assays. The cell morphology showed both HUVEC and BEAS-2B cells suffered significant but different degrees of damage and demonstrated features indicating carcinogenesis when these cell lines were exposed to Cr(IV)-DPO for different time durations. Results from viability and morphological assays indicated that genotoxic damages of Cr(IV)-DPO to HUVEC and BEAS-2B cells were both concentration and time dependent. With longer time exposure up to 72 hr or higher concentration up to 100 μM, these damages were more pronounced. To understand the specific nature of these damages, expressions of apoptotic and DNA repair genes by RT^2-PCR arrays, and cDNA sequencing studies were carried out. Expressions of most apoptotic genes of HUVEC were altered; in particular, they were over-expressed due to the chronic Cr(IV)-DPO exposure (5 μM, 48 hr), indicating that Cr(IV) inhibited cellular proliferation in response to the oxidative damage. When BEAS-2B cells were treated with the same concentration of Cr(IV)-DPO, DNA repair genes displayed responses less actively as the exposure time increased. Gene sequencing experiments on Cr(IV)-treated BEAS-2B cells exhibited remarkable mutations with transverse mutations dominated the variants. These gene mutations were random and not confined to guanine bases as reported in the literature.

ACKNOWLEDGMENTS

First, I would like to give my deepest gratitude to my advisor, Dr. Rathindra Bose, without whose encouragement and support, it would have been impossible to conduct this highly complex research project. I have gathered a great deal of experience in the isolation, separation, and quantification of proteins, and as well as the expression and sequencing of genes. Many times, he used his rich knowledge both in the platinum and chromium research areas in guiding me to find the correct research directions, to understand the key points, and to work for the goal efficiently in my research project.

I should also thank all the members of Dr. Bose's group, Dr. Shadi Moghaddas, Homa Dezvareh, and Lu Yang. They gave me generous help in my research. The discussions with them on any problems I came across in my project were so insightful and informative.

I also would like to give my deepest thanks to all the faculty members in the Chemistry Department, especially, Dr. Lee, Dr. Moeller, Dr. Guloy, Dr. Gilbertson, Dr. Thummel, and Dr. Zaitsev, who helped me many times with all kinds of situations related or unrelated to research. I also thank Dr. Yuhong Wang from Biochemistry for being a committee member and Dr. Robert Schwartz from Biochemistry for letting me use their equipment. They are so kind-hearted people who do their best for the all graduate students.

Finally, words seem pale to express my gratitude and love for my friends, my roommate, my parents, and my boyfriend who gave me the warmest comforts when I was upset and never stopped me from trying whenever I had problems in research or in my life. Thanks!

TABLE OF CONTENTS

LIST OF TABLES

LIST OF FIGURES

CHAPTER I: INTRODUCTION AND BACKGROUND

Chromium is a naturally occurring element which is found in rocks, soil, water, and living organisms. In nature, there exist three stable oxidation states of chromium: chromium(0), chromium(III), and chromium(VI). Chromium compounds usually exhibit various bright colors depending on their oxidation states and ligand environment. Due to their versatile chemical properties, chromium compounds are widely used in manufacturing processes such as welding, chrome plating and chrome pigmenting, leather tanning, and textile production.[1] Burning of natural gas, oil, or coal[2] also contributes to chromium accumulation in the environment. In the human body, a small amount of chromium(III) is required to function as a binding receptor of insulin.[3] But an excessive uptake of chromium is regarded as one of the important factors for inducing cancer, especially lung cancer, because it cause DNA damage.[2] It is well documented that many industrial workers are frequently exposed to a high dose of chromium in their working conditions. Therefore, chromium pollution leading to health problems is exacerbated by the fast industrialization in modern society. Cigarette-smoke-extract containing chromium[2] was also proven to be one factor inducing DNA damage and causing lung cancer.[4] Therefore, an unhealthy living style also increases the chances of getting cancer. Usually, excessive chromium is not taken in by our body, since most of the chromium entering in our body can be detoxified by various enzymes and proteins and excreted through urine. However, some forms of chromium compounds can remain in the lungs for several years or longer,[2] resulting in chromium accumulation to a hazardous level and consequently severe DNA damage. Furthermore, high levels of chromium have been reported in tap water that are suspected

to cause cancer in some areas.[5] Based on the plethora of evidence, the International Agency for Research on Cancer (IARC) has determined that chromium(VI) compounds are highly carcinogenic.[2]

Thus, there is a need to investigate the genotoxic mechanisms of chromium(VI). However, chromium(VI) has been found to have low bioactivity, therefore it may not be the ultimate cause of DNA damage. In contrast, chromium(V), chromium(III), and chromium(IV) show good bioactivities by binding to DNAs and proteins, thus these chromium species are thought to be putative agents that causes DNA damage.[6] However, the exact nature of the chromium species that causes cancer and the mechanisms of carcinogenesis are yet to be determined. The chromium(IV) and chromium(V) oxidation states are the two intermediates observed in the reduction reactions of chromium(VI) to chromium(III). In cellular milieu, the reduction reactions proceed efficiently in the presence of small thiol-containing molecules including glutathione and cysteine, or enzymes including cytochrome P450 reductase, mitochondrial electron transport complexes and glutathione reductase, and aldehyde oxidase.[7, 8]

Chromium(III), once reduced from chromium(VI), can first bind to GSH or amino acid and subsequently bind to DNA to form the Cr-DNA ternary adducts.[9] These adducts, however, do not lead to DNA replication arrests and may not cause severe damages to DNA. Chromium(III) could also incorporate with the DNA bases or phosphodiester backbones directly through the covalent linkage or electrostatic/ionic interactions to form the Cr-DNA mono-adducts,[10] leading to DNA structures distortions. It is also possible that the chromium(III) ions insert into the grooves of dsDNAs, leading to the formation of Cr-DNA

inter/intrastrand crosslinks. These structural damages resulting from chromium/DNA adducts in cellular milieu break the high integrity of DNA structure required for DNA's full functions regarding the regulations of gene expressions.[11] Consequently, the DNA replications and transcriptions are severely affected leading to a variety of cellular responses including initiation of cancer or apoptosis.

One of the intermediates, chromium(V), is long-lived in cellular milieu and could interact with DNAs directly or indirectly through various mechanisms, as reported in literature. With similar bioactivity as chromium(III), chromium(V) also binds with DNAs to form mono/ternary Cr-DNA adducts or Cr-DNA intra- and inter-strand crosslinks.[12] However, the genotoxicity of chromium(V) does not solely result from its association with DNAs that DNA structure due to many other interactions with molecules in the cellular milieu.

In particular, the oxidization of DNAs by chromium(V) is an important reason for the DNA damage. Usually, it plays a more important role in causing DNA damage and leading to DNA mutations. The DNA structural damages: Cr(III)-DNA or Cr(V)-DNA adducts and crosslinks, might be repaired by a multitude of DNA repair pathways including base excision repair (BER), nucleotide excision repair (NER), mismatch repair (MMR), and double-strand break repair (DSB) genes. In contrast, the DNA oxidization damages result in base oxidation, base release, and DNA strand scission, and therefore produce modified bases and "gaps" in the DNA strands. These gaps, once not filled correctly, lead to DNA infidelity and eventually lead to various gene mutations.[13, 14] Furthermore, the occurrence of DNA mutations increases when the DNA repair system tries to correct the damages by eliminating the oxidized bases or nucleotide breakages, because the elimination processes

produce repair intermediates and introduce more gaps. In addition, it has been observed that the genes activated in the cells by oxidations are different from those activated by the exposure to hydrogen peroxide, oxygen, or X-rays.[6]

The mechanisms of DNA oxidization by chromium(V) have been reported from our laboratory, and are shown in Scheme 1[14] and Scheme 2.[15] By conducting the experiments with reactions between the oligonucleotides with length of up to 35mers, the single-strand, or the double-strand DNA molecules[13-16] and the chromium(V)-oxo-compounds, the cleaved base, sugar, and phosphodiester were detected with LC-MS after the reactions. Specially, base cleavage was mostly observed at the guanine (G) position with a significantly lesser extent observed at cytosine (C), adenine (A), and thymine (T) positions.[13] Further, three primary oxidation products, 5-methylene-2-furanone (5-MF), furfural and 8-oxo-deoxyguanosine and one minor product base-propenal were detected. 8-oxo-deoxyguanosine, usually repaired by the base excision repair (BER) pathway in the cellular milieu, was generated from deoxyguanosine due to oxygen atom transfer from the oxo-metallates to the double bond between C8 and N7 or cycloaddition reaction of the purine ring. The two oxidized cleaved sugar derivatives, furfural and 5-MF, resulted from hydrogen abstraction or hydride transfer from C1' and C5' positions of the ribose respectively to the oxo-chromium(V) center. The discovery that more furfural was produced compared to 5-MF in dsDNA reactions was postulated due to the hydrogen abstraction (or hydride transfer) from the C5' position within a Cr(V)–dsDNA intermediate was easier to proceed.[13]

Scheme 1. Proposed mechanism of DNA cleavage by Cr(V) complexes

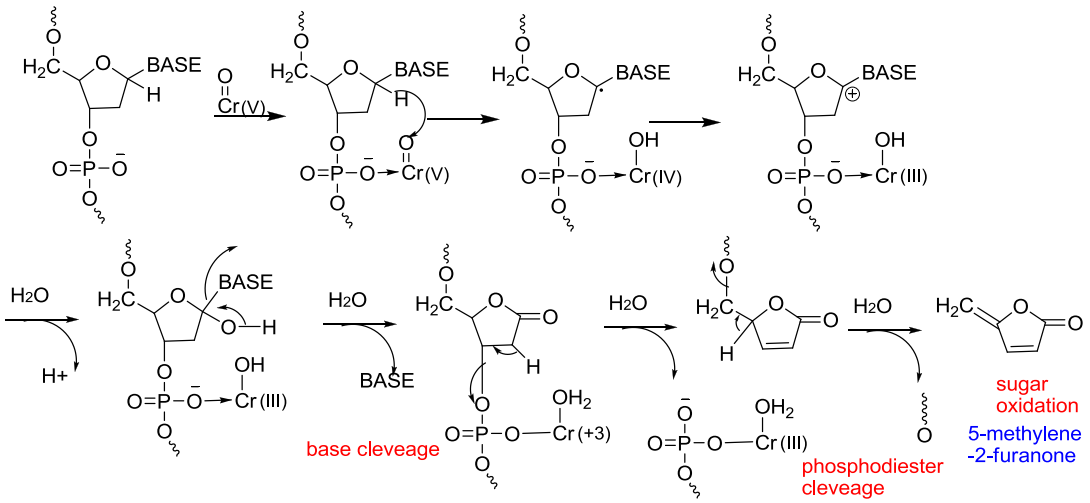

Scheme 2. Sugar and base oxidation products formed by chromium(V) oxidation of DNA

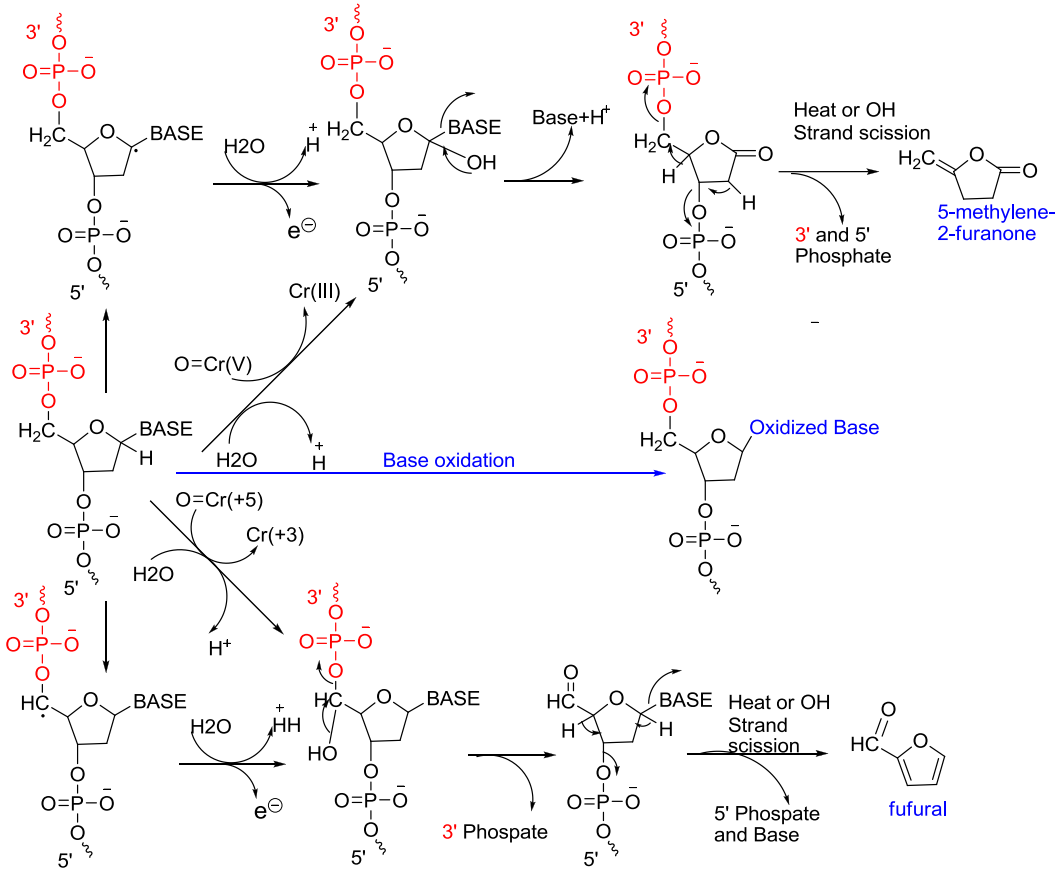

The cleavage of base, phosphate and sugar caused by the chromium oxidation leads to DNA double-strand breakage and DNA synthesis arrest, resulting in cell death. Specially, when the apurinic/ apyrimidinic sugars (where base is missing, AP sites) are involved in the DNA synthesis, adenine is usually preferred to be inserted to the opposite strand, namely X-A where X is the missing base in the parent strand and A belongs to the synthesized new strand. Under this condition, mutations will occur if the missing base is not a thymine, causing A to T, G to T, or C to T transitions (**A**-T→X-A→A-**T**, **G**-C→X-A→A-**T**, **C**-G→X-A→A-**T**).

Free radicals, such as the reactive oxygen species ·OH and $\cdot O_2$ that are initiated by Cr oxidation in the Fenton-like reactions (Scheme 3), were also reported to induce DNA damage.[17] The hypothesis has been validated by the observation that the reactions products of ss-DNAs, ds-DNAs or oligonucleotides with chromium(VI), including oxidized bases, DNA strand break residues and Cr-DNA or DNA-protein-Cr crosslinks, decrease in the presence of radical scavengers. The mechanisms of radical-initiated cascading nucleotides damages have been discussed in several articles,[18-20] in which the radicals are produced from the reaction of chromium or other metals with hydrogen peroxide (Schemes 4 through 6[19]). Mutations occur when the damaged DNA sequence is copied to the daughter DNAs during replications. DNA polymerase may fail to read the damaged bases and consequently the replication process is arrested, leading to cell death or apoptosis; for example, FAPyG is reported to be a strong DNA synthesis blockage.[21] But the polymerase may successfully pass through by misreading the incorrect information. Therefore, the incorrect bypass results in DNA mutations, which are regarded as the initiations of cancer. These theories

have been reported in the living organisms that, in *E.coli*, though at very low frequency, the polymerase passed the thymine glycol (T*) DNA lesion, leading to T to C transition mutations by following **T***-A→T*-G→G-**C**.[22] The 5-hydroxyl-cytosine (C*) can also be passed through in DNA synthesis, resulting to C to T mutation when the C* mismatches with A, **C***-G→C*-A→A-**T**.[23] Furthermore, in both bacteria and simian cells, the G to T transition mutations are also observed with higher frequency by following the process:**G***-C→G*-A→A-**T**, where the 8-hydroxyl-G (G*) and adenine are mis-paired. 8-hydroxyl-A (A*) is known to possess the potential to bind with G, forming the A*-G mismatch couple, but it is less mutagenic compared to G* because the mismatch is usually repaired by the DNA repair system in living organisms.[24]

Scheme 3. Hydroxyl radical produced in Cr(V) and Cr(IV) Fenton-like reactions

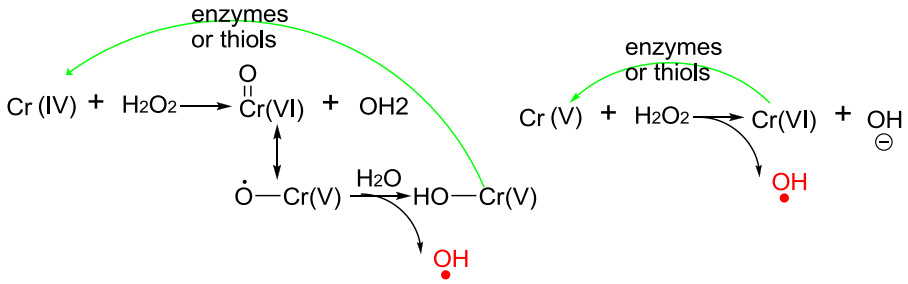

Scheme 4. Reaction of the hydroxyl radical with adenine base.

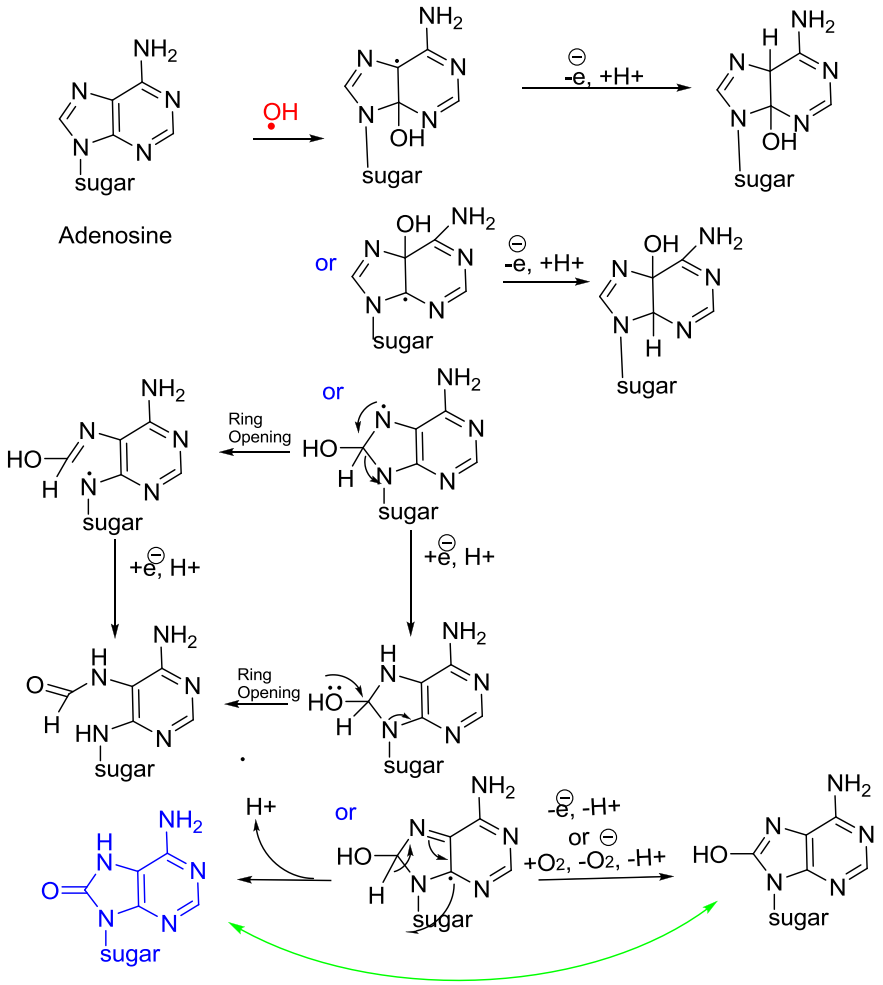

Scheme 5. Reaction of the hydroxyl radical with gaunine base.

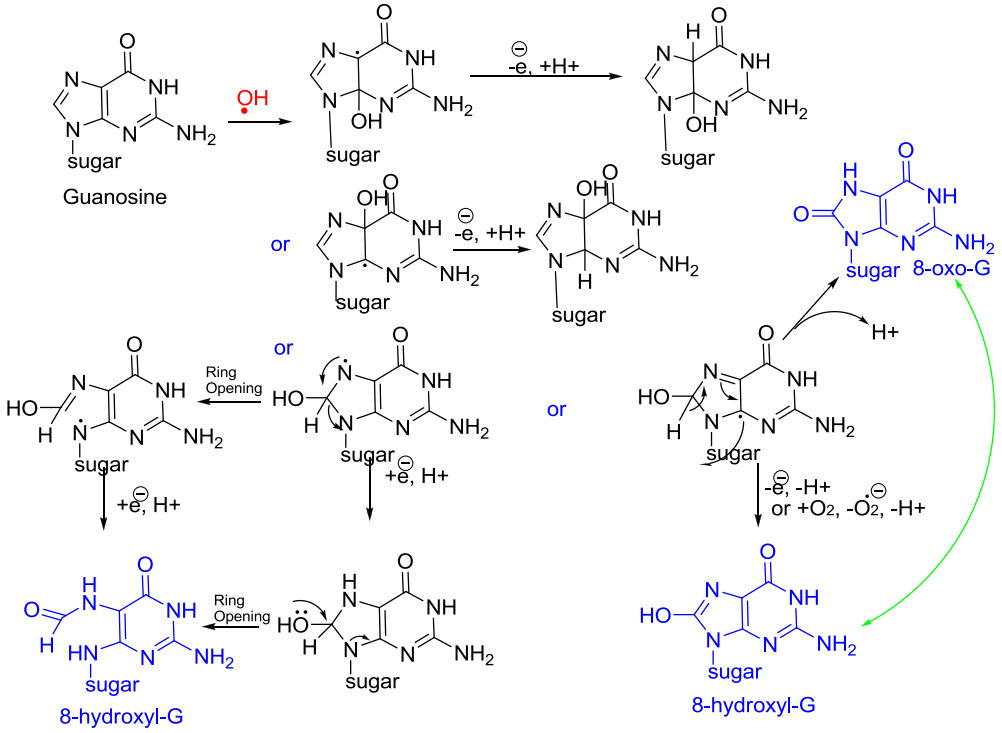

Scheme 6. Reaction of the hydroxyl radical with the thymine and cytosine bases.

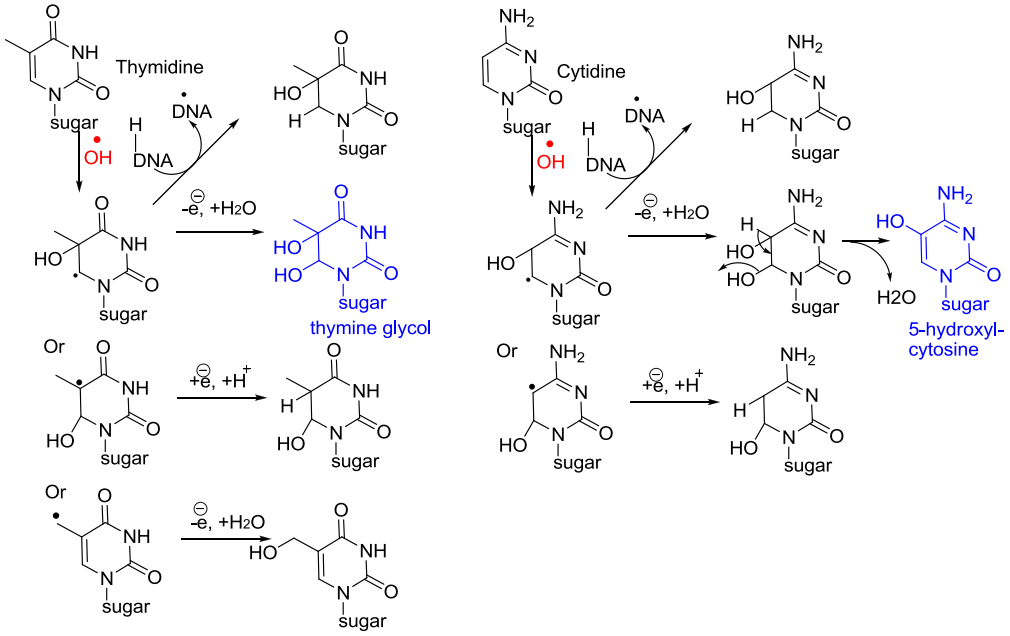

Although chromium(IV) and chromium(V) are both intermediates of the reduction from chromium(VI) to chromium(III), and that both species can damage the DNAs structure by oxidization reactions, reports regarding the genotoxicity of chromium(IV) are rare compared to the vast literature reporting chromium(V) as a potential carcinogen. In order to fully understand the fate of two intermediates in cellular milieu and the consequences of their interactions with DNAs, an assessment of the relevance of chromium (IV) in causing DNA damage leading to DNA mutations, is necessary. Previous work in our laboratory measured the formal potential of the couple Cr(IV/III) showing that chromium (IV) is a more powerful oxidizing agent compared to chromium (V).[25] These results suggested that chromium (IV) might be the real intermediate and contributes to DNA oxidative damages. Consequently, chromium (IV) compounds might be more carcinogenic than chromium (V). However, there are no reports that systematically examined the nature of cellular responses upon Cr(IV) exposure and its ability to mutate DNA. Hence, the project described in this thesis was designed to focus on the investigations of the genotoxicity of chromium (IV) compound by selecting a model compound, Cr(IV)-DPO.

It is also noted that most of the investigations on DNA damage caused by chromium compounds were performed with isolated DNA. In these experiments, chromium compounds react with isolated DNAs or oligonucleotides instead of DNAs in vitro (living cells). So, it is obvious to us that the mimic-cellular milieu in test tubes should not be regarded as the real microenvironment in cellular cytosol or nucleus. This is because, in living cells, there exist many enzymes or co-factors, such as the 3'-5' proofreading enzymes, replication co-factors (PCNA, RPA), bypass polymerases, and DNA repair

enzymes,[11] correcting the DNA damage to maintain the integrity of DNA structures. In reality, tumorigenesis caused by Cr(VI) exposure is regarded as a multistep process that includes DNA damage, mutation, chromosome instability, aneuploidy, and epigenetic modulation.[26] Therefore, the research of the chromium genotoxicity mechanism in cultured cells, in the presence of the comprehensive DNA repair system, is more realistic.. Furthermore, the gene expression profiles of living cells which have been treated with chromium compounds would also help us understand the mechanisms of chromium genotoxicity. Recently, replication-blocking lesions in Cr-treated DNA and in DNA isolated from Cr(VI)-treated yeast and Cr(VI)-treated A549 cells (lung carcinoma cells) were detected by the application of quantitative PCR (QPCR).[27] Suppressions of inducible and constitutive gene expressions in CHO cells (Chinese hamster ovary carcinoma cells) has also been proven to be associated with the treatment of chromium (VI).[28] In addition, both the gene expression profiles of A549 cells treated with acute Cr(VI) (high dosage up to 300 μM, short time down to 15 min) and BEAS-2B cells treated with chronic Cr(VI) (low dosage down to 0.25 μM, exposure up to four weeks) have been reported[29-31] and shown gene alternations induced by the chromium treatments.

Considering the relevance of adverse effects of chromium on human health, the research projects that evaluate DNA repair responses when cells are exposed to chromium compounds should be informative. Furthermore, the DNA repair intermediates themselves brought more complications because, in many cases, DNA mutations are produced when the repair system tries to fix sequence deletions or insertions by synthesizing a new sequence without the correct template.[32, 33] For example, to find out the exact DNA repair

pathways involved in repairing Cr-lesions, some works have been carried out to identify the specific mechanisms for survival after Cr(VI) exposure with repair-deficient mammalian cells.[34, 35] Though the DNA repair system plays a key role in preventing gene mutations, unfortunately until now, literature on the alternations in profiling of gene expressions of DNA repair genes is still rare.[36] Furthermore, research on the specific mutated positions in genes, which are regarded as the ultimate consequence of oxidative DNA strand scissions caused by chromium(IV), has not been discussed although the observation that single-strand DNA (oligonucleotides) was damaged by chromium(IV) was reported previously by our laboratory[37]. Therefore, my specific research project also focused on identifying the mutated genes caused by chromium (IV) compound which has been hypothesized as a more mutagenic reagent than chromium(V) and also trying to locate the positions of mutated genes. In order to achieve this goal, the DNA transcription profiling experiments (RT^2-PCR gene expression array) and cDNA sequencing have been carried out. Furthermore, how the exposure time of treatment influences the expression of DNA repair genes been investigated in the project described in this thesis.

CHAPTER II: EXPERIMENTAL METHODS

2.1. Synthesis of diperoxoaquoethylenediaminechromium (IV) monohydrate

Diperoxoaquoethylenediaminechromium (IV) monohydrate (Cr(IV)-DPO) was prepared following the method described by House[38] (see Scheme 7). In a typical synthesis, 1.25ml ethylenediamine was dissolved into 25mL ice, magnetically stirred while 1.5 grams chromium trioxide in 5mL ice water and 5mL 30% hydrogen peroxide were added drop by drop simultaneously in 20 minutes. All ice used in the reaction was prepared beforehand with distilled water. Reaction was kept in an ice bath while stirring for 2~3 hr until olive greenish precipitate was formed. The precipitate was filtered and washed with cold acetone, ethanol and water twice and kept in desiccator overnight to dry. The olive-greenish solid was diperoxoaquoethyl- enediaminechromium (IV) monohydrate and was stored at 0 ºC.

Scheme 7. Synthesis of diperoxoaquoethylenediaminechromium (IV) monohydrate

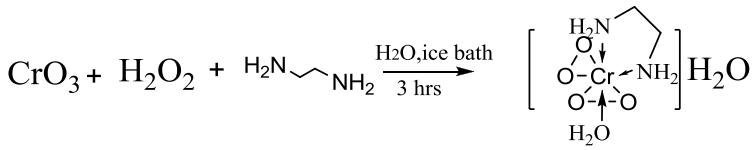

2.2. Cell culture

2.2.1 Culture method of HUVEC cell line

Human umbilical vein endothelial cell line (HUVEC, CRL-1730) was obtained from ATCC®. HUVECs were cultured in M199 medium (Lonza) supplemented with 7 units/mL Heparin (Sigma-Aldrich, Heparin sodium salt from porcine intestinal mucosa, Grade I-A), 0.04mg/mL endothelial cell mitogen (Biomedical Technologies Inc.), 20% (v/v) Fetal

Bovine Serum (ATCC® 30-2020™), 100 units/mL penicillin, and 100 µg/mL streptomycin (Sigma-Aldrich). FBS was filtered through 0.22 µm vacuum filter system (Corning®) before using. The Heparin sodium salt solid was dissolved in Hanks Balanced Salt Solution (HBSS, Lonza®). Lyophilized endothelial cell mitogen powder was dissolved in HBSS. The whole medium which had been added with all the required supplements was filtered through 0.22 µm vacuum filter system (Corning®), stored at 4 °C and warmed up in 37 °C water bath before using. A proper number of HUVECs were seeded in tissue culture petri dishes or flasks (TPP®) pre-coated with 0.1% pre-filtered gelatin solution (Sigma-Aldrich, Type B, tissue culture grade, sterile) overnight. HUVECs were cultured at 37 °C in a culture incubator with humidified atmosphere containing 5% CO_2. The culture medium was refreshed every two to three days to keep the cells growing healthily. For Cr(IV) compound exposure, once HUVECs were growing up to 75%~80% confluence in petri-dish, they were treated with various concentration of Cr(IV)-DPO complex for specific exposure time, different according to various experiment designs. When treating the cells, the complex was dissolved into the culture medium and diluted to the required concentration with fresh culture medium to make the treatment medium. Both in the treated groups and untreated control groups, the culture medium was changed every other day. All the Cr(IV)-DPO complex used in the series of experiments for various assays was from the same synthesis batch.

2.2.2. Culture method of BEAS-2B cell line

Human bronchial epithelium cell line (BEAS-2B, CRL-9609™) was obtained from ATCC®. BEAS-2B cells were cultured in BEGM™ bronchial epithelial cell growth medium with additive BEGM single quot kit suppl&Growth Factors (Lonza®, excluding gentamycin-amphotericin B mix), 100 units/mL penicillin, and 100 μg/mL streptomycin. Cells were seeded in tissue culture petri dishes or flasks which were pre-coated with BEAS-2B culture coating solution at 37 ^{o}C overnight. The coating solution was prepared following ATCC® instruction: a mixture of 0.01 mg/mL fibronectin (Sigma-Aldrich, fibronectin from bovine plasma Powder was dissolved in sterile cell culture grade water), 0.03 mg/mL bovine collagen type I (Sigma-Aldrich, collagen from bovine achilles tendon) and 0.01 mg/mL bovine serum albumin (BSA, Sigma-Aldrich) dissolved in whole culture medium. For Cr(IV) exposure, once BEAS-2B cells were growing to 75% to 80% confluence, they were treated with various concentrations of Cr(IV)-DPO complex for expected exposure time according to different experiment designs. The treatment medium was made in a similar way as above. Both the treatment medium and untreated medium was changed every other day. As in the previous experiments, the Cr(IV)-DPO complex used here for various assays was also from the same synthesis batch.

2.3. Cellular morphological assay

The same passage of HUVECs treated with various concentration of Cr(IV)-DPO complex, ranging from 0.5 μM, 1.0 μM, 2.5 μM, 5.0 μM, and 10.0 μM, and without treatment, were photographed in tissue culture petri-dish with an inverted microscope to observe the morphological changes at different time points. After removing the treatment medium,

being washed with phosphate buffered saline (PBS, Lonza®) four times and growing under fresh medium again for another 48 hr, the HUVECs were photographed again with the same method. The same passage of BEAS-2B Cells treated with various concentrations of Cr(IV)-DPO complex were also photographed similarly to observe the morphologies.

2.4. Cell viability assay

The cell viability of both HUVEC and BEAS-2B cells were tested in in an identical manner as described below. The same number of cells (15,000 to 20,000 cells each well) were seeded into pre-coated opaque-walled 96-well plate (Greiner Bio-One 96-Well CELLSTAR® black microplates for tissue culture) with multichannel pipet, up to 300 μL culture medium was added to each well, and the plate was incubated for 8 hr or overnight at 37 ^{o}C in a culture incubator with a humidified atmosphere containing 5% CO_2 to allow the cells to adhere to the well bottom. Cell number was calculate after concentration of cell solution was determined with TC20™ automated cell counter (Bio-Rad) following the manufacturer instruction. After the cells were suspended uniformly in culture medium by pipetting, 20 μL of the cell solution was mixed with 20 μL trypan blue solution, 0.4% (Gibco®, Life technologies), 15 μL of the mixture solution was loaded into the chamber of the counting slide (Bio-Rad) and then the sample was read immediately with a TC20 automated cell counter. After all the cells were adherent, freshly made different concentrations of Cr(IV)-DPO treatment medium or control untreated medium was added into the wells, 300 μL each well. The plate was incubated in a culture incubator with a humidified atmosphere containing 5% CO_2 for 24 hr, 48 hr, 72 hr or 96 hr. For the 72 hr and 96 hr treatment groups, the medium was changed every other day. After incubation for

the required time course, the medium in each well was removed very gently without touching the cell layer at the bottom. In each well, 100 μL CellTiter-Glo® reagent (prepared beforehand by thoroughly mixing the lyophilized CellTiter-Glo® substrate with the CellTiter-Glo® buffer provided in the CellTiter-Glo® Luminescent Cell Viability Assay kit, Promega) and 100 μL PBS were added with multichannel pipet. The plate was shaken gently for 15 mins at room temperature, incubated at 37ºC for 30 mins, and equilibrated to room temperature in 20 mins. The intensity of luminescence in each well was read with Synergy HT multi-mode microplate reader (BioTek). The intensity of luminescence reflects the percentage of viability. If the intensity is higher, the number of living cells is higher, and vice versa. The viability ratio of control samples was set as 1 and the viability ratio of each treated sample was calculated by comparing the luminescence intensity to the control samples.

2.5. Western blotting assay

2.5.1. Protein extraction from cells

Protein samples for Western immunoblot were prepared following the protocol: Cells after treatment were washed four times with a large volume of cold PBS (for BEAS-2B cells) or HBSS (for HUVECs). The cell culture dish was placed in ice while the washing solution was discarded, then the pre-chilled lysis buffer was added. The lysis buffer was prepared beforehand by mixing 1000 μL radio-immunoprecipitation assay buffer (RIPA buffer, Sigma-Aldrich) with 90 μL protease inhibitor cocktail (Thermo Scientific) (1 mL for 55cm^2 culture dish and 0.4 mL for 21 cm^2 culture dish). The adherent cells was scraped and crashed off the bottom of dish by using a plastic cell scraper and lifter (sterile,

Chamlab). The cell lysate was then transferred into a pre-chilled microfuge tube and centrifuged in at 4°C, 20,000g for 20 minutes. The tubes with samples were gently removed from the centrifuge and placed on ice to keep them chilled. The supernatant, namely the protein solution, was kept and gently transferred to a new microtube while the pellet was discarded. Protein concentration was determined with Copper/ BCA assay kit (Pierce™ BCA Protein Assay Kit) following the manufacturer instructions. Bovine serum albumin (BSA, 1 mg/ mL, Thermo scientific) was used as the standard sample. In each clean glass test tube, 5 µL of each sample or 2.5 µL, 5.0 µL, 7.5 µL, 10.0 µL, 15 µL, and 20 µL of BSA standard solution was added and labeled separately, then the sample was diluted to 2000 µL by adding 1000 µL freshly made BCA mixture solution (3.125 mL Solution A, 0.125 mL solution C and 3.00 mL solution B were mixed thoroughly) and corresponding volume of MiliQ water. After dilution, all the samples were cooked at 60^{o}C for 30 mins and then cooled down to room temperature in 5 mins before measuring their absorbance at 562nm with the Synergy HT multi-mode Microplate reader. The concentration (µg/ µL) of each protein sample was calculated after plotting the standard curve based on the absorbance intensity. Once the concentration of each protein sample was determined, they were stored at -80°C for later use for loading onto a gel.

2.5.2. Protein electrophoresis

When protein samples were ready for being run by electrophoresis, samples were thawed and placed in ice to keep them cold. Electrophoresis running buffer solution (25 mM Tris base, 190 mM glycine, 0.1% SDS, pH=8.3) was made and cooled at 4 ^{o}C beforehand. A vertical electrophoresis apparatus (Amersham Pharmacia biotech AB MightySmall^{TM} II

for 8*9 gels) was set up and two 7.5% precast polyacrylamide 10-well gels (Bio-Rad 7.5% Ready Gel® Tris-HCl Gel) were mounted tightly between the anode and cathode chambers which held the electrophoresis running buffer. The whole apparatus was placed in ice to keep the running buffer cool during the electrophoresis process. Protein loading samples were prepared by mixing the same weight amount of protein (25 μg to 50 μg) based on their protein concentration with 10 μL loading buffer. The loading buffer was prepared following the manufacturer's instruction by mixing 450 μL 2x Laemmli sample buffer (Bio-Rad) with 50 μL 2-mercaptoethanol (Fisher Scientific). Then protein loading samples were cooked at 95ºC for 5 mins to allow the 2-mercaptoethanol denature protein structure by breaking the inter- and intra-chain disulfide bonds. The denatured sample was loaded into each well of the pre-casted gels and at the same time 10 μL SeeBlue Plus2 pre-stained standard (life technologies) was loaded as protein loading standard maker. To keep running balance, all the wells without any loading sample were also loaded with 10 μL loading buffer. Once the loading process was completed, a 250V, 150mA current was set and provided by electrophoresis power supply (Life technologies, EPS601). Then the denatured protein molecules were forced through the gel under this voltage while larger molecules were retarded more than the smaller molecules in migration. After around one hour, electrophoresis was completed, and the protein molecules with specific molecular weight in each sample migrated to their specific positions in gel based on the size and charge.

2.5.3. Protein transfer from gel to membrane after electrophoresis

When the electrophoresis was completed, the proteins staying on the gel were transferred to a nitrocellulose membrane in dry method with Original iBlot® Gel Transfer Device and

the complementary mini transfer nitrocellulose stack (life technologies). The voltage applied was 20V and transfer time was set ranging from 7 to 13 mins depending on the targeted proteins. If the proteins to be detected were lower molecular weight, transfer time was shorter, and vice versa. With the completion of protein transfer, the gel was incubated with Coomassie blue stain solution (Bio-Rad) at room temperature to check whether the protein in gel was fully transferred to the membrane. The membrane was washed with TBST (25 mM Tris base, 140 mM NaCl, 0.1% Tween-20, adjust to pH=7.4 with concentrated HCl) buffer two times and then blocked overnight at 4 ^{o}C or 3 hr at room temperature with the blocking solution under agitating. This preliminary blocking process is necessary and required to prevent non-specific background binding of the primary and/or secondary antibodies to the membrane. The 5% blocking solution was freshly made every time by dissolving non-fat dry milk (LabScientfic) or bovine serum albumin (BSA) into TBST.

2.5.4. Inmmunoblotting with antibodies and blot visualization

With the completion of membrane preliminary blocking, the membrane was washed with TBST three times, 5 mins each time on an agitator and was blocked with primary antibody for 3 hr at room temperature. Primary antibody (Santa Cruz Biotechonoly, Inc.) was dissolved and diluted with 5% non-fat dry milk or 5% BSA TBST buffer solution to a proper ratio following the manufacturer's instructions. The proper ratio of antibody dilution was important to ensure enough targeted protein bound to the antibody. After primary antibody incubation, the blocking solution was discarded and the membrane was washed with 30 mL~50 mL TBST buffer, three times, 10 mins each time, to wash off the

residue of primary antibody. Then the membrane was blocked with secondary antibody solution for 1~1.5 hr at room temperature to allow secondary antibody (IgG-HRP, Santa Cruz) to bind with primary antibody which already bound to targeted protein after first incubation. Secondary antibody was also diluted with 5% non-fat dry milk or 5% BSA TBST buffer. After second incubation, the blocking solution was discarded and the membrane was washed again with TBST buffer for three times (10 mins each time). The membrane was detected with ECL Select Western Blotting Detection Reagents (GE Healthcare Life Sciences). The membrane was fully covered with the detection solution in darkness for five minutes and then the chemiluminescent intensity emitted by the targeted immnuo-blotted protein was detected with C-DiGit® Blot Scanner (LI-COR).

2.6. Profiler RT^2-PCR array assay

2.6.1. RNA isolation and purification from cells

After treatment of cells with various concentrations of Cr(IV)-DPO and with variable time exposures, the treated and control cells growing in 100 mm petri dishes (making sure all the cells were the same passage, P4) were thoroughly washed with HBSS or PBS buffer four times. Then 2 mL PBS diluted trypsin-EDTA solution (0.1% for BEAS-2B cells and 0.05% for HUVECs, 0.25% Trypsin, Life Technologies) was added to fully cover the cells. The cells treated with trypsin-EDTA were incubated at 37 ºC for 7~9 mins to facilitate the cells detachment. Longer time treatment with trypsin will damage cell viabilities, so after incubation at 37 ºC 6.0 to 8.0 mL of complete growth medium was added to dilute and deactivate trypsin. The detached cells were aspirated by gently pipetting. The cell

suspension solution was transferred to 15 mL centrifuge tube and centrifuged at 300xg for 5 to 8 min. Cells pellet at the tube bottom was kept after centrifugation and suspended, washed with 10 mL PBS buffer. Centrifugation was performed again to wash off any residue of trypsin. This time, the pellet after centrifugation was kept and re-suspended with 1.5 mL PBS buffer. The number of cells in each sample was determined by counting the cells in PBS with a TC20 automated cell counter (Bio-Rad). If the total cell number was smaller than 5×10^6, all of the cell solution was transferred into 1.5 mL centrifuge tube and centrifuged at 500 xg for 5 min. If not, partial solution containing 5×10^6 cells was transferred into a 1.5 mL micro tube and then proceed to next step. After obtaining cell pellet from each sample, the RNA of each sample was isolated at room temperature by following the protocols provided with the RNeasy Mini Kit (QIAGEN). First, the cell solution of each sample was centrifuged, and the cell pellet was kept and mixed with 350 µL provided Buffer RLT. (RLT buffer was used to immediately inactivate RNases to remove impurities and ensure purification of intact RNA since RLT was a highly denaturing guanidine-thiocyanate-containing buffer that it disrupted the cells and loosened the compact pellet by flicking the tube.) The cell lysate was homogenized by passing it through an RNase-free 27G syringe (27 G x 1 1/2 inch BD PrecisionGlide™ needle, sterile) at least 5 times. The homogenized lysate was mixed thoroughly with 350 µL 70% ethanol (Ethanol was added to provide the appropriate binding conditions to silica-based membrane in the spin column) and transferred carefully to the provided RNeasy spin column placed in a 2 mL collection tube. Column was tightly closed and centrifuged for 15s at 8000 x g. The flow-through was discarded and the column with to a new 2 mL provided collection tube. Then 700 µL provided Buffer RW1 was added to the RNeasy spin column to wash

away the unbinding contaminants. Column was closed gently and centrifuged for 15 s at 8000 x g to wash the spin column. The flow-through was discarded and the column was transferred to a new 2 mL collection tube. Then the column for each sample was washed to remove the residue of salts left with 500 µL 1x 100% ethanol diluted Buffer RPE two times, centrifuge at 8000 x g for 15s and 2min respectively. Then the RNeasy spin column was centrifuged at 8000 x g, 1min again to completely remove the ethanol and was placed in a supplied new 1.5 mL collection tube. Finally, 30~40 µL supplied RNase-free water was added to the spin column membrane directly and tube was centrifuged for 1 min at 8000 x g to elute the RNA. Usually, after the first time elution, additional 15~30 µL RNase-free water was added while using the same collection tube to completely elute all the RNA bound to the silica membrane. After this process, all the RNA molecules from each sample with size longer than 200 nucleotides which mainly consisted of mRNA were purified and collected. At the same time, the shorter RNA within, like 5.8S rRNA, 5S rRNA, and tRNAs molecules were selectively excluded and washed away because they were so small to form sediment efficiently through the CsCl cushion staying in the silica membrane when they were undergoing high speed centrifugation. RNA samples were labelled and stored at -80^{o}C for later use.

2.6.2. cDNA synthesis from RNA samples

Before preparing cDNA samples, the quality and quantity of each RNA sample was tested with Nanodrop 1000 (Thermo) following the manufacturer instructions. This test gave the absorbance of each sample at wavelength 260 nm and 230 nm simultaneously. The standard that the absorbance reading of 1.0 at 260 nm in a 1 cm detection path corresponded

to an RNA concentration of 40 ng/ μL was used by the device to calculate the RNA concentration of each sample. The samples to proceed to the next step qualified to a concentration higher than 125 ng/ μL with a ratio of A260:A230 greater than 1.7 and a ratio of A260:A280 staying in range of 1.8 to 2.0. cDNA synthesis was completed by using RT^2 First Strand Kit (QIAGEN), following the protocols provided. For all experiments, the same weight amount of RNA from each sample was calculated by referring to the concentration got previously and was added to the PCR microtube. Then 2 μL supplied Buffer GE (Genomic DNA elimination buffer) and RNase-free water were added in sequence to bring the Genomic DNA elimination mix solution up to 10 μL in total. The genomic DNA elimination mix was then cooked for 5 min at 42°C and cooled in ice for at least 1 minute. At the same time, reverse-transcription mix solution per reaction was prepared by mixing 4 μL 5x Buffer BC3, 1uL Control P2, 2 μL RE3 reverse transcriptase Mix and 3 μL RNase-free water (all were provided in the kit). For each sample, the reaction solution was made by thoroughly mixing the 10 μL of reverse-transcription mix solution with the 4°C-cooled genomic DNA elimination mix solution by gentle pipetting. Then each reaction solution was placed into a T100™ Thermal Cycler (Bio-Rad) to proceed with cDNA synthesis under the thermal cycle: incubated at 42°C for exactly 15 min, immediately stopped by incubating at 95°C for 5 min and cooled to 4 ºC to hold. After synthesis, 91 μL RNase-free water was added to dilute the products in each tube by pipetting up and down several times gently. cDNA samples were labeled carefully and placed in ice to proceed with PCR assay or stored at -20 ºC prior to the PCR assay.

2.6.3. RT^2 profiler PCR array analysis

Before preparing the plate for the PCR assay, the working bench was carefully cleaned up by spraying 10% bleach used to chemically degrade any possible DNA contaminants left on the bench. The RT^2 profiler PCR array was prepared following the manufacturer instructions. First, the PCR components mix was prepared in a loading reservoir (QIAGEN) by thoroughly mixing 102 µL cDNA synthesis product prepared before with 1350 µL (for 96-well plate) or 650 µL (for 96 x 4 plate) 2x RT^2 SYBR Green Mastermix (QIAGEN) and 1248 µL (for 96 x 4 plate) or 548 µL (for 96 x 4 plate) RNase-free water. The RT^2 profiler PCR Array plate was not be removed from the sealed bag before the PCR components mix was prepared. In each well of the RT^2 Profiler PCR array plate, 25 µL (for 96-well plate) or 10 µL (for 96 x 4 well plate) PCR components mix was added as accurately as possible using a multichannel pipettor. Once finishing the sample loading, the RT^2 Profiler PCR array plate was carefully and tightly sealed with optically clear adhesive film (Thermo Scientific) to avoid the sample contamination as well as evaporation during thermal cycler in PCR instrument. The array plate was centrifuged for 1 min at 1000 g at room temperature (15–25°C) to remove the bubbles and allow the sample to settle down to the well bottom. The presence of bubbles in the well would interfere with the results, so visual inspection of the plate from underneath was necessary to make sure no bubbles were present in each well. While setting up the PCR cycling program in ABI PRISM® 7900HT (Life technologies®, Applied Biosystems™), the RT^2 Profiler PCR Array plate ready to be detected was placed on ice or stored at -20°C wrapped in aluminum foil for up to one week. The real-time cycler program was set as three stages: stage one is the activation stage which

was set as 10mins, 95°C heating, 1 cycle; stage two is the amplification which was set as 15s, 95°C heating followed by 1 min 60°C heating, 40 cycles; stage three is the disassociation stage which was set as 95°C heating, 1 minute followed by 65°C heating, 2 minutes and no repeat. The fluorescence data was collected both in stage 2 and stage 3. After around 2.5 hours, the PCR running was completed and the raw data was exported and processed by using SDS.2.4 software (Life technologies®, Applied Biosystems™) following manufacturer instruction. The final data for each array was exported as a "txt" file. The gene information of each well of each specific array was obtained from the website www.sabiosciences.com. Data were translated in an Excel form and was analyzed following the manufacturer instructions to calculate each gene expression variations between the chromium(IV) treated samples and the untreated control samples.

2.7. cDNA sequencing

Four cDNA samples prepared from BEAS-2B cells (4th passage of cell line obtained from ATCC®), two untreated control samples and two 5 μM Cr(IV)-DPO 48 hr treated samples were prepared with the method stated above and were sent to the Sequencing Core located in University of Houston. After further purification by running agarose gel and amplification by PCR for each sample, in the core, sequencing analysis was run on Ion Torrent™ with Ion 316™ Chip (Life technologies®). After sequencing, data was collected and the variants calling was performed to export all the sequence variants in reference with human genome library, giving the FASTAQ files, bam files, vcf (variant calling file) files and excel forms including detailed information on each variant. The information consisted of genomic position, frequency, quality, reads in the plus and minus strands that cover this

position, and numbers of reads both in plus and minus strands that match the variant. The vcf files were uploaded to the IGV (Integrative Genomics Viewer) java software downloaded from the Broad Institute website http://www.broadinstitute.org/igv/home where the human genome library, hg19, was provided as FASTA file. Then the vcf files were analyzed in two ways. The first way was that I narrowed my views to DNA damage related signaling pathways including the cellular apoptosis pathway, the DNA repair pathway, and the cell cycle check pathway. So the variants of each sample were viewed referring to human genome by choosing the three gene lists in the region option. Respectively, the information about the apoptosis gene list including 129 genes was viewed, DNA damage repair gene list including 104 genes, and cellular cycle checkpoints gene list including 110 genes. Once the variants calling was performed by Ion System™ analyzer (Ion Torrent™, Life technologies®), the variants were shown after choosing a specific gene list if there existed any variant, otherwise, the software gave the response "NO VARIANTS FOUND". Then in the software screen, the position of one variant belonging to one specific gene was located and its position was recorded, which was used to pick out all the other variants existing in this very gene by checking the excel form providing all the location information of each variant. The second way was that the genomic location, obtained from the http://www.genecards.org/ website, of each interested gene was input manually in the search bar of the IGV software. After searching, the software displayed the variants if existed of each uploaded vcf file, then the variants were checked in the four excel forms to identify the locations of all variants for each sample. The second way was applied when the published oncogenes of lung cancer were viewed. But, for both ways, one important thing worth noting is that the control samples had large quantities of overlapping variants

as the treated samples. Thus, when analyzing the variants to find out the influence resulting from the Cr(IV)-DPO treatment, the overlapping variants were subtracted manually from treated samples. It is worth mentioning that many of the variants had very low coverage. The parameter “coverage” of each genomic location reflects how many times this variant was detected. Because the running sample was cDNA samples converted from mRNA rather than whole genomic samples, in the transcription process from genomic DNA to mRNA, more than 98% of DNA information was not transcribed. Thus, overall, the finding that the data showed low coverage was reasonable. But, even the lower coverage was normal to happen in cDNA sample sequencing; the higher the coverage, the better the reliability. Therefore, if the coverage of a variant is smaller than 10, that variant was regarded as not significant and neglected. This analysis process might introduce accidental errors, but based on the large quantities of total number of variants, these errors might be negligible.

CHAPTER III: RESULTS AND ANALYSIS

3.1. Characterizations of Cr(IV)-DPO complex

The authenticity of Cr(IV)-DPO complex was verified by HPLC separation, atomic absorption spectroscopy (AAs, AAnalyst^{TM} 600, PerkinElmer$^{®}$), and LC-MS (Thermo Scientific$^{®}$). HPLC (Thermo Scientific$^{®}$) separation, using 5%-95% acetone nitrile gradient mobile phase, showed one sharp peak detected at wavelength 370 nm. A peak m/z 177 was detected in LC-MS, indicating that the Cr(IV)-DPO lost one water ligand. The atomic absorption spectroscopy was used to identify the percentage of Cr in the synthesized complex. The experimental data of synthesized complex, with 2% variation compared to the theoretical data calculated from pure Cr(IV)-DPO, was regarded as pure enough to be used in vivo analysis in the next steps.

3.2. The cellular morphological changes of HUVECs over time with and without Cr(IV)-DPO treatment.

HUVECs adherently growing in petri dish with treatment of different concentrations of Cr(IV)-DPO were photographed at different time points in the method stated before. The images at the 24 hr time point are shown from Figure 1a to 1f. The image shown in Figure 1a is the shapes of HUVECs after 24 hr incubation with the normal whole medium (no chromium(IV) treatment), Figure 1b shows the shapes of HUVECs after 24 hr incubation with 0.5 μM Cr(IV)-DPO dissolved whole medium, Figure 1c shows the shapes of HUVECs after 24 hr incubation with 1.0 μM Cr(IV)-DPO dissolved whole medium, Figure 1d shows the shapes of HUVECs after 24 hr incubation with 2.5 μM Cr(IV)-DPO dissolved whole medium, the image in Figure1e is the shapes of HUVECs after 24 hr incubation with

the 5.0 μM Cr(IV)-DPO dissolved medium, Figure 1f shows the shapes of HUVECs after 24 hr incubation with the 10.0 μM Cr(IV)-DPO dissolved medium.

These images displayed the influence of treatment with Cr(IV)-DPO on HUVECs. Figure 1a shows clearly that HUVECs were tube-shaped meaning that the cells were growing healthily. Figure 1b shows some cells were round and short, but the majority of them were still tube-shaped, implying that the cells were struggling against low-level growth stress. The image in Figure 1c shows nearly the same results as Figure 1b though the treatment concentration was a little bit higher. The image displayed in Figure 1d shows nearly half the cells in the visualization area were round and short instead of long-tube-shaped like that were seen in image exhibited in Figure 1a, which means that the growth stress was increasing as the treatment concentration increased. The image in Figure 1e shows most of the cells were alive but obviously damaged due to the treatment since no tube-shaped cells existed any more. And all the cells were shown short-and-round, indicating that the growth stress was high to suppress the growth of HUVECs. Finally, Figure 1f shows that most of the HUVECs were dying due to too high survival stress caused by the high dosage of Cr(IV)-DPO.

These images together indicated that the Cr(IV)-DPO complex was toxic to HUVECs and influenced the normal growth of HUVECs, but the effects were dose-dependent. When the treatment concentration of Cr(IV)-DPO was low, HUVECs were able to defend the cellular pressure and survived for at least 24 hr, but as the Cr(IV)-DPO concentration increased, HUVECs were severely damaged by high cellular pressure and died.

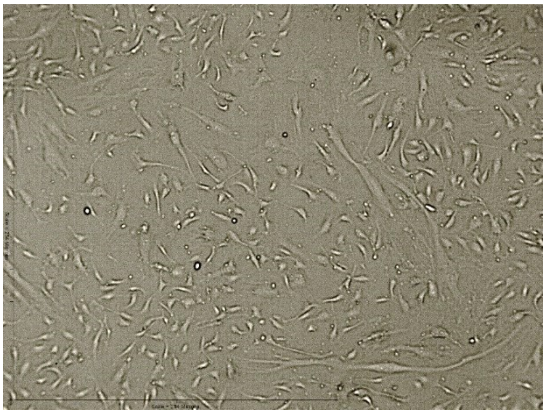

(1a)

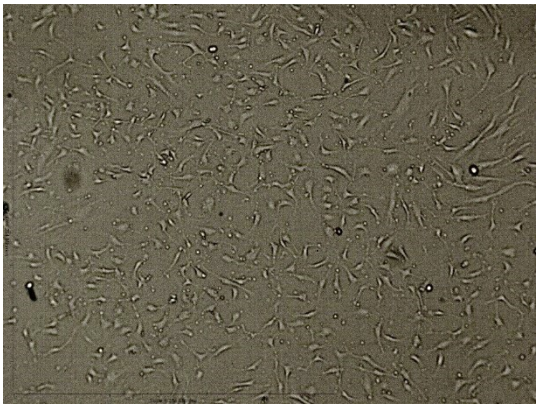

(1b)

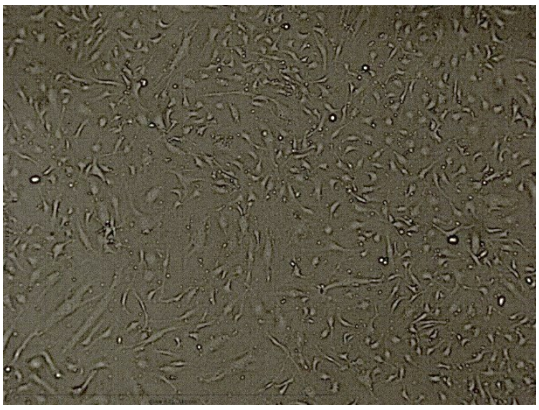

(1c)

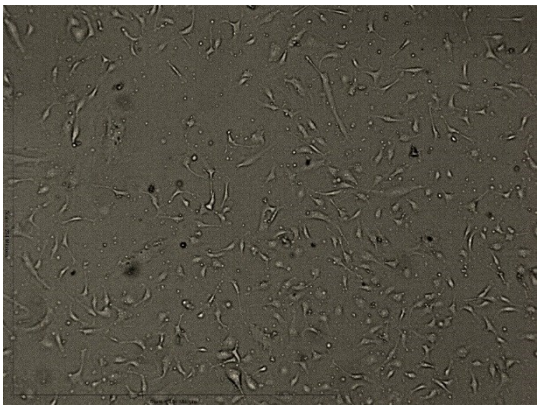

(1d)

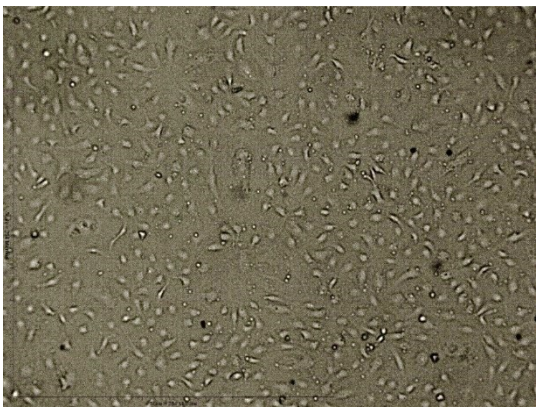

(1e)

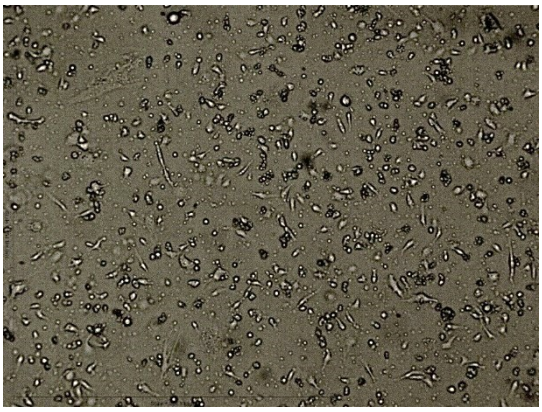

(1f)

Figure 1. Images of HUVEC cells after being treated with various concentrations of Cr(IV)-DPO for 24 hr; (1a) cells without treatment (control); (1b) 0.5 μM; (1c) 1.0 μM; (1d) 2.5 μM; (1e) 5.0 μM; (1f) 10.0 μM.

After the 24 hr incubation under Cr(IV)-DPO treatment, the dead cells that were detached and suspended were removed by aspiration, the rest attached cells were continued to be cultured in the method as stated before, and pictures of their morphologies were taken at various time points, +1hr, +3 hr, +5 hr,+9 hr, +18 hr, +24 hr, +28 hr, +32 hr, +40 hr, +44 hr, and +48 hr. The Figures of HUVECs treated with 0uM (untreated control group), 0.5 μM, 1.0 μM, 2.5 μM, 5.0 μM, and 10.0 μM Cr(IV)-DPO for 24 hr, and cultured for another 24 hr with chromium-free whole medium are shown here as Figure 2a to 2f respectively. The image in Figure 2a shows clearly that HUVECs were growing fast and healthily, most of them were still tube-shaped, though some were not because they were competitively growing in the space-limited petri dish. Figure 2b shows HUVECs were growing well and forming tube-like morphology but half cells were short-triangular and were randomly scattered. The image in Figure 2c is almost identical to that in Figure 2b except that the HUVECs were more colonized with each other, which might be caused by higher cell density. The image shown in Figure 2d obviously shows more round-short cells than Figure 2a to 2c, which means that the cell damages caused by previous 24 hr, 2.5 μM-Cr(IV)-DPO treatment continued to influence HUVECs in the following 24 hr incubation even without the presence of Cr(IV)-DPO complex. The image in Figure 2e shows most of the cells died in the following 24 hr culture after discarding the 5 μM Cr(IV)-DPO treatment. The image shown in Figure 2f shows nearly all of the cells were dead caused by previous high-dosage treatment. These observations indicate that the cellular damages caused by exposure to the Cr(IV) complex might exist in the gene level, consequently the DNA damaged and dysfunctional during the Cr(IV)-DPO treatment hardly support the normal cellular metabolism for further growth.

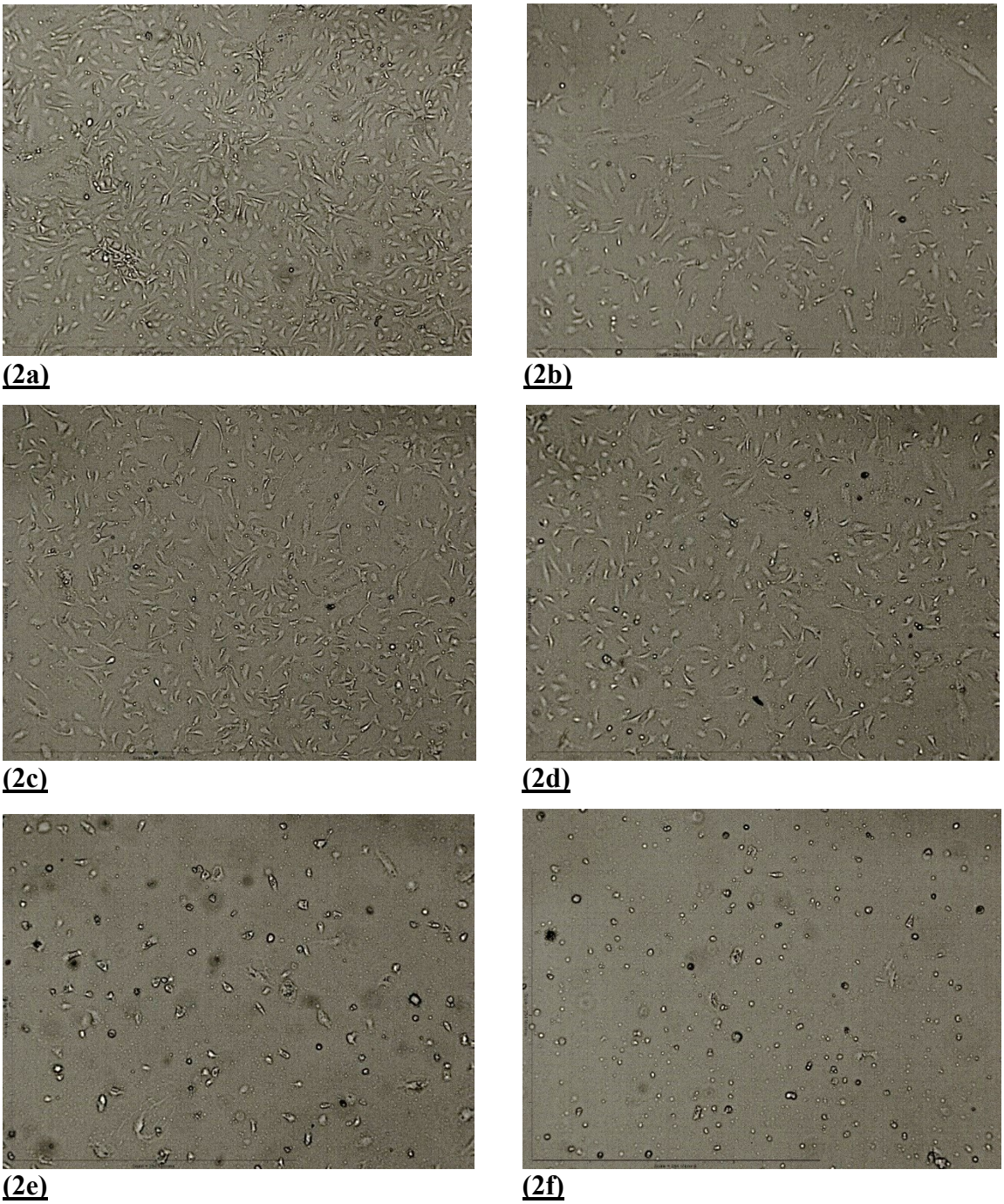

(2a) **(2b)**

(2c) **(2d)**

(2e) **(2f)**

Figure 2. Images of HUVEC cells after another 24 hr incubation with Chromium(IV)-free medium following the of 24 hr Cr(IV)-DPO treatment; (2a) cells without treatment, +24 hr (control); (2b) 0.5 μM, +24 hr; (2c) 1.0 μM, +24 hr; (2d) 2.5 μM, +24 hr; (2e) 5.0 μM, +24 hr; (2f) 10.0 μM, +24 hr.

The images of HUVECs treated with 0 μM (untreated control group), 0.5 μM, 1.0 μM, 2.5 μM, 5.0 μM, and 10.0 μM Cr(IV)-DPO for 24 hr and cultured for another 48 hr with chromium(IV)-free whole medium culture are shown in Figure 3a to 3f. The image shown in Figure 3a shows the HUVECs in the control group were growing well with the tube-like morphology, although some cells were seen as a short and round morphology which can be explained by the reason that long time growing in petri dish caused some mutations coming from environmental influence. Figure 3b shows that HUVECs under this condition tended to colonize and their shapes were mostly short and round, which were regarded as some of the initial markers of carcinogenesis. The image shown in Figure 3c is nearly identical to that in Figure 3b except that cells were more colonized and round. Figure 3d to 3f, all show that all the cells died in this 48 hr post-treatment culture period. These observations confirmed the hypothesis that the toxicity of Cr(IV)-DPO was produced because the complex damage DNA molecules during exposure. Therefore, during the treatment period, some of the DNA damage were not repaired that the gene expressions of HUVECs were interfered, leading to the demonstration that HUVECs died later on without any treatment.

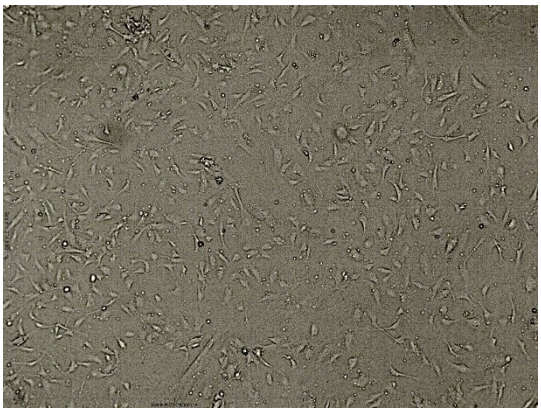

(3a)

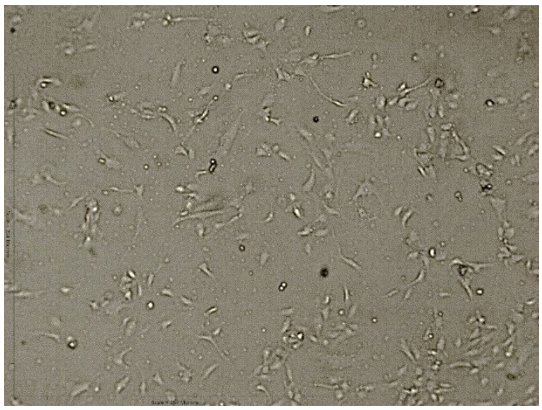

(3b)

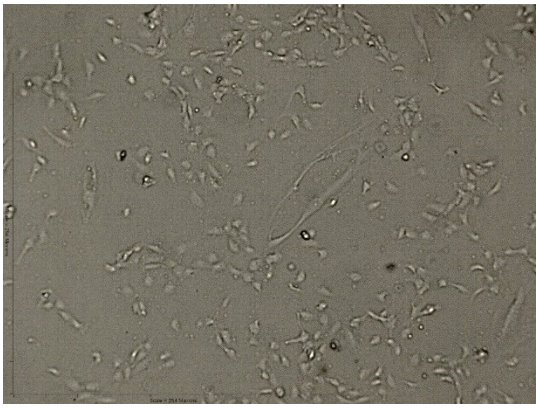

(3c)

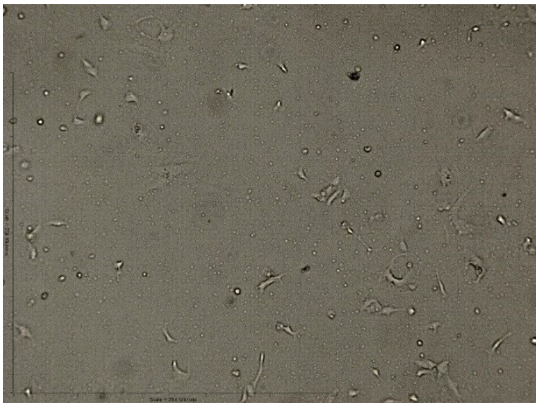

(3d)

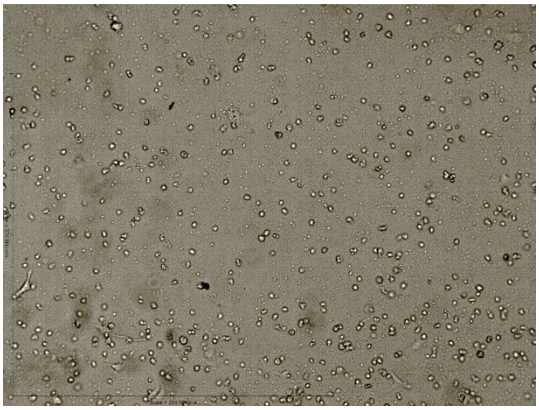

(3e)

(3f)

Figure 3. Images of HUVEC cells after another 48 hr incubation with Chromium(IV)-free medium following the of 24 hr Cr(IV)-DPO treatment; (3a) cells without treatment, +48 hr (control); (3b) 0.5 µM, +48 hr; (3c) 1.0 µM, +48 hr; (3d) 2.5 µM, +48 hr; (3e) 5.0 µM, +48 hr; (3f) 10.0 µM, +48 hr.

3.3. The cellular morphological changes of BEAS-2B cells over time under Cr(IV)-DPO treatment.

BEAS-2B cells growing in one layer at the bottom of the tissue-culture petri-dish were treated with different concentrations of Cr(IV)-DPO, ranging from 0 μM (untreated control), 0.5 μM, 1 μM, 2.5 μM, 5 μM, 10.0 μM, 20.0 μM, 30.0 μM, 50.0 μM, to 100.0 μM. They were photographed at various time points in the method as before. The pictures are shown here, from Figure 4a to 4j, are the images of BEAS-2B cells at 24 hr treatment time point. Initially, the same number of BEAS-2B cells were seeded in a 96-well plate, and then the cells were treated variously according to experimental design. The cells were photographed at the same time point.

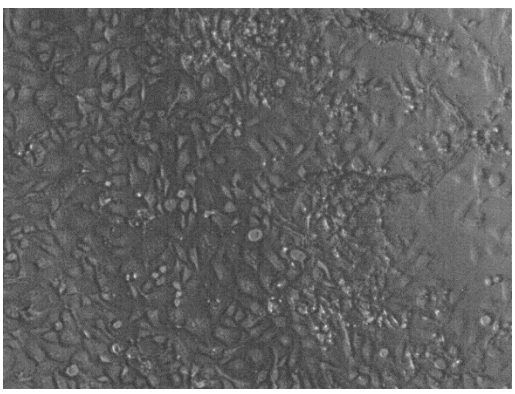

(4a)

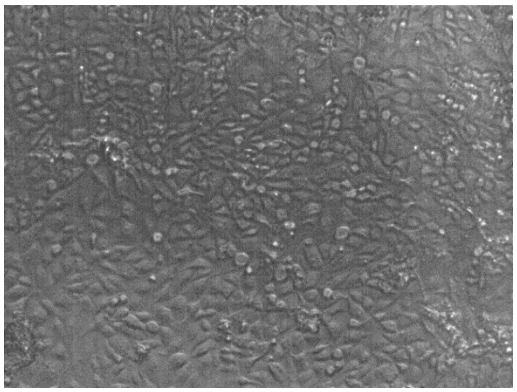

(4b)

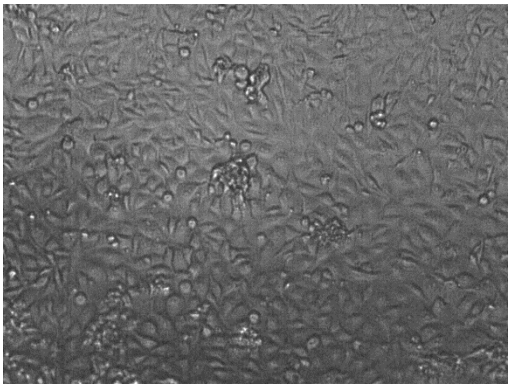

(4c)

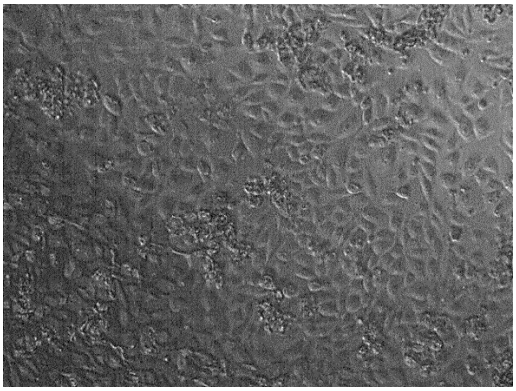

(4d)

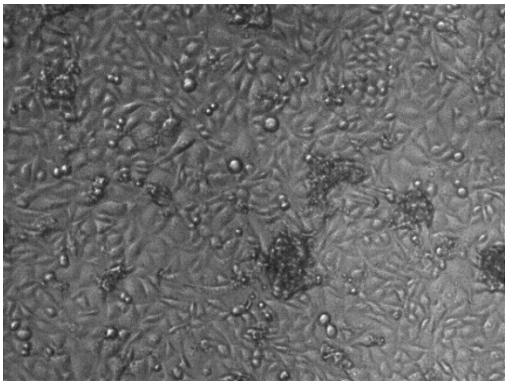

(4e)

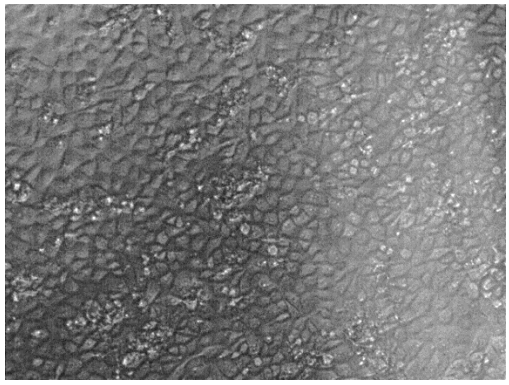

(4f)

Figure 4. Images of BEAS-2B cells after being treated with various concentrations of Cr(IV)-DPO for 24 hr; (4a) cells without treatment (control); (4b) 0.5 μM; (4c) 1.0 μM; (4d) 2.5 μM; (1e) 5.0 μM; (4f) 10.0 μM; (4g) 20.0 μM; (4h) 30.0 μM; (4i) 50.0 μM; (4j) 100.0 μM.

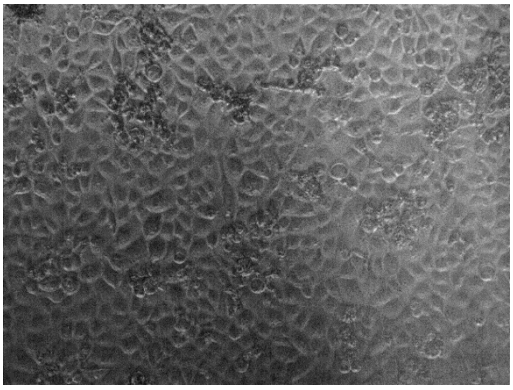

(4g)

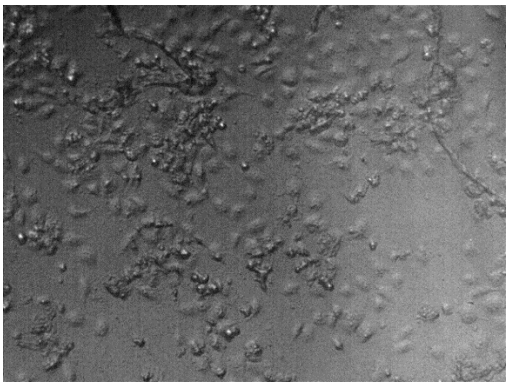

(4h)

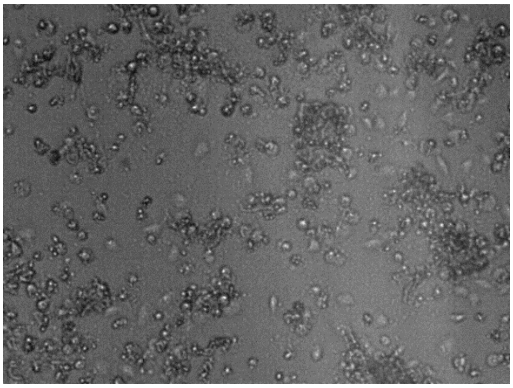

(4i)

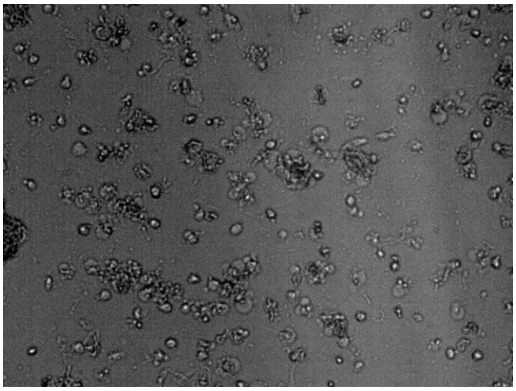

(4j)

(**Figure 4** continued)

The image shown in Figure 4a is the morphology of BEAS-2B cells in the untreated control group, showing the cells looked triangular which were the normal shape of healthy BEAS-2B cells. The image shown in Figure 4a works as a reference to all the other figures that if the cells did not look like triangle, the cells were negatively influenced by Cr(IV)-DPO. The Image shown in Figure 4b is the morphology of BEAS-2B cells after treatment with 0.5 μM Cr(IV)-DPO for 24 hr. The cells were seen to be triangular and nearly identical to those in Figure 4a. Figure 4c to 4e are pictures of the morphologies of BEAS-2B cells after the 24 hr treatment with 1.0 μM, 2.5 μM, and 5.0 μM Cr(IV)-DPO. Based on these observations, we can conclude that the BEAS-2B cells under these treatment conditions were not influenced much in the 24 hr growth period. The image shown in Figure 4f is the

morphological shapes of BEAS-2B cells treated with 10.0 μM Cr(IV)-DPO for 24 hr, from which we can see most of the cells are round rather than triangular shape as in the control group. Figure 4g is the picture of morphological shapes of the BEAS-2B cells treated with 20.0 μM Cr(IV)-DPO for 24hr, showing that some cells were undergoing dying process since their morphologies tended to be amorphous. Figure 4h shows the morphologies of BEAS-2B cells treated with 30.0 μM Cr(IV)-DPO for 24 hr, from which the phenomenon that more than half of the cells died and detached from the bottom was observed. It is caused by the high concentration of Cr(IV)-DPO producing high survival pressure. Figure 4i and 4j show the cells were dying under the increasing survival pressure caused by the increasing Cr(IV)-DPO concentrations. These observations gave a similar conclusion that the damages to BEAS-2B cells caused by Cr(IV)-DPO were dose-dependent. The damages were first demonstrated on the cellular morphologies, therefore this conclusion exactly corresponds to some news report that the workers frequently contacting with chromium-contaminated water had skin diseases. By comparing the Figures of HUVECs and BEAS-2B cells, we can also conclude that BEAS-2B cells have higher tolerance against Cr(IV)-DPO than HUVECs.

In addition, after another 24 hr incubation with various concentrations of the Cr(IV)-DPO complex that made the incubation time up to 48 hr, images of the BEAS-2B cells were taken in the method stated before. The pictures are were shown below through Figure 5a to 5j. This additional step was done to check whether the damages to BEAS-2B cells caused by Cr(IV)-DPO treatment was also time-dependent.

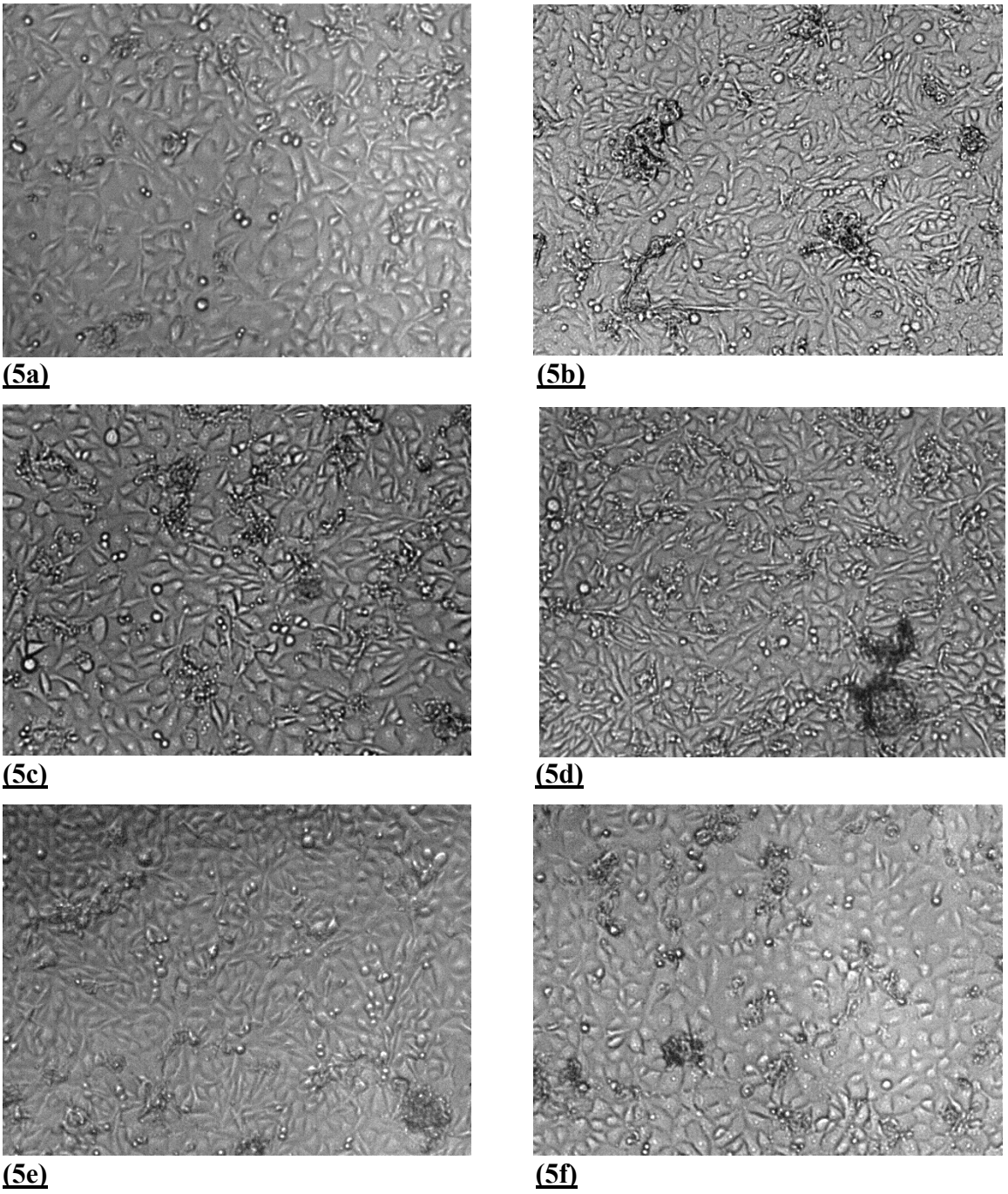

(5a) **(5b)**

(5c) **(5d)**

(5e) **(5f)**

Figure 5. Images of BEAS-2B cells after being treated with various concentrations of Cr(IV)-DPO for 48 hr; (5a) cells without treatment (control); (5b) 0.5 μM; (5c) 1.0 μM; (5d) 2.5 μM; (5e) 5.0 μM; (5f) 10.0 μM; (5g) 20.0 μM; (5h) 30.0 μM; (5i) 50.0 μM; (5j) 100.0 μM.

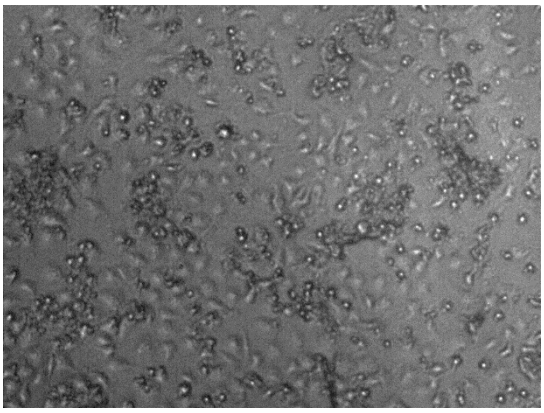

(5g)

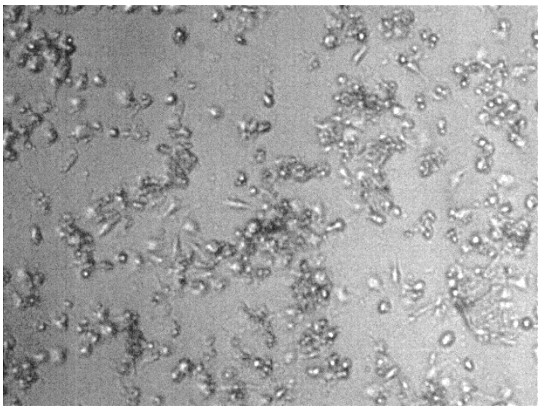

(5h)

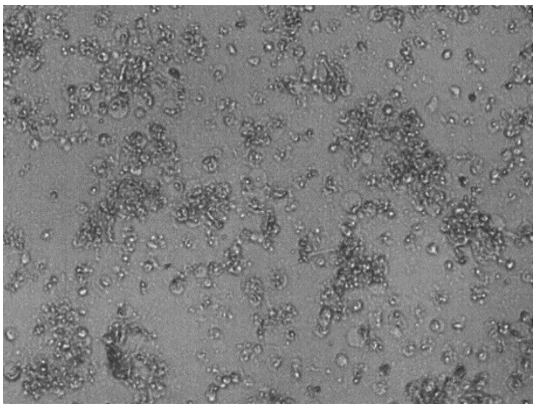

(5i)

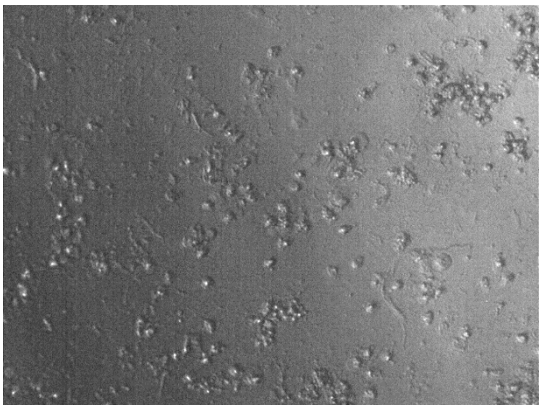

(5j)

(**Figure 5** continued)

The changes in morphologies of BEAS-2B cells treated with Cr(IV)-DPO for 48 hr were nearly identical to the 24 hr treatment group except that the apparent morphological changes happened at a lower concentration of Cr(IV)-DPO, 10 μM instead of around 20 μM in the group with 24hr exposure time. This result confirms the prevailing conclusion that toxicity of Cr complex is time-dependent and dose-dependent.

3.4 Cellular viability assay

The viabilities of HUVECs against Cr(IV)-DPO concentrations for an exposure time of 24 hr were determined according to the method stated above and are shown in Figure 6. The horizontal axis is the concentration of Cr(IV)-DPO (μM), and the vertical axis indicates the viability ratio which is calculated in the method listed above based on the comparative luminescence intensity with reference to control samples. From the graph in Figure 6, the IC_{50} of HUVECs against Cr(IV)-DPO for the 24 hr treatment was determined as 7.2 μM.

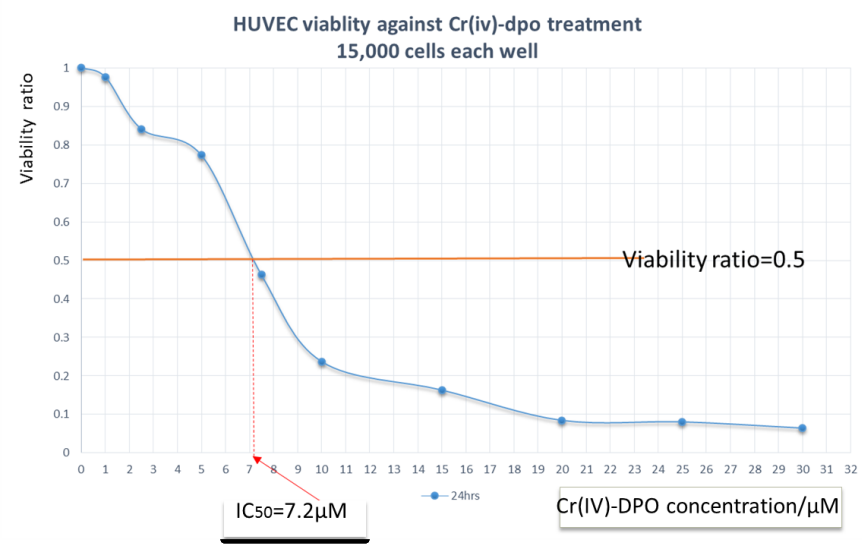

Figure 6. Percent survival of HUVEC cells upon treatment with various concentrations of Cr(IV)-DPO for 24 hr

The viabilities of BEAS-2B cells against Cr(IV)-DPO for the exposure time of 6 hr, 24 hr, 48 hr, and 72 hr were determined respectively in the method stated above. The results are shown as the plotting lines in Figure 7. As stated before, the horizontal axis is also the concentration of Cr(IV)-DPO (μM), the vertical axis is the viability ratio calculated in the same way stated above.

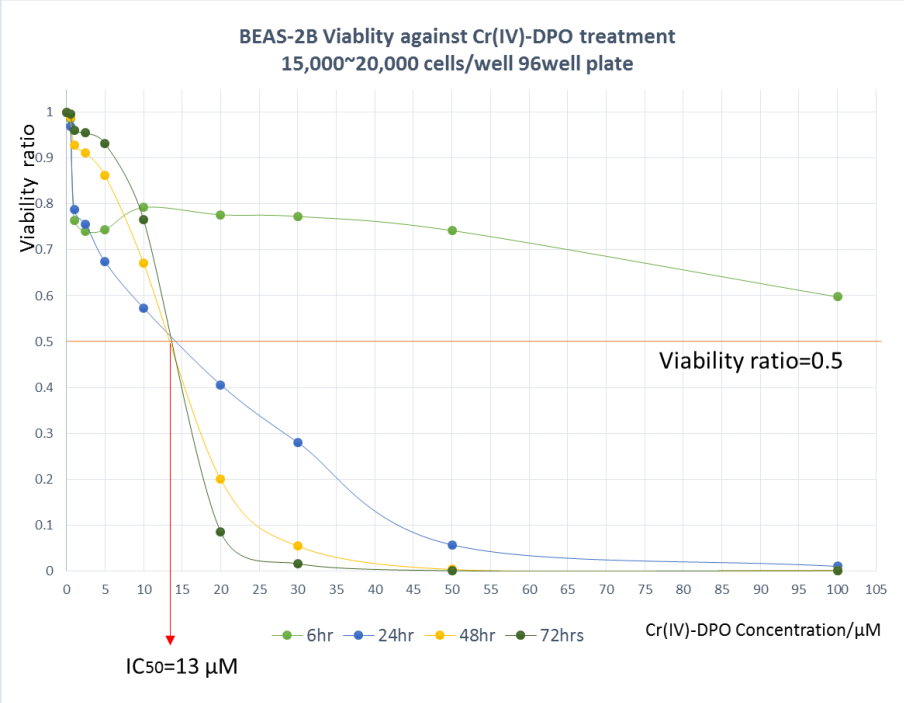

Figure 7. Percent survival of BEAS-2B cells upon treatment with various concentrations of Cr(IV)-DPO for 6 hr, 24 hr, 48 hr, and 96 hr

Figure 7 includes four plotted lines, the light green one represents the group with treatment time of 6 hr, the blue line represents the group with treatment time of 24 hr, the yellow line represents the group with treatment time of 48 hr, and the dark green line represnts the group with treatment time of 72 hr. As stated before, each point at a specific treated concentration was an average number from six wells with the same treatment. It is worth noting that, as shown in Figure 7, the IC_{50} of BEAS-2B cells against Cr(IV)-DPO with treatment time for 24 hr, 48 hr, and 72 hr was almost identical, around 13 µM. However, the IC_{50} of the group with Cr(IV)-DPO treatment for 6 hr is unable to be determined because 6 hr exposure was too short to cause severe damge to the BEAS-2B cells.

3.5. Western blotting, probed with P53, PTEN, BCL and PUMA antibodies.

Proteins, extracted following the method stated before from HUVECs, which were treated with 0.25 μM, 0.5 μM, 1 μM, 2.5 μM, 5 μM, 7 μM, 10 μM, and 20 μM Cr(IV)-DPO complex respectively for 24 hr, were immunoblotted with primary antibodies: P53, PTEN, BCL2, and PUMA. Proteins extracted from HUVECs which were treated with 2.5 μM and 5 μM Cr(IV)-DPO for 48 hr and 72 hr respectively were also immunoblotted with P53 antibody and PTEN antibody. Proteins extracted from the HUVECs which were treated with 2.5 μM and 5.0 μM Cr(IV)-DPO for 24 hr and 48 hr followed by additional 24 hr incubation in chromium-free whole medium were immunoblotted with P53 antibody and PTEN antibody respectively. Figures 8 and 9 show the results from Western blotting assays on different samples. Each nitrocelluse membrane with the transferred proteins was blotted twice. The first time, it was blotted with the targeted antibody, and the second time, it was blotted with Beta-Actin which worked as loading control since the expression intensity of Beta-Actin should be the same in all samples given the loading amout of protein in each sample is the same.

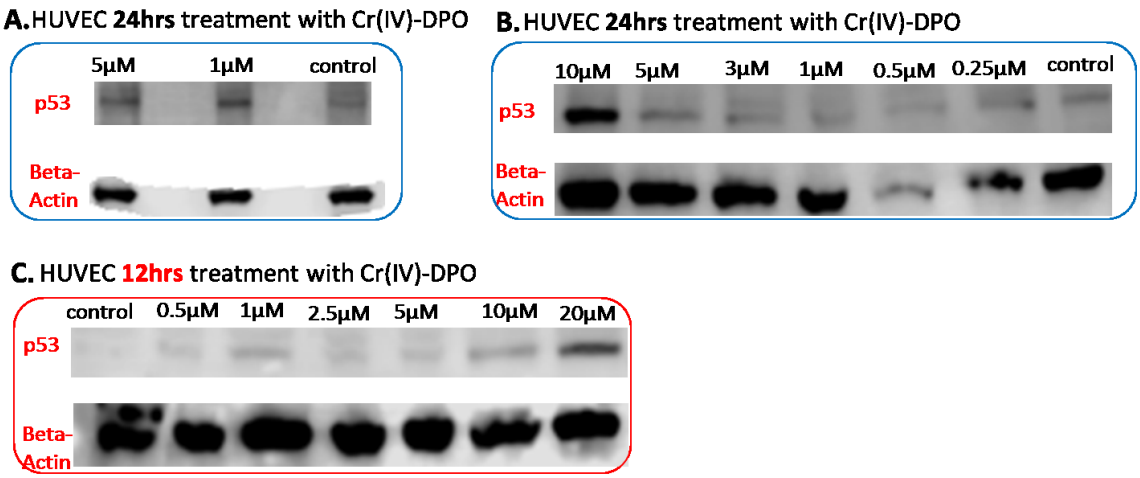

Figure 8. Western blot displaying expression of P53 protein compared to Beta-Actin control

P53 is a protein encoded by the *TP53* gene that plays crucial roles in apoptosis, cell cycle arrest and many other cancer-related signaling pathways since it is a tumor suppressor gene. P53 protein is activated when the DNA is damaged since it activates the DNA repair genes, thus P53 protein expression variants will be an important marker of indicating the DNA damage resulting from the Cr(IV)-DPO treatment. The Western blots in Figure 8 show that the P53 protein in HUVECs under Cr(IV)-DPO treatment was over-expressed compared to the control. In addition, as the dosage increased, P53 was more over-expressed and as the incubation time increased from 12hr to 24hr, the P53 was also more over-expressed. This result indicated that under higher dosage or longer exposure time of Cr(IV)-DPO the cells were producing more P53 protein to maintain cell health and defend against the DNA damage resulting from the chromium(IV) treatment.

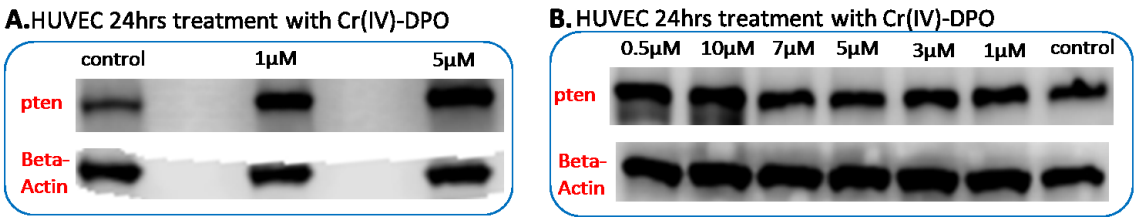

Figure 9. Western blot displaying expression of Pten protein compared to Beta-Actin control

PTEN is a protein in human cells encoded by the *PTEN* gene which is a tumor-suppressor gene whose mutation is usually a key step in the initiation of cancers. Specifically, the PTEN protein acts as an enzyme catalyzing the dephosporylating of the 3'-phosphate of the inositol ring in PIP3 and consequently inhibiting PI3K-AKT signaling pathway. Under this regulation, the cell proliferation is balanced. Thus the variations of PTEN expression in different protein samples extracted from HUVECs with various treatment conditions will be an important marker showing the possibility of *PTEN* gene mutation under the Cr(IV)-DPO treatment. The two Western blots shown in Figure 9 indicate that as the Cr(IV)-DPO concentration increased, the pten protein expression in HUVECs was decreased. This result means that the *PTEN* gene expression was interrupted by the chromium treatment. Since the increase of pten expresson would defend against cellular damages, but in treated samples, PTEN expression was in contrast lacked when the cells were severely damaged by chromium, leading HUVECs inadequately regulate cell proliferation.

BCL-2 is an anti-apoptotic protein of the BCL-2 family of proteins that regulate and contribute to apoptosis. In human cells, BCL-2 protein, encoded by the *BCL2* gene, either promotes or inhibits apoptosis. Thus, mutations in the *BCL-2* gene will affect cellular proliferation balance leading to cancer. Because of its pivotal role in cancer development,

BCL2 gene has been classified as an oncogene. Our results show that BCL-2 protein was not significantly changed by Cr(IV)-DPO treatment, as compared to control in HUVECs (results not shown). This suggests that BCL-2 was not affectted by the treatement condition.

PUMA (also called Bcl-2-binding component 3) is a pro-apoptotic protein regulated by P53. Once activated it frees the mitochondrial pro-apoptotic proteins BAX and/or BAK by interacting with the anti-apoptotic BCL-2 family protein members. Consequently it results in the activation of initiator and effector caspases, yielding cell death. Because of puma's importance in cell death, we evaluated the puma expression in untreated and Cr(IV)-DPO-treated HUVECs using Western blot analysis. Our results show that PUMA expression was unchanged by Cr(IV)-DPO treatment, it was not significantly shown both in the control and treated samples (Figure not provided).

Modulation of the expressions of proteins: P53, PTEN, PUMA, BCL-2, FAS, FASL, BAX, CASPASE3, and CASPASE8 were investigated in the untreated control and Cr(IV)-DPO-treated HUVECs. But only protein P53 (Figure 8) and protein PTEN (Figure 9) were markedly increased following the Cr(IV)-DPO treatments. Unchanged protein expressions of PUMA, CASPASE-3, CASPASE-8, FAS, and BCL-2 may be due to the lack of sensitivity of the Western blotting. Alternatively, these proteins might be present in their phosphorylated forms, which can not be detected using total protein lysates in my experimental method. Therefore, the absence of changes in the protein expressions post chromium(IV)-treatment of HUVECs may not exclude the presence of cell mutation under the Cr(IV)-DPO treatment.

3.6. Variations in gene expressions observed by RT^2-PCR due to Cr(IV)-DPO-treated cells compared to untreated control cells

3.6.1 Apoptosis RT^2-PCR Array on HUVECs

Cellular morphology, cell viability, and protein expression experiments provided valuable insight, to further understand the mechanisms of Cr(IV)-DPO treatment caused cellular damages RT^2-PCR was performed. Due to the fact that the genotoxicity of chromium compounds is too complicated to be simply explained by some specific signaling pathways or specific genes, in this project, the apoptosis RT^2-PCR profiler array was carried on to find out the apoptotic genes expression variations. The array contained 84 key genes involved in the apoptosis signaling pathway. The PCR was performed in the method stated before and the data analysis was also processed as the method described earlier.

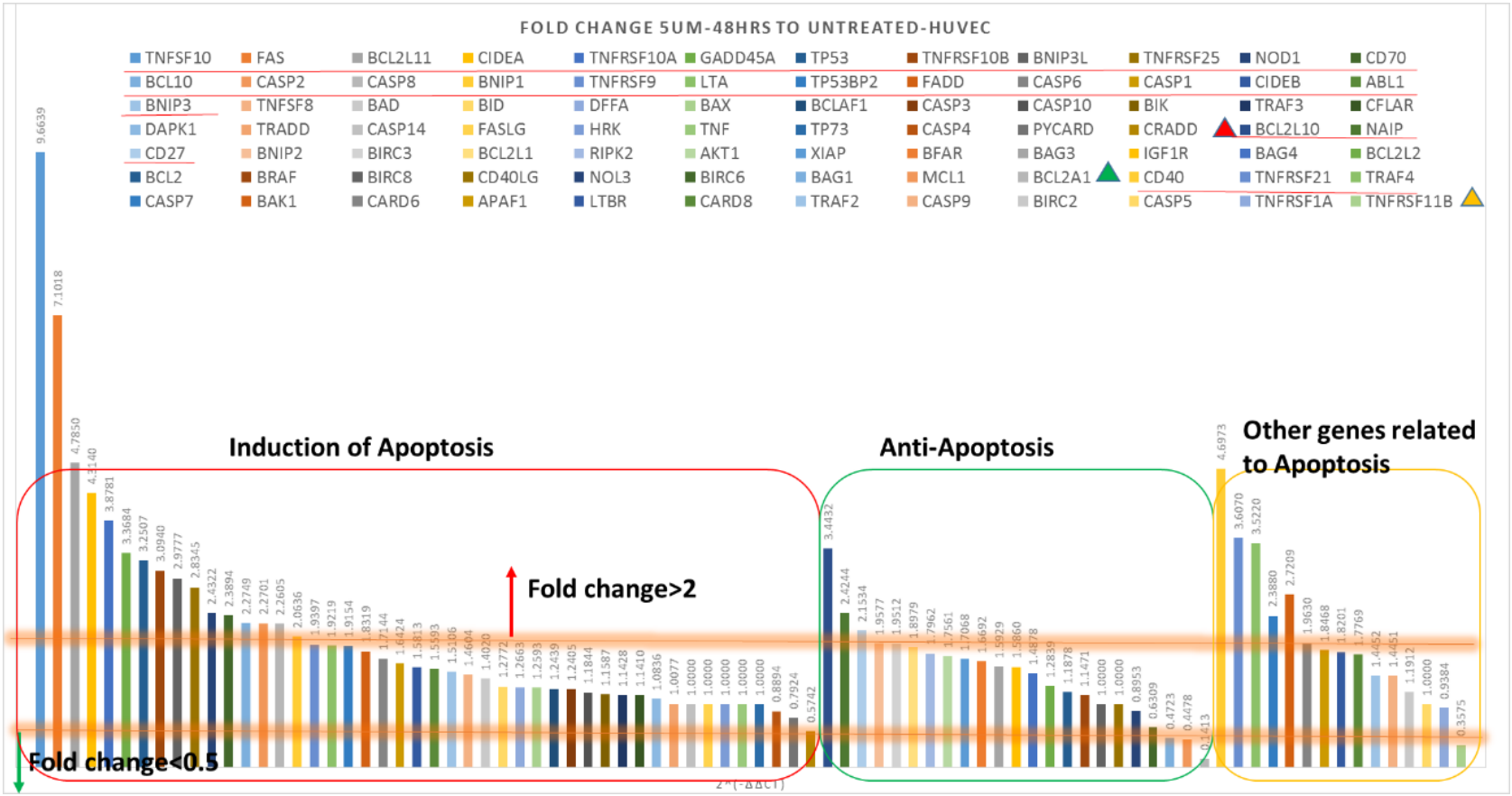

Figure 10. Fold changes of apoptotic genes expression (HUVEC cells) by Cr(IV)-DPO (5 μM 48hr treatment) compared to the untreated control

Figure 10 shows gene expression fold change between untreated control and HUVECs treated groups. Each column height represents one gene, and the higher the column, the more the gene is expressed. The 84 genes were grouped into three categories based on their functions in response to apoptosis (Figure 10). The first group includes 49 genes that induce the apoptosis, among those, 19 genes (*TNFSF10, FAS, BCL2L11, CIDEA, TNFRSF10A, TNFRSF21, TRAF4, BCL2L10, GADD45A, TP53, TNFRSF10B, BNIP3L, TNFRSF25, NOD1, CD70, BCL10, CASP2, CASP8,* and *BNIP1*) were overexpressed by 2-fold, 3 genes (*TNFRSF9, LTA,* and *TP53BP2*) were near over-expressed by over 1.9-fold and none the 49 genes showed less than 0.5-fold change, following the 5 μM Cr(IV)-DPO treatment for 48 hrs. These observations demonstrated that HUVECs treatment with 5 μM Cr(IV)-DPO for 48 hrs resulted in substantial cells apoptotic gene alterations reflected by the change in at least 22 genes.

In the second group, which includes 22 anti-apoptotic genes, only NAIP and CD27, were over-expressed. We postulate that in order to survive the HUVECs react against apoptosis by activating the anti-apoptotic genes when the cellular integrity was threatened by the treatment. Concomitantly, 3 out of the 22 anti-apoptotic genes (*BAG1, MCL1,* and *BCL2A1*), were suppressed over 2-fold, suggesting that the apoptotic process overwhelmed the anti-apoptotic process, which could explain the excess of cell death.

In the third group, which includes 13 apoptosis regulator genes, there were 3 genes (*CD40, BAK1*, and *CASP7*) over-expressed in the HUVECs with Cr(IV)-DPO treatment compared to the untreated control. Specially, *CD40* and *BAK1* are the positive regulation genes, and *CASP7* is the gene encoding Caspase7 responsible for cleaving the downstream substrates

and executes cellular apoptosis. *TNFRSF11B* (Tumor Necrosis Factor Receptor) was down-regulated. These observations, together, lead to the conclusion that the HUVECs gradually died under Cr(IV)-DPO treatment through apoptosis pathway rather than the necrosis pathway which is regarded as the other cell death pathway. The expression of these three group of genes is listed in Tables 1 through 3.

Table 1. Fold changes of apoptosis induction genes expression of HUVEC cells by Cr(IV)-DPO compared to the untreated cells.

GENE Symbol	**Fold change**	**Description**	**Gene Name**
TNFSF10	9.66	Tumor necrosis factor (ligand) superfamily, member 10	*APO2L, Apo-2L, CD253, TL2, TRAIL*
FAS	7.10	Fas (TNF receptor superfamily, member 6)	*ALPS1A, APO-1, APT1, CD95, FAS1, FASTM, TNFRSF6*
BCL2L11	4.79	BCL2-like 11 (apoptosis facilitator)	*BAM, BIM, BOD*
CIDEA	4.31	Cell death-inducing DFFA-like effector a	*CIDE-A*
TNFRSF10A	3.88	Tumor necrosis factor receptor superfamily, member 10a	*APO2, CD261, DR4, TRAILR-1, TRAILR1*
TNFRSF21	3.61	Tumor necrosis factor receptor superfamily, member 21	*BM-018, CD358, DR6*
TRAF4	3.52	TNF receptor-associated factor 4	*CART1, MLN62, RNF83*
BCL2L10	3.44	BCL2-like 10 (apoptosis facilitator)	*BCL-B, Boo, Diva*
GADD45A	3.37	Growth arrest and DNA-damage-inducible, alpha	*DDIT1, GADD45*
TNFRSF10B	3.09	Tumor necrosis factor receptor superfamily, member 10b	*CD262, DR5, KILLER, KILLER, DR5, TRAIL-R2, TRAILR2, TRICK2, TRICK2A, TRICK2B, TRICKB, ZTNFR9*

Table 1 continued

GENE Symbol	**Fold change**	**Description**	**Gene Name**
BNIP3L	2.98	BCL2/adenovirus E1B 19kDa interacting protein 3-like	*BNIP3a, NIX*
TNFRSF25	2.83	Tumor necrosis factor receptor superfamily, member 25	*APO-3, DDR3, DR3, LARD, TNFRSF12, TR3, TRAMP, WSL-1, WSL-LR*
NOD1	2.43	Nucleotide-binding oligomerization domain containing 1	*CARD4, CLR7.1, NLRC1*
CD70	2.39	CD70 molecule	*CD27L, CD27LG, TNFSF7*
BCL10	2.27	B-cell CLL/lymphoma 10	*CARMEN, CIPER, CLAP, c-E10, mE10*
CASP2	2.27	Caspase 2, apoptosis-related cysteine peptidase	*CASP-2, ICH1, NEDD-2, NEDD2, PPP1R57*
CASP8	2.26	Caspase 8, apoptosis-related cysteine peptidase	*ALPS2B, CAP4, Casp-8, FLICE, MACH, MCH5*
BNIP1	2.06	BCL2/adenovirus E1B 19kDa interacting protein 1	*NIP1, SEC20, TRG-8*
TNFRSF9	1.94	Tumor necrosis factor receptor superfamily, member 9	*4-1BB, CD137, CDw137, ILA*
LTA	1.92	Lymphotoxin alpha (TNF superfamily, member 1)	*LT, TNFB, TNFSF1*
TP53BP2	1.92	Tumor protein P53 binding protein, 2	*53BP2, ASPP2, BBP, P53BP2, PPP1R13A*
FADD	1.83	Fas (TNFRSF6)-associated via death domain	*MORT1*
CASP6	1.71	Caspase 6, apoptosis-related cysteine peptidase	*MCH2*
CASP1	1.64	Caspase 1, apoptosis-related cysteine peptidase (interleukin 1, beta, convertase)	*ICE, IL1BC, P45*
CIDEB	1.58	Cell death-inducing DFFA-like effector b	-
ABL1	1.56	C-abl oncogene 1, non-receptor tyrosine kinase	*ABL, JTK7, bcr, abl, c-ABL, c-ABL1, p150, v-abl*
BNIP3	1.51	BCL2/adenovirus E1B 19kDa interacting protein3	*NIP3*

Table 1 continued

GENE Symbol	**Fold change**	**Description**	**Gene Name**
TNFSF8	1.46	Tumor necrosis factor (ligand) superfamily, member 8	*CD153, CD30L, CD30LG*
BAD	1.40	BCL2-associated agonist of cell death	*BBC2, BCL2L8*
BID	1.28	BH3 interacting domain death agonist	*FP497*
DFFA	1.27	DNA fragmentation factor, 45kDa, alpha polypeptide	*DFF-45, DFF1, ICAD*
BAX	1.26	BCL2-associated X protein	*BCL2L4*
BCLAF1	1.24	BCL2-associated transcription factor 1	*BTF, bK211L9.1*
CASP3	1.24	Caspase 3, apoptosis-related cysteine peptidase	*CPP32, CPP32B, SCA-1*
CASP10	1.18	Caspase 10, apoptosis-related cysteine peptidase	*ALPS2, FLICE2, MCH4*
BIK	1.16	BCL2-interacting killer (apoptosis-inducing)	*BIP1, BP4, NBK*
TRAF3	1.14	TNF receptor-associated factor 3	*CAP-1, CAP1, CD40bp, CRAF1, IIAE5, LAP1*
CFLAR	1.14	CASP8 and FADD-like apoptosis regulator	*CASH, CASP8AP1, CLARP, Casper, FLAME, FLAME-1, FLAME1, FLIP, I-FLICE, MRIT, c-FLIP, c-FLIPL, c-FLIPR, c-FLIPS*
DAPK1	1.08	Death-associated protein kinase 1	*DAPK*
TRADD	1.01	TNFRSF1A-associated via death domain	-
CASP14	1.00	Caspase 14, apoptosis-related cysteine peptidase	-
HRK	1.00	Harakiri, BCL2 interacting protein (contains only BH3 domain)	*DP5, HARAKIRI*
TNF	1.00	Tumor necrosis factor	*DIF, TNF-alpha, TNFA, TNFSF2*
TP73	1.00	Tumor protein p73	*P73*
CASP4	0.89	Caspase 4, apoptosis-related cysteine peptidase	*ICE(rel)II, ICEREL-II, ICH-2, Mih1, TX, TX*

Table 1 continued

GENE Symbol	**Fold change**	**Description**	**Gene Name**
PYCARD	0.79	PYD and CARD domain containing	*ASC, CARD5, TMS, TMS-1, TMS1*
CRADD	0.57	CASP2 and RIPK1 domain containing adaptor with death domain	*MRT34, RAIDD*

Table 1 listed above includes the 49 genes whose activations or over expressions lead to apoptosis, and vice versa, the down-expression means that the genes are inactive to DNA damage leading to apoptosis. The genes with fold number in red color indicated the over-expressed genes. Naturally, 19 genes with fold change larger than 2 indicate that $\Delta\Delta C_t$ (equals to $\Delta C_{t(treated)} - \Delta C_{t(control)}$) is smaller than -1.

Table 2. Fold changes of anti-apoptosis genes expression of HUVEC cells by Cr(IV)-DPO compared to the untreated cells.

GENE Symbol	**Fold change**	**Description**	**Gene Name**
NAIP	2.42	NLR family, apoptosis inhibitory protein	*BIRC1, NLRB1, psiNAIP*
CD27	2.15	CD27 molecule	*S152, S152. LPFS2, T14, TNFRSF7, Tp55*
BNIP2	1.96	BCL2/adenovirus E1B 19kDa interacting protein 2	*BNIP-2, NIP2*
BIRC3	1.95	Baculoviral IAP repeat containing 3	*AIP1, API2, CIAP2, HAIP1, HIAP1, MALT2, MIHC, RNF49, c-IAP2*
BCL2L1	1.90	BCL2-like 1	*BCL-XL, S, BCL2L, BCLX, BCLXL, BCLXS, Bcl-X, PPP1R52, bcl-xL, bcl-xS*
RIPK2	1.80	Receptor-interacting serine-threonine kinase 2	CARD3, CARDIAK, CCK, GIG30, RICK, RIP2

Table 2 continued

GENE Symbol	Fold change	Description	Gene Name
AKT1	1.76	V-akt murine thymoma viral oncogene homolog 1	AKT, CWS6, PKB, PKB-ALPHA, PRKBA, RAC, RAC-ALPHA
XIAP	1.71	X-linked inhibitor of apoptosis	API3, BIRC4, IAP-3, ILP1, MIHA, XLP2, hIAP-3, hIAP3
BFAR	1.67	Bifunctional apoptosis regulator	BAR, RNF47
BAG3	1.59	BCL2-associated athanogene 3	BAG-3, BIS, CAIR-1, MFM6
IGF1R	1.59	Insulin-like growth factor 1 receptor	CD221, IGFIR, IGFR, JTK13
BAG4	1.49	BCL2-associated athanogene 4	BAG-4, SODD
BCL2L2	1.28	BCL2-like 2	BCL-W, BCL2-L-2, BCLW, PPP1R51
BCL2	1.19	B-cell CLL/lymphoma 2	Bcl-2, PPP1R50
BRAF	1.15	V-raf murine sarcoma viral oncogene homolog B1	B-RAF1, BRAF1, NS7, RAFB1
BIRC8	1.00	Baculoviral IAP repeat containing 8	ILP-2, ILP2, hILP2
CD40LG	1.00	CD40 ligand	CD154, CD40L, HIGM1, IGM, IMD3, T-BAM, TNFSF5, TRAP, gp39, hCD40L
NOL3	0.90	Nucleolar protein 3 (apoptosis repressor with CARD domain)	ARC, FCM, MYP, NOP, NOP30
BIRC6	0.63	Baculoviral IAP repeat containing 6	APOLLON, BRUCE
BAG1	0.47	BCL2-associated athanogene	BAG-1, HAP, RAP46
MCL1	0.45	Myeloid cell leukemia sequence 1 (BCL2-related)	BCL2L3, EAT, MCL1-ES, MCL1L, MCL1S, Mcl-1, TM, bcl2-L-3, mcl1, EAT
BCL2A1	0.14	BCL2-related protein A1	ACC-1, ACC-2, BCL2L5, BFL1, GRS, HBPA1

Table 2 listed above includes the 22 genes whose activation or over expression means responding to defend the apoptosis process when DNA is damaged, and vice versa, the down-expressed genes failed to protect the HUVECs against the Cr(IV)-DPO treatment,

consequently leading to apoptosis. Genes with fold number highlighted in red indicated over-expressed genes, whereas genes with fold number highlighted in blue represented down-expressed genes. In this table four genes had fold change larger than 2, meaning their $\Delta\Delta C_t$ is smaller than -1, while three other genes had fold number small than 0.5 meaning their $\Delta\Delta C_t$ is bigger than 1.

Table 3. Fold changes of apoptosis regulation genes expression of HUVEC cells by Cr(IV)-DPO compared to the untreated cells.

GENE Symbol	Fold change	Description	Gene Name
CD40	4.70	CD40 molecule, TNF receptor superfamily member 5	*Bp50, CDW40, TNFRSF5, p50*
BAK1	2.72	BCL2-antagonist/killer 1	*BAK, BAK-LIKE, BCL2L7, CDN1*
CASP7	2.39	Caspase 7, apoptosis-related cysteine peptidase	*CASP-7, CMH-1, ICE-LAP3, LICE2, MCH3*
CARD6	1.96	Caspase recruitment domain family, member 6	*CINCIN1*
APAF1	1.85	Apoptotic peptidase activating factor 1	*APAF-1, CED4*
LTBR	1.82	Lymphotoxin beta receptor (TNFR superfamily, member 3)	*CD18, D12S370, LT-BETA-R, TNF-R-III, TNFCR, TNFR-RP, TNFR2-RP, TNFR3, TNFRSF3*
CARD8	1.78	Caspase recruitment domain family, member 8	*CARDINAL, DACAR, DAKAR, NDPP, NDPP1, TUCAN*
TRAF2	1.45	TNF receptor-associated factor 2	*MGC:45012, TRAP, TRAP3*
CASP9	1.45	Caspase 9, apoptosis-related cysteine peptidase	*APAF-3, APAF3, ICE-LAP6, MCH6, PPP1R56*
BIRC2	1.19	Baculoviral IAP repeat containing 2	*API1, HIAP2, Hiap-2, MIHB, RNF48, c-IAP1, cIAP1*
CASP5	1.00	Caspase 5, apoptosis-related cysteine peptidase	*ICE(rel)III, ICEREL-III, ICH-3*

Table 3 continued

GENE Symbol	Fold change	Description	Gene Name
TNFRSF1A	0.94	Tumor necrosis factor receptor superfamily, member 1A	*CD120a, FPF, MS5, TBP1, TNF-R, TNF-R-I, TNF-R55, TNFAR, TNFR1, TNFR1-d2, TNFR55, TNFR60, p55, p55-R, p60*
TNFRSF11B	0.36	Tumor necrosis factor receptor superfamily, member 11b	*OCIF, OPG, TR1*

Table 3 listed above includes 13 genes which regulated cellular apoptosis. Among these 13 genes, *CD40, BAK1*, and *CASP7* are significantly over-expressed and *CARD6* with fold change around 1.96 is regarded as near over-expressed. Only *TNFRSF11B* alone is down-regulated which might indicate that the pathway going through necrosis death of HUVECs caused by Cr(IV)-DPO treatment was inactive.

3.6.2. Responses to DNA repair genes due to the exposure of BEAS-2B cells to Cr(IV) by RT^2-PCR

Since it had been known that chromium damaged DNAs of cells, and consequently causes cancer when the damages could not be repaired, it is desirable to investigate how the gene expressions responding to DNA repair changed gradually over time upon exposure of Cr(IV)-DPO to cells. Therefore, the expression of DNA repair arrays that includes 84 genes were carried by RT^2-PCR by treating BEAS-2B cells with 5 μM Cr(IV)-DPO for 24r, 48 hr, and 72 hr. These 84 genes were classified into five groups: base excision repair genes (BER), nucleotide excision repair genes (NER), mismatch repair genes (MMR), double-strand break repair genes (DSB), and other DNA repair-related genes. With the completion of PCR, data were analyzed in the method stated before. For convenient visualization, each

gene expression variations between the treated group and the untreated control group were plotted as a bar graph, separated into five groups, as shown in Figures 11 through 13. Same as before, the gene with expression fold change larger than 1.91 was regarded as an over-expressed gene, and the gene with expression fold change smaller than 0.52 was regarded as a down-expressed gene compared to the untreated control.

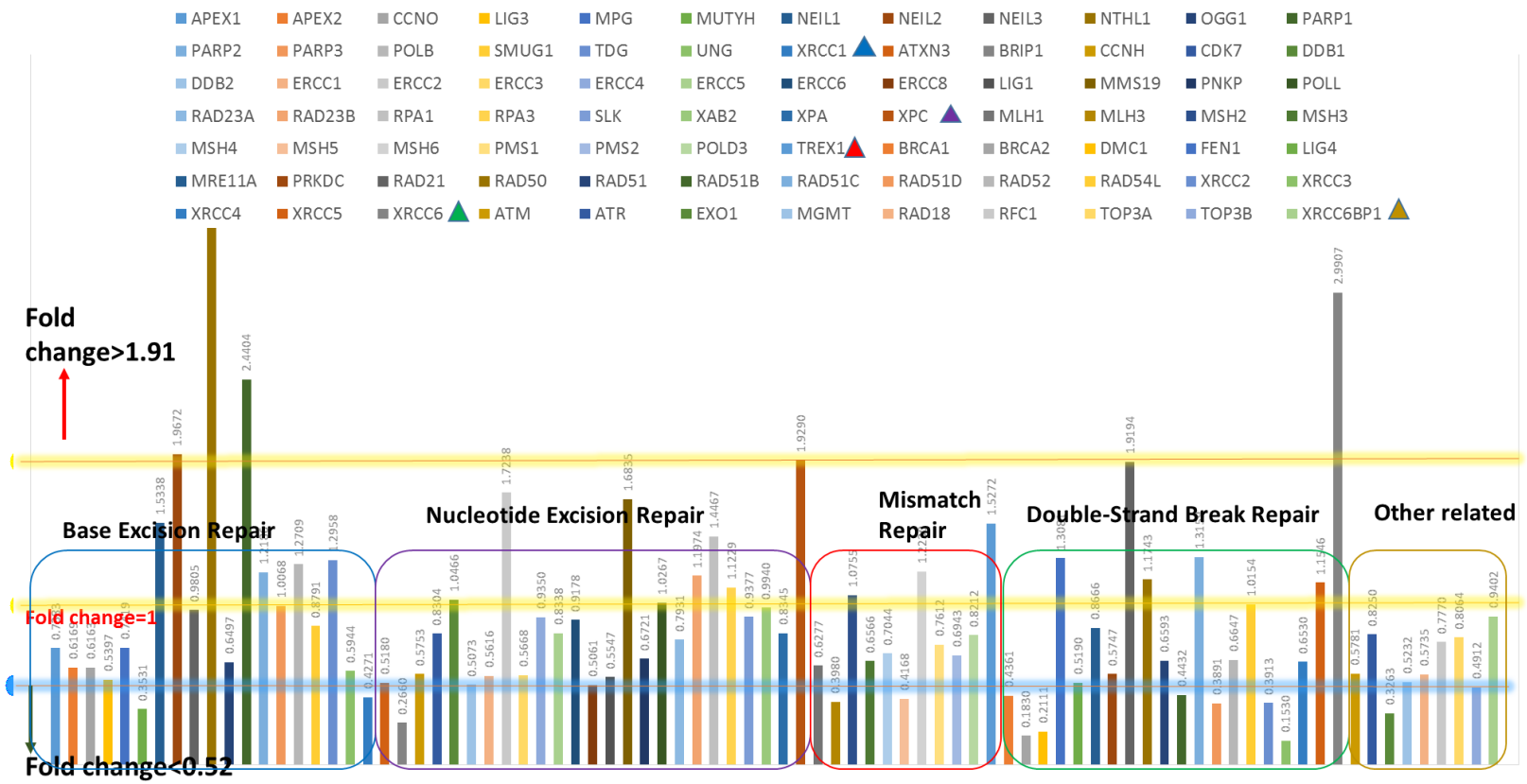

Figure 11. Fold changes of DNA repair genes expression (BEAS-2B cells) by Cr(IV)-DPO (5 μM 24hr treatment) compared to the untreated control

Figure 11 showed DNA repair gene expression fold change in BEAS-2B untreated control and treated cell groups after 24 hrs post 5 μM Cr(IV)-DPO treatment. Statistical analysis showed that 18 from these 84 DNA repair-related genes (*XRCC1, MUTYH, ATXN3, DDB2, ERCC8, BRIP1, MSH5, MLH3, LIG4, RAD51B, BRCA1, XRCC2, RAD51D, DMC1, BRCA2, XRCC3, TOP3B*, and *EXO1*) were down expressed. Further, they belong to all five groups, no specificity is shown. However, only 6 from these 84 genes were demonstrating over-expressed, they are *NTHL1, PARP1, NEIL2, XPC, XRCC6*, and *RAD21*. Genes *NTHL1, PARP1*, and *NEIL2* belong to base excision repair genes. *XPC* is a nucleotide excision repair gene. *XRCC6* and *RAD21* are double-strand break repair genes.

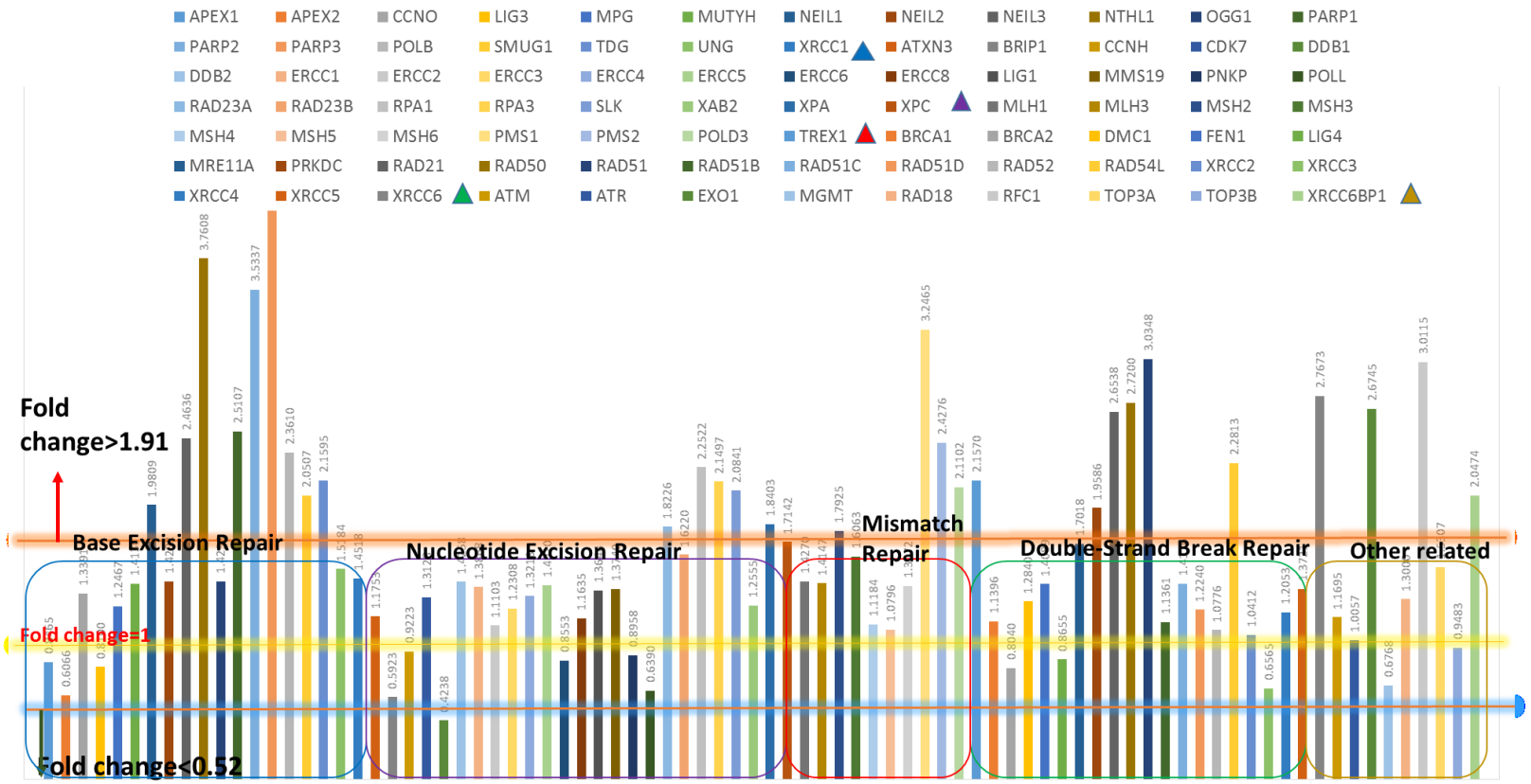

Figure 12. Fold changes of DNA repair genes expression (BEAS-2B cells) by Cr(IV)-DPO (5 μM 48hr treatment) compared to the untreated control

Figure 12 showed DNA repair gene expression fold change in BEAS-2B untreated control and treated cell groups after 24 hr post 5 μM Cr(IV)-DPO treatment. Among the 84 DNA repair-related genes, 18 genes (*PARP3, NTHL1, PARP2, PARP1, NEIL3, POLB, TDG, SMUG1, NEIL1, RPA1, RPA3, SLK, RAD51, XRCC6, RAD50, RAD21, RAD54L*, and *PRKDC*) were over-expressed. These 18 genes belong to all five groups of DNA repair genes indicating that DNA damage caused by Cr(IV)-DPO was diverse and mediated through complex mechanisms. Conversely 5 other DNA repair genes (*OGG1, SMUG1, MUTYH, APEX2*, and *DBB1*) were down-expressed which imply that were either not activated or suppressed under Cr(IV)-DPO treatment.

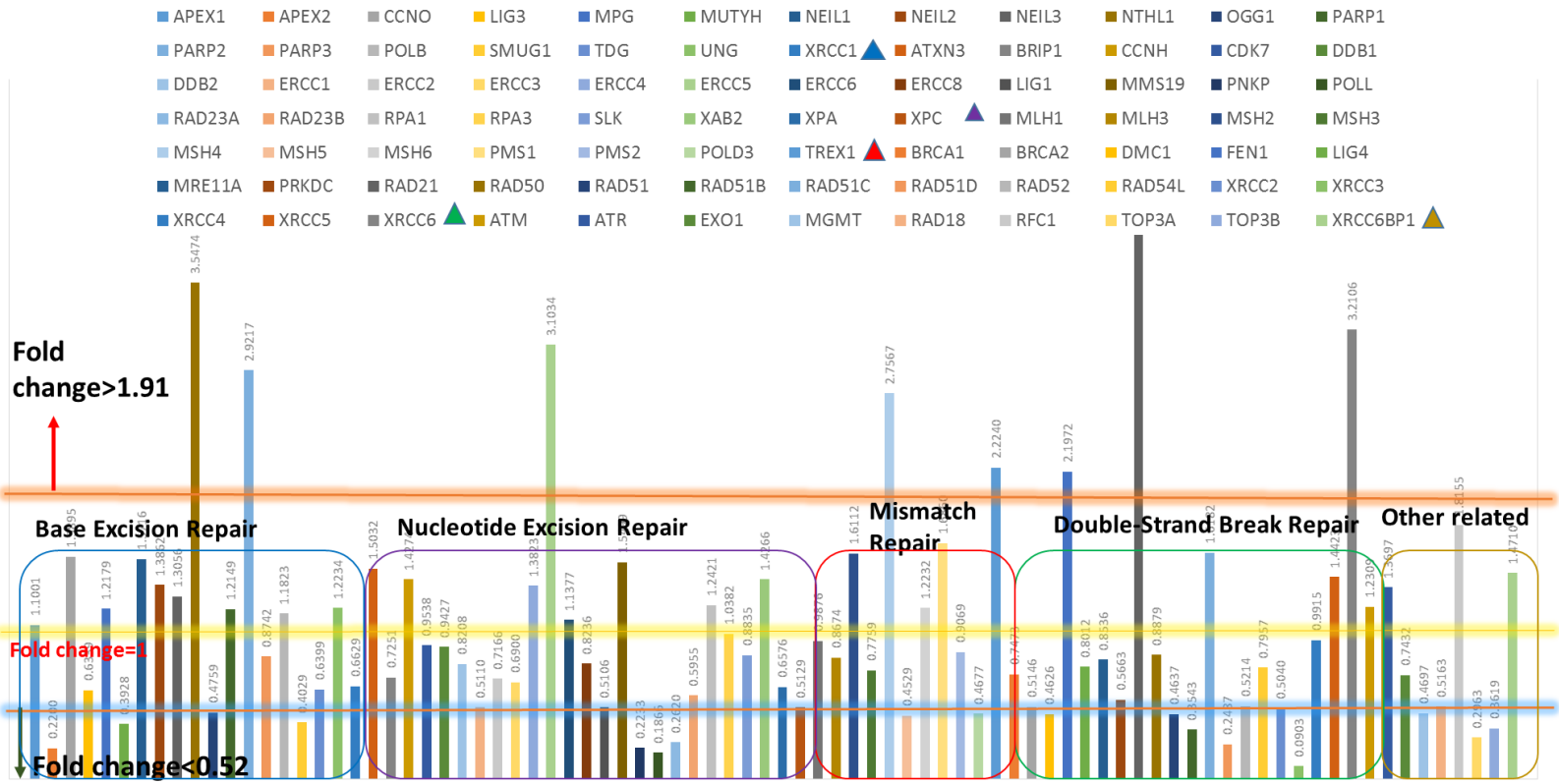

Figure 13. Fold changes of DNA repair genes expression (BEAS-2B cells) by Cr(IV)-DPO (5 µM 72hr treatment) compared to the untreated control

Similarly, Figure 13 is the column graph plotted based on the gene expression variations between the 5 μM-72 hr treated BEAS-2B cells and the untreated control BEAS-2B cells. Among these 84 DNA repair-related genes, 23 were down-expressed. They are *OGG1, SMUG1, MUTYH, APEX2, XPC, ERCC1, LIG1, RAD23A, PNKP, POLL, POLD3, MSH5, BRCA2, XRCC2, RAD51, DMC1, RAD51B, RAD51D, XRCC3, RAD18, MGMT, TOP3B,* and *TOP3A*. Six of these 84 genes were over-expressed; they are *NTHL1, PARP2, ERCC5, RAD21, XRCC6,* and *FEN1*.

Detailed information of the genes in five groups: Base excision repair genes, nucleotide excision repair genes, mismatch repair genes, double-stranded break repair genes, and other DNA repair-related genes, is listed in the Tables 4, 5, 6, 7, and 8.

Table 4. Changes in expression of base excision genes upon treatment of BEAS-2B cells with Cr(IV)-DPO (5 μM treated) compared to the untreated control group

Gene Symbol	**Base Excision Repair GENES Fold change of treated to control**			**Description**	**Gene Name**
	24 hr	**48 hr**	**72 hr**		
APEX1	0.74	0.85	1.10	APEX nuclease (multifunctional DNA repair enzyme) 1	*APE, APE1, APEN, APEX, APX, HAP1, REF1*
APEX2	0.62	0.61	0.22	APEX nuclease (apurinic/apyrimidinic endonuclease) 2	*APE2, APEXL2, XTH2*
CCNO	0.62	1.34	1.59	Cyclin O	*CCNU, UDG2*
LIG3	0.54	0.81	0.63	Ligase III, DNA, ATP-dependent	*LIG2*
MPG	0.74	1.25	1.22	N-methylpurine-DNA glycosylase	*AAG, ADPG, APNG, CRA36.1, MDG, Mid1, PIG11, PIG16,*
MUTYH	0.35	1.41	0.39	MutY homolog (E. coli)	*CYP2C, MYH*
NEIL1	1.53	1.98	1.57	Nei endonuclease VIII-like 1 (E. coli)	*FPG1, NEI1, hFPG1*

Table 4 continued

Gene Symbol	Base Excision Repair GENES Fold change of treated to control			Description	Gene Name
	24 hr	**48 hr**	**72 hr**		
NEIL2	1.97	1.43	1.39	Nei endonuclease VIII-like 2 (E. coli)	*NEH2, NEI2*
NEIL3	0.98	2.46	1.31	Nei endonuclease VIII-like 3 (E. coli)	*FGP2, FPG2, NEI3, hFPG2, hNEI3*
NTHL1	4.12	3.76	3.55	Nth endonuclease III-like 1 (E. coli)	*NTH1, OCTS3*
OGG1	0.65	1.43	0.48	8-oxoguanine DNA glycosylase	*HMMH, HOGG1, MUTM, OGH1*
PARP1	2.44	2.51	1.21	Poly (ADP-ribose) polymerase 1	*ADPRT, ADPRT 1, ADPRT1, ARTD1, PARP, PARP-1, PPOL, pADPRT-1*
PARP2	1.22	3.53	2.92	Poly (ADP-ribose) polymerase 2	*ADPRT2, ADPRTL2, ADPRTL3, ARTD2, PARP-2, pADPRT-2*
PARP3	1.01	4.38	0.87	Poly (ADP-ribose) polymerase family, member 3	*ADPRT3, ADPRTL2, ADPRTL3, ARTD3, IRT1, PADPRT-3*
POLB	1.27	2.36	1.18	Polymerase (DNA directed), beta	-
SMUG1	0.88	2.05	0.40	Single-strand-selective monofunctional uracil-DNA glycosylase 1	*FDG, HMUDG, UNG3*
TDG	1.30	2.16	0.64	Thymine-DNA glycosylase	*hTDG*
UNG	0.59	1.52	1.22	Uracil-DNA glycosylase	*DGU, HIGM4, HIGM5, UDG, UNG1, UNG15, UNG2*
XRCC1	0.43	1.45	0.66	X-ray repair complementing defective repair in Chinese hamster cells 1	*RCC*

Table 4 shows that fold change in base excision repair gene (BER) is variable among three treatment conditions. Normally base excision repair genes are activated to remove the small,

non-helix distorting base lesions caused by metal coordination or base oxidation to maintain the integrity of DNA structure. In Table 4, the numbers in red indicate over-expressed genes and the numbers in blue signify the down-regulated genes. Notably, the expression of many genes in the different treatment groups were not proportional to the exposure time of treatments. The expressions of *OGG1* and *MUTYH* are two "hot spots" as they are the two genes related to the 8-oxoguanine clean-up (one of the guanine oxidation products). *MUTYH* is a gene encoding a DNA glycosylase protein, which functions as an enzyme to excise the adenine bases from the DNA backbone when the adenines are wrongly paired with guanine, cytosine or 8-oxo-7,8-dihydroguanine. *OGG1* is a gene encoding the 8-hydroxyguanine DNA glycosylase protein, which functions as an enzyme to excise 8-oxoguanine. Hence, if the two genes were down-expressed, there was a high possibility that damaged guanine is not repaired and accumulated, and potentially might cause cancer.

Table 5. Changes in expression of nucleotide excision repair genes upon treatment of BEAS-2B cells with Cr(IV)-DPO (5 μM treated) compared to the untreated control group

Gene Symbol	**Nucleotide excision repair Genes Fold change of treated to control**			**Description**	**Gene Name**
	24 hr	**48 hr**	**72 hr**		
ATXN3	0.52	1.18	1.50	Ataxin 3	*AT3, ATX3, JOS, MJD, MJD1, RP11-529H20.5, SCA3*
BRIP1	0.27	0.59	0.73	BRCA1 interacting protein C-terminal helicase 1	*BACH1, FANCJ, OF*
CCNH	0.58	0.92	1.43	Cyclin H	*CAK, p34, p37*
CDK7	0.83	1.31	0.95	Cyclin-dependent kinase 7	*CAK1, CDKN7, HCAK, MO15, STK1, p39MO15*

Table 5 continued

Gene Symbol	Nucleotide excision repair Genes Fold change of treated to control			Description	Gene Name
	24 hr	48 hr	72 hr		
DDB1	1.05	0.42	0.94	Damage-specific DNA binding protein 1, 127kDa	*DDBA, UV-DDB1, XAP1, XPCE, XPE, XPE-BF*
DDB2	0.51	1.43	0.82	Damage-specific DNA binding protein 2, 48kDa	*DDBB, UV-DDB2*
ERCC1	0.56	1.39	0.51	Excision repair cross-complementing rodent repair deficiency, complementation group 1 (includes overlapping antisense sequence)	*COFS4, RAD10, UV20*
ERCC2	1.72	1.11	0.72	Excision repair cross-complementing rodent repair deficiency, complementation group 2	*COFS2, EM9, TTD, XPD*
ERCC3	0.57	1.23	0.69	Excision repair cross-complementing rodent repair deficiency, complementation group 3 (xeroderma pigmentosum group B complementing)	*BTF2, GTF2H, RAD25, TFIIH, XPB*
ERCC4	0.94	1.32	1.38	Excision repair cross-complementing rodent repair deficiency, complementation group 4	*ERCC11, FANCQ, RAD1, XPF*
ERCC5	0.83	1.40	3.10	Excision repair cross-complementing rodent repair deficiency, complementation group 5	*COFS3, ERCM2, UVDR, XPG, XPGC*
ERCC6	0.92	0.86	1.14	Excision repair cross-complementing rodent repair deficiency, complementation group 6	*ARMD5, CKN2, COFS, COFS1, CSB, RAD26, UVSS1*
ERCC8	0.51	1.16	0.82	Excision repair cross-complementing rodent repair deficiency, complementation group 8	*CKN1, CSA, UVSS2*

Table 5 continued

Gene Symbol	Nucleotide excision repair Genes Fold change of treated to control			Description	Gene Name
	24 hr	48 hr	72 hr		
LIG1	0.55	1.36	0.51	Ligase I, DNA, ATP-dependent	-
MMS19	1.68	1.37	1.55	MMS19 nucleotide excision repair homolog (S. cerevisiae)	*MET18, MMS19L, hMMS19*
PNKP	0.67	0.90	0.22	Polynucleotide kinase 3'-phosphatase	*EIEE10, MCSZ, PNK*
POLL	1.03	0.64	0.19	Polymerase (DNA directed), lambda	*BETAN, POLKAPPA*
RAD23A	0.79	1.82	0.26	RAD23 homolog A (S. cerevisiae)	*HHR23A, HR23A*
RAD23B	1.20	1.62	0.60	RAD23 homolog B (S. cerevisiae)	*HHR23B, HR23B, P58*
RPA1	1.45	2.25	1.24	Replication protein A1, 70kDa	*HSSB, MST075, REPA1, RF-A, RP-A, RPA70*
RPA3	1.12	2.15	1.04	Replication protein A3, 14kDa	*REPA3*
SLK	0.94	2.08	0.88	STE20-like kinase	*LOSK, STK2, bA16H23.1*
XAB2	0.99	1.26	1.43	XPA binding protein 2	*HCNP, HCRN, NTC90, SYF1*
XPA	0.83	1.84	0.66	Xeroderma pigmentosum, complementation group A	*XP1, XPAC*
XPC	1.93	1.71	0.51	Xeroderma pigmentosum, complementation group C	*RAD4, XP3, XPCC*

Table 5 shows that the fold change of the nucleotide excision repair gene (NER) varies among the three treatment conditions. Nucleotide excision repair genes are activated when some bulky helix-distorting DNA lesion is recognized. After the activation, a short single strand DNA segment or the base coordinated with the bulky compounds are removed, consequently a gap in the DNA sequence is formed, which is filled by the new synthesized DNA sequence. It is worth noting that several genes were becoming from down-regulated at 24 hr treatment to over-expressed after 48-hr Cr(IV)-DPO treatment, relative to untreated cells, indicating that many bulky DNA lesions occurred when BEAS-2B cells were treated with Cr(IV)-DPO for an extended length of time.

Table 6. Changes in expression of mismatch repair genes upon treatment of BEAS-2B cells with Cr(IV)-DPO (5 µM treated) compared to the untreated control group

Gene Symbol	**Mismatch repair GENES Fold change of treated to control**			**Description**	***Gene Name***
	24 hr	**48 hr**	**72 hr**		
MLH1	0.63	1.43	0.99	MutL homolog 1, colon cancer, nonpolyposis type 2 (E. coli)	*COCA2, FCC2, HNPCC, HNPCC2, hMLH1*
MLH3	0.40	1.41	0.87	MutL homolog 3 (E. coli)	*HNPCC7*
MSH2	1.08	1.79	1.61	MutS homolog 2, colon cancer, nonpolyposis type 1 (E. coli)	*COCA1, FCC1, HNPCC, HNPCC1, LCFS2*
MSH3	0.66	1.61	0.78	MutS homolog 3 (E. coli)	*DUP, MRP1*
MSH4	0.70	1.12	2.76	MutS homolog 4 (E. coli)	-
MSH5	0.42	1.08	0.45	MutS homolog 5 (E. coli)	*G7, MUTSH5, NG23*
MSH6	1.22	1.40	1.22	MutS homolog 6 (E. coli)	*GTBP, GTMBP, HNPCC5, HSAP, p160*
PMS1	0.76	3.25	1.69	PMS1 postmeiotic segregation increased 1 (S. cerevisiae)	*HNPCC3, PMSL1, hPMS1*
PMS2	0.69	2.43	0.91	PMS2 postmeiotic segregation increased 2 (S. cerevisiae)	*HNPCC4, PMS2CL, PMSL2*
POLD3	0.82	2.11	0.47	Polymerase (DNA-directed), delta 3, accessory subunit	*P66, P68*
TREX1	1.53	2.16	2.22	Three prime repair exonuclease 1	*AGS1, CRV, DRN3, HERNS*

Table 6 shows the fold change of the same mismatch repair gene varies among these three treatment conditions. Mismatch repair genes work when the base in daughter strand is not exactly matched to parent strand during DNA replication and recombination. These mis-matched bases, erroneous insertion or deletion are recognized and repaired to maintain the integrity and high-accuracy of DNA structure. Interestingly, the group with 5 µM-48 hr

treatment again show that most of the genes over-expressed which are barely seen in the other two treatment groups.

Table 7. Changes in expression of double-strand break repair genes upon treatment of BEAS-2B cells with Cr(IV)-DPO (5 μM treated) compared to the untreated control group

Gene Symbol	**Double-strand break repair genes Fold changes of treated to control**			**Description**	***Gene Name***
	24 hr	**48 hr**	**72 hr**		
RCA1	0.44	1.14	0.75	Breast cancer 1, early onset	*BRCAI, BRCC1, BROVCA1, IRIS, PNCA4,PPP1R53 PSCP, RNF53*
BRCA2	0.18	0.80	0.51	Breast cancer 2, early onset	*BRCC2, BROVCA2, FACD, FAD, FAD1, FANCB, FANCD, FANCD1, GLM3, PNCA2*
DMC1	0.21	1.28	0.46	DMC1 dosage suppressor of mck1 homolog, meiosis-specific homologous recombination (yeast)	*DMC1H, LIM15, dJ199H16.1*
FEN1	1.31	1.41	2.20	Flap structure-specific endonuclease 1	*FEN-1, MF1, RAD2*
LIG4	0.52	0.87	0.80	Ligase IV, DNA, ATP-dependent	-
MRE11A	0.87	1.70	0.85	MRE11 meiotic recombination 11 homolog A (S. cerevisiae)	*ATLD, HNGS1, MRE11, MRE11B*
PRKDC	0.57	1.96	0.57	Protein kinase, DNA-activated, catalytic polypeptide	*DNA-PKcs, DNAPK, DNPK1, HYRC, HYRC1, XRCC7, p350*
RAD21	1.92	2.65	4.45	RAD21 homolog (S. pombe)	*CDLS4, HR21, HRAD21, MCD1, NXP1, SCC1, hHR21*
RAD50	1.17	2.72	0.89	RAD50 homolog (S. cerevisiae)	*NBSLD, RAD502, hRad50*

Table 7 continued

Gene Symbol	Double-strand break repair genes Fold changes of treated to control			Description	*Gene Name*
	24 hr	**48 hr**	**72 hr**		
RAD51	0.66	3.03	0.46	RAD51 homolog (S. cerevisiae)	*BRCC5, HRAD51, HsRad51, HsT16930, MRMV2, RAD51A, RECA*
RAD51B	0.44	1.14	0.35	RAD51 homolog B (S. cerevisiae)	*R51H2, RAD51L1, REC2*
RAD51C	1.32	1.41	1.62	RAD51 homolog C (S. cerevisiae)	*BROVCA3, FANCO, R51H3, RAD51L2*
RAD51D	0.39	1.22	0.25	RAD51 homolog D (S. cerevisiae)	*BROVCA4, R51H3, RAD51L3, TRAD*
RAD52	0.66	1.08	0.52	RAD52 homolog (S. cerevisiae)	*RP11-359B12.2*
RAD54L	1.02	2.28	0.80	RAD54-like (S. cerevisiae)	*HR54, RAD54A, hHR54, hRAD54*
XRCC2	0.39	1.04	0.50	X-ray repair complementing defective repair in Chinese hamster cells 2	-
XRCC3	0.15	0.66	0.09	X-ray repair complementing defective repair in Chinese hamster cells 3	*CMM6*
XRCC4	0.65	1.21	0.99	X-ray repair complementing defective repair in Chinese hamster cells 4	-
XRCC5	1.15	1.37	1.44	X-ray repair complementing defective repair in Chinese hamster cells 5 (double-strand-break rejoining)	*KARP-1, KARP1, KU80, KUB2, Ku86, NFIV*
XRCC6	2.99	2.77	3.21	X-ray repair complementing defective repair in Chinese hamster cells 6	*CTC75, CTCBF, G22P1, KU70, ML8, TLAA*

Table 7 shows that double-strand breaks repair gene fold changes are variable among the three treatment conditions. Double-strand breaks repair genes are activated when the two strands of DNA molecules are damaged at the same time, and cannot serve as a template for repair. Both the two strands are removed. Double-strand lesions are formed when a metal, like platinum or chromium, bound to two or more bases from the two strands. Table 7 demonstrates some genes are over-expressed, indicating the hypothesis that with the treatment of Cr(IV)-DPO, the chromium was inserted into the grooves of DNA molecules and bound to the two strands, resulting in double-strand break DNA lesions.

Table 8. Changes in expression of other genes related to DNA repair upon treatment of BEAS-2B cells with Cr(IV)-DPO (5 µM treated) compared to the untreated control group

Gene Symbol	**Other GENES, Fold change of treated to control**			**Description**	***Gene Name***
	24 hr	**48 hr**	**72 hr**		
ATM	0.58	1.17	1.23	Ataxia telangiectasia mutated	*AT1, ATA, ATC, ATD, ATDC, ATE, TEL1, TELO1*
ATR	0.83	1.01	1.37	Ataxia telangiectasia and Rad3 related	*FCTCS, FRP1, MEC1, SCKL, SCKL1*
EXO1	0.33	2.67	0.74	Exonuclease 1	*HEX1, hExoI*
MGMT	0.52	0.68	0.47	O-6-methylguanine-DNA methyltransferase	-
RAD18	0.57	1.30	0.52	RAD18 homolog (S. cerevisiae)	*RNF73*
RFC1	0.78	3.01	1.82	Replication factor C (activator 1) 1, 145kDa	*A1, MHCBFB, PO-GA, RECC1, RFC, RFC140*
TOP3A	0.81	1.53	0.30	Topoisomerase (DNA) III alpha	*TOP3*
TOP3B	0.49	0.95	0.36	Topoisomerase (DNA) III beta	*TOP3B1*
XRCC6 BP1	0.94	2.05	1.47	XRCC6 binding protein 1	*KUB3*

Table 8 shows that fold change in expression of each DNA repair-related gene is variable among the three treatments. These genes represent DNA repair regulators. Table 8 shows that most of the regulatory genes were unchanged after 24 hr and 48 hr Cr(IV)-DPO treatments except for three genes (*EXO1, RFC1, XRCC6BP1*) that were over-expressed. A possible explanation is that these regulators were required when more repair genes were activated after 48 hr treatment to fix DNA lesions caused by the Cr(IV)-DPO treatment.

3.7. cDNA Sequencing results

Prepared cDNA samples from 5 μM-48 hr Cr(IV)-DPO-treated BEAS-2B and the untreated control BEAS-2B cells were sequenced in duplicate on an Ion PGM System™ (Ion Torrent™, Life Technologies®) using with Ion 316™ Chip kit v2. The data were retrieved and analyzed and Ion Reporter™ Software. Four vcf.(variant calling file) files, four bam files and four corresponding Excel files were exported after the analysis and processing, two for the untreated control samples and two for the 5 μM-48 hr Cr(IV)-DPO-treated samples. The vcf. files were uploaded to IGV (integrative genomics viewer) analysis software (Java) to view the sequence variants in the genes of three DNA-damage-related signaling pathways between the two treated samples and the two control samples. The three pathways are: the cellular apoptosis signaling pathway (129 genes), the DNA repair signaling pathway (104 genes), and the cell cycle signaling pathway (110 cell cycle checkpoints genes). Some of the genes were involved in multiple signaling pathways, but, in total, around 300 genes were viewed by the software and identified for the variants. The Figures showing the variants of each gene list for the four samples compared to the human genome (hg19) are listed as Figures 14-19. Information related to each significant variant

is listed in Table 9 through Table 12. Positions with sequence insertions were highlighted in blue, and positions with sequence deletions were highlighted in red.

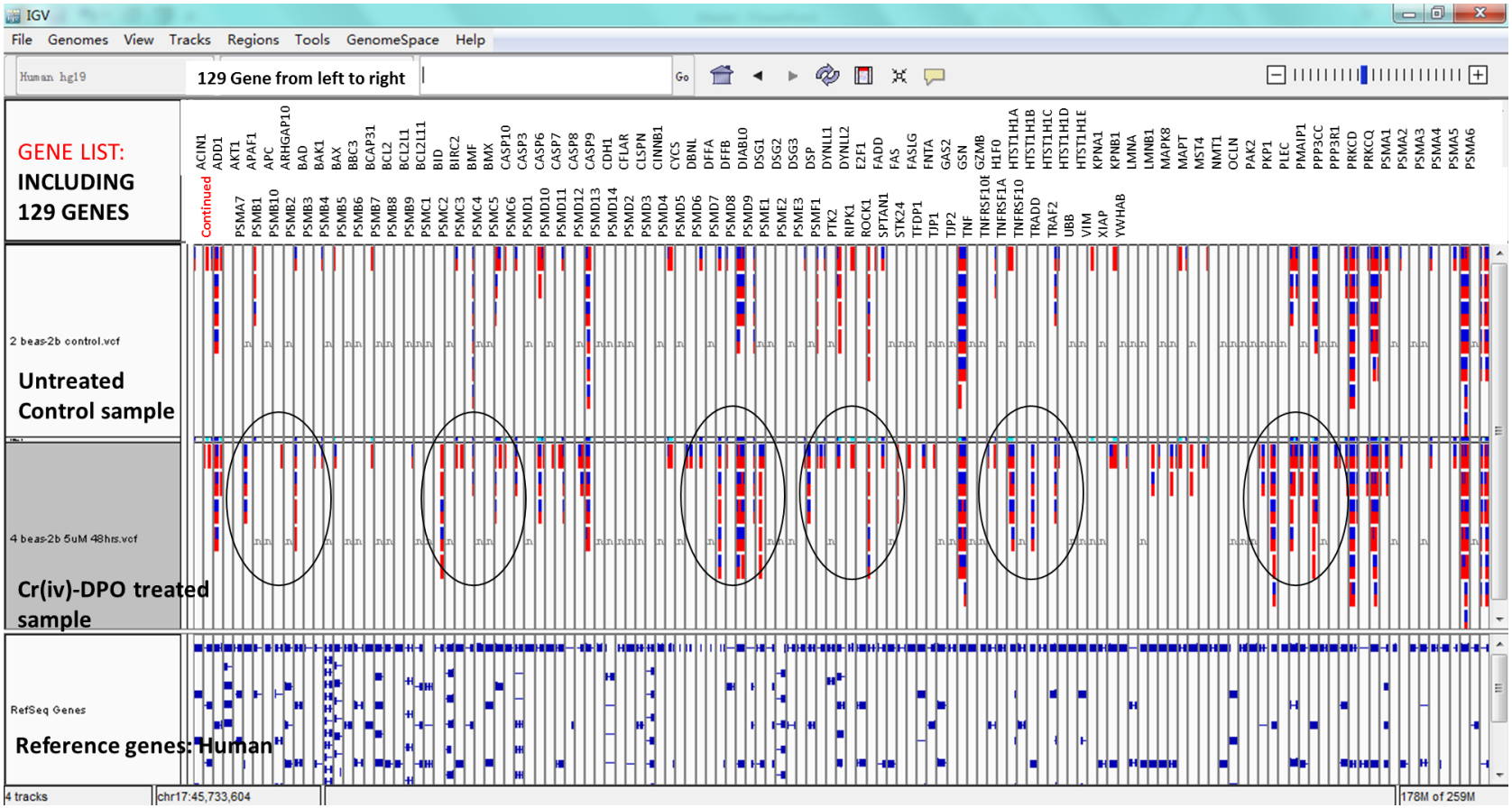

Figure 14. Gene sequence variants of control sample (sample#2) and Cr(IV)-DPO-treated sample (sample#4) of cellular apoptosis gene with reference to human genome library

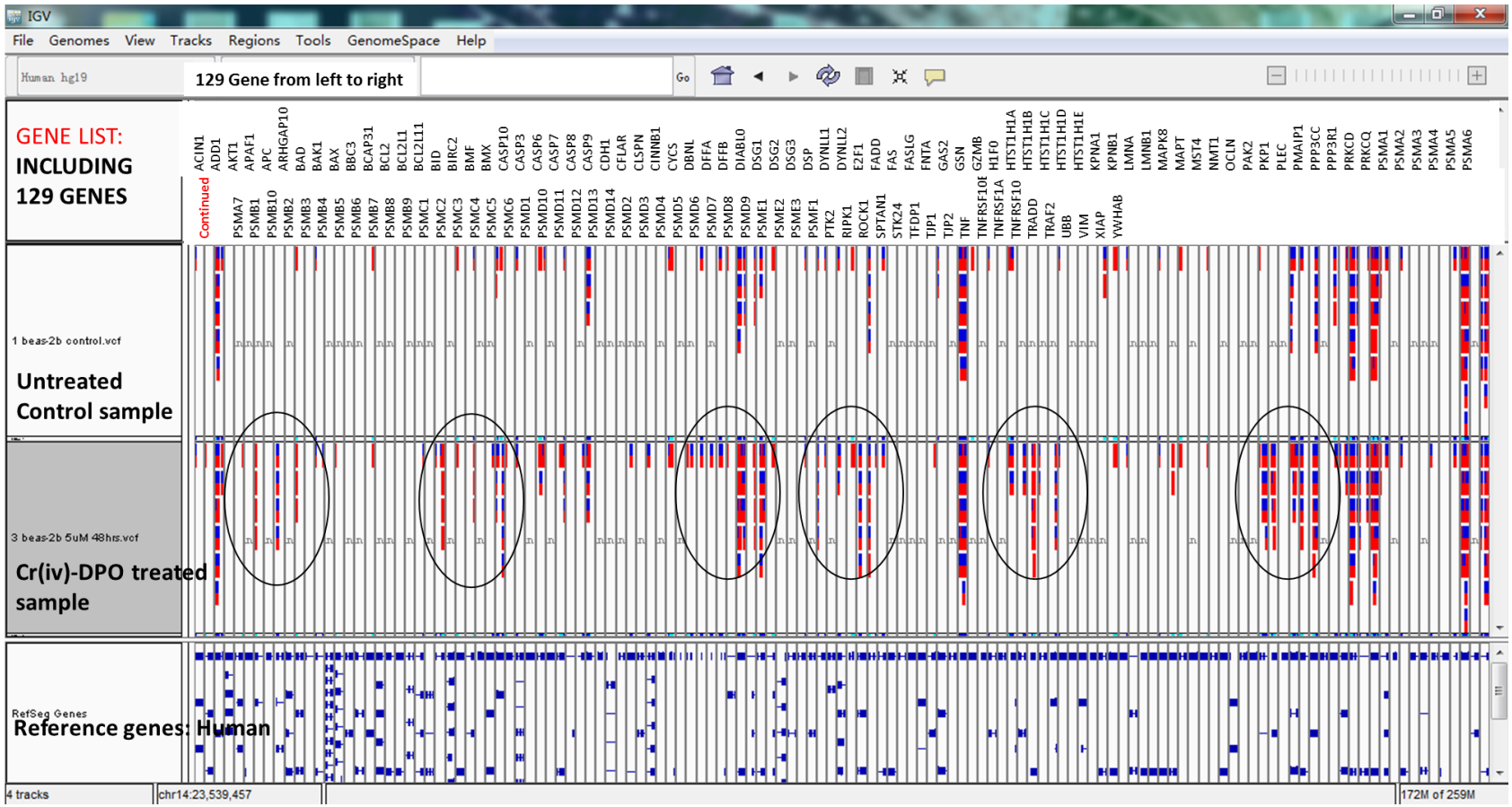

Figure 15. Gene sequence variants of control sample (sample#1) and Cr(IV)-DPO-treated sample (sample#3) of cellular apoptosis gene with reference to human genome library

Figure 14, that lists apoptotic genes, shows the variations between the variants of control sample (sample#2) and variants of treated sample (sample#4). Figure 15 shows the duplicate sequencing data (control sample (sample#1) compared to the treated sample (sample#3)). The blue color shows the length of inserts is small than expected based on the hg19 library and the red color shows the length of inserts is larger than expected. Each gene in the list of 129 genes was checked by localizing the position of each specific variant. Because many variants, coming from natural mutation occurrence, were detected in the control samples, all the variants of the treated samples and of the control samples were compared with each other to subtract the variants not caused by the Cr(IV)-DPO treatment. Some of the variant differences were neglected because their coverage was too low to be significant.

Table 9 lists the significant variants of 13 genes from the 129 apoptotic genes qualified to the requirements that the control sample didn't contain, but the treated samples did, or the variants in the control samples were too low (coverage<10) that they were eliminated, but those in the treated samples were high enough to be considered significant.

Table 9. Variants between the treated (5 μM, 48 hr treatment) and untreated control samples of the apoptotic genes

Position	Reference	Variant	Allele Call	Coverage
	1. ***AKT1*** chr14: 105,235,687-105,262,080			
105,236,506	T	A	Heterozygous	22
105,241,340	CCTGTAAAGCAGGGCTGG GTGAGCTGCCACCCCGCA CCCTCATCTCCACCCTGC CCCACCGCCCCGGCCCCA	-	Heterozygous	48
105,243,108	C	G	Homozygous	20
105,243,109	T	C	Homozygous	20

Table 9 continued

Position	Reference	Variant	Allele Call	Coverage
	2. ***BAX*** chr19: 49,458,117-49,465,055			
49,459,592	-	CCC	Heterozygous	15
49,464,971	G	A	Homozygous	11
	3. ***BCAP31*** chrX:152,965,947-152,990,201			
152,967,563	C	T	Homozygous	17
	4. ***E2F1*** chr20:32,263,292-32,274,210			
32,265,137	CTGGGTGGAAGCAGCA GGCAGGGTAAACTGAG GCCCAGGTGACCACCA GCCCAGCCCAGCCCAG CCCAGTTGGGCCCGGA GTTCCCAGATCTCAC	-	Heterozygous	47
	5. ***H1F0*** chr22: 38,201,114-38,203,443			
38,202,642	G	T	Homozygous	33
38,202,734	G	C	Homozygous	38
	6. ***KPNB1*** chr17: 45,727,204-45,761,004			
45,727,650	GGTAGGACGCAGGAGC CGGGGGTAGGGCTGAG GTGATTGGGGTGGGGG AGGGGAGGCCCGGCCC CTCTGACCCCGCTCCG TCTCCCACTTTCCTCC CCCTA	-	Homozygous	30
45,727,414	G	A	Heterozygous	38
45,730,245	G	T	Heterozygous	22
45,730,246	A	G	Heterozygous	18
45,730,246	A	T	Heterozygous	18
45,730,247	G	T	Heterozygous	17
45,730,248	T	G	Heterozygous	15
45,734,221	T	A	Heterozygous	12
45,734,222	G	C	Heterozygous	12
45,734,223	C	A	Heterozygous	12
45,734,223	C	T	Heterozygous	12
45,734,226	-	TCAAGAAC TAT	Heterozygous	15
45,734,225	G	T	Heterozygous	15
45,740,545	G	A	Homozygous	11
45,740,547	A	C	Heterozygous	10
45,740,549	G	C	Heterozygous	10
45,760,056	G	A	Heterozygous	21
45,760,551	G	T	Heterozygous	83
	7. ***LMNA*** chr1: 156,052,369-156,107,657			
156,106,185	T	C	Heterozygous	30
156,107,534	C	T	Heterozygous	26
	8. ***LMNB1*** chr5: 126,112,315-126,172,712			

Table 9 continued

Position	Reference	Variant	Allele Call	Coverage
126,140,625	G	T	Heterozygous	17
126,140,631	TC	-	Homozygous	14
126,140,639	A	C	Homozygous	14
126,140,642	-	TAG	Homozygous	13
126,140,644	T	G	Homozygous	12
126,140,645	G	C	Heterozygous	13
126,141,390	-	AGAT	Homozygous	40
126,141,390	T	A	Heterozygous	13
126,141,391	A	G	Heterozygous	13
126,141,393	C	T	Heterozygous	11
126,146,043	G	C	Heterozygous	16
126,146,043	G	T	Heterozygous	16
126,146,048	-	AATGCCAGA	Homozygous	12
126,146,048	C	A	Heterozygous	12
126,146,049	T	A	Heterozygous	11
126,146,050	C	G	Heterozygous	11
126,146,050	C	T	Heterozygous	11
126,171,999	T	C	Heterozygous	15
9. ***PPP3R1*** chr2: 68,405,989-68,479,651				
68,415,823	C	A	Heterozygous	15
68,415,823	C	G	Heterozygous	15
68,415,824	T	G	Heterozygous	15
68,415,825	A	G	Homozygous	12
68,413,597	T	A	Heterozygous	19
10. ***STK24*** chr13: 99,102,455-99,229,396				
99,118,818	G	T	Homozygous	10
99,118,820	A	G	Homozygous	10
99,118,822	C	G	Heterozygous	10
99,127,502	A	C	Heterozygous	10
99,134,504	C	T	Homozygous	10
99,134,507	-	TGGG	Heterozygous	13
99,134,506	A	G	Heterozygous	13
99,171,485	T	C	Heterozygous	31
11. ***TJP1*** chr15: 29,992,357-30,114,706				
30,034,841	C	G	Heterozygous	11
30,064,379	A	G	Homozygous	12
30,064,380	A	C	Homozygous	12
30,064,381	A	T	Homozygous	12
30,064,384	G	T	Heterozygous	12
30,011,276	C	T	Heterozygous	10
30,033,528	G	T	Heterozygous	11
30,033,529	T	C	Homozygous	11
30,033,532	T	G	Homozygous	11
30,033,533	A	G	Homozygous	12
30,033,643	-	GG	Homozygous	28

Table 9 continued

Position	Reference	Variant	Allele Call	Coverage
30,058,751	A	T	Heterozygous	10
30,064,256	A	C	Homozygous	10
30,064,257	A	T	Homozygous	10
30,064,258	G	T	Homozygous	14
30,064,259	A	C	Homozygous	15
30,064,261	A	T	Heterozygous	18
30,064,262	C	A	Heterozygous	21
30,064,265	A	C	Heterozygous	22
30,064,265	A	G	Heterozygous	22
30,064,267	-	TTCTAATTGT	Heterozygous	22
30,064,266	C	T	Heterozygous	22
30,064,372	A	C	Heterozygous	12
30,064,372	A	T	Heterozygous	12
30,064,376	G	T	Homozygous	10
30,064,378	-	TCCTTC	Homozygous	10
30,065,414	C	T	Heterozygous	10
30,065,418	G	C	Heterozygous	14
30,065,564	A	G	Heterozygous	12
30,065,565	A	T	Heterozygous	11
12. ***VIM*** chr10: 17,270,258-17,279,592				
17,271,991	C	A	Homozygous	14
17,271,992	T	G	Homozygous	14
17,271,994	C	A	Homozygous	14
17,272,716	A	T	Heterozygous	18
17,272,720	T	A	Heterozygous	12
17,272,721	C	A	Heterozygous	12
17,272,631	A	C	Homozygous	13
17,272,638	A	C	Homozygous	18
17,272,639	A	T	Homozygous	18
17,272,641	T	C	Heterozygous	18
17,272,643	T	G	Homozygous	22
17,272,644	T	G	Homozygous	22
17,272,645	T	A	Homozygous	23
17,272,723	C	G	Heterozygous	10
17,275,572	T	A	Homozygous	11
17,275,573	C	A	Homozygous	11
17,275,575	G	C	Homozygous	17
17,275,578	C	T	Homozygous	18
17,275,579	A	C	Homozygous	20
17,275,581	A	G	Homozygous	22
17,275,583	T	C	Homozygous	25
17,275,693	G	T	Heterozygous	11
17,275,694	A	G	Heterozygous	14
17,275,695	C	G	Heterozygous	14
17,275,696	T	A	Heterozygous	11

Table 9 continued

Position	Reference	Variant	Allele Call	Coverage
17,275,696	T	C	Heterozygous	11
17,275,931	G	T	Homozygous	21
17,275,933	A	T	Homozygous	20
17,275,935	G	C	Heterozygous	20
17,276,830	C	G	Heterozygous	16
17,276,835	A	-	Homozygous	15
17,276,835	A	G	Heterozygous	15
17,276,834	C	A	Heterozygous	15
17,276,836	G	A	Heterozygous	12
17,276,838	A	G	Homozygous	11
17,276,818	G	A	Homozygous	24
17,276,824	A	C	Homozygous	16
17,276,827	-	TGG	Homozygous	13
17,277,156	C	G	Heterozygous	10
17,277,158	C	G	Heterozygous	12
17,277,162	C	T	Heterozygous	18
17,277,391	A	C	Heterozygous	11
17,277,392	G	T	Heterozygous	13
17,277,394	G	C	Heterozygous	10
17,277,394	G	T	Heterozygous	10
17,277,395	A	C	Heterozygous	10
17,277,395	A	T	Heterozygous	10
17,277,396	A	T	Homozygous	10
17,278,384	T	A	Heterozygous	13
17,278,384	T	C	Heterozygous	13
17,278,386	T	A	Heterozygous	12
13. ***YWHAB*** chr20: 43,514,240-43,537,175				
43,514,538	C	A	Homozygous	17
43,514,539	G	T	Heterozygous	16
43,514,540	C	A	Heterozygous	15
43,514,541	G	A	Heterozygous	14
43,514,541	G	T	Heterozygous	14
43,514,542	G	A	Heterozygous	14
43,514,543	G	A	Heterozygous	12
43,514,386	C	G	Heterozygous	13
43,516,385	T	G	Heterozygous	10
43,516,389	T	A	Heterozygous	10
43,516,389	T	G	Heterozygous	10
43,530,153	T	G	Heterozygous	12
43,530,157	T	-	Heterozygous	15
43,530,157	T	C	Heterozygous	15
43,530,161	T	A	Heterozygous	24
43,530,161	T	C	Heterozygous	24
43,530,162	C	G	Heterozygous	26
43,530,166	T	C	Heterozygous	40

Table 9 continued

Position	Reference	Variant	Allele Call	Coverage
43,530,478	A	G	Heterozygous	24
43,530,480	A	G	Heterozygous	21
43,530,480	A	T	Heterozygous	21
43,530,481	G	T	Heterozygous	22
43,530,482	G	A	Heterozygous	19
43,530,483	C	A	Heterozygous	20
43,530,484	C	A	Heterozygous	20
43,530,486	G	A	Heterozygous	18
43,530,487	T	A	Heterozygous	15
43,530,488	G	A	Heterozygous	11
43,530,489	C	A	Heterozygous	11
43,532,615	A	T	Heterozygous	13
43,532,616	A	G	Heterozygous	18
43,532,626	T	A	Heterozygous	30
43,532,627	T	G	Heterozygous	33
43,532,628	T	G	Heterozygous	36
43,532,630	T	C	Heterozygous	39
43,532,632	A	-	Heterozygous	39
43,532,631	TA	CT	Heterozygous	39
43,532,760	A	G	Heterozygous	20
43,532,762	G	C	Heterozygous	16
43,532,763	T	G	Heterozygous	18
43,532,764	A	C	Heterozygous	14
43,533,601	T	A	Homozygous	12

Despite the low number of variants in the treated samples, we still concluded that DNA sequences were altered when BEAS-2B cells were treated with 5 μM Cr(IV)-DPO for 48 hr because the modifications were unique to the treated samples. Furthermore, the position for each specific alternation was identified. Among these 184 mutation positions listed in Table 9, when doing statistical analysis on each kind of mutations, the number of mutated T (thymine) is 43 (23.4%), the number of mutated G (Guanine) is 41 (22.3%); the number of mutated C (Cytosine) is 37 (20.1%), the number of mutated A (Adenine) is 46 (25.0%), the number of deleted sequence is 7 (3.8%) and the number of inserted sequence is 10 (5.4%). These observations seem to contradict the prevailing assumption that G was the most easily oxidized base by chromium complex. The rationale to explain this anomaly is

discussed in later part of the thesis. Moreover, the number of base alternation to T is 44 (23.9%), the number of base alternation to G is 42 (22.8%), the number of base alternation to C is 39 (21.2%), and the number of base alternation to A is 42 (22.8%).

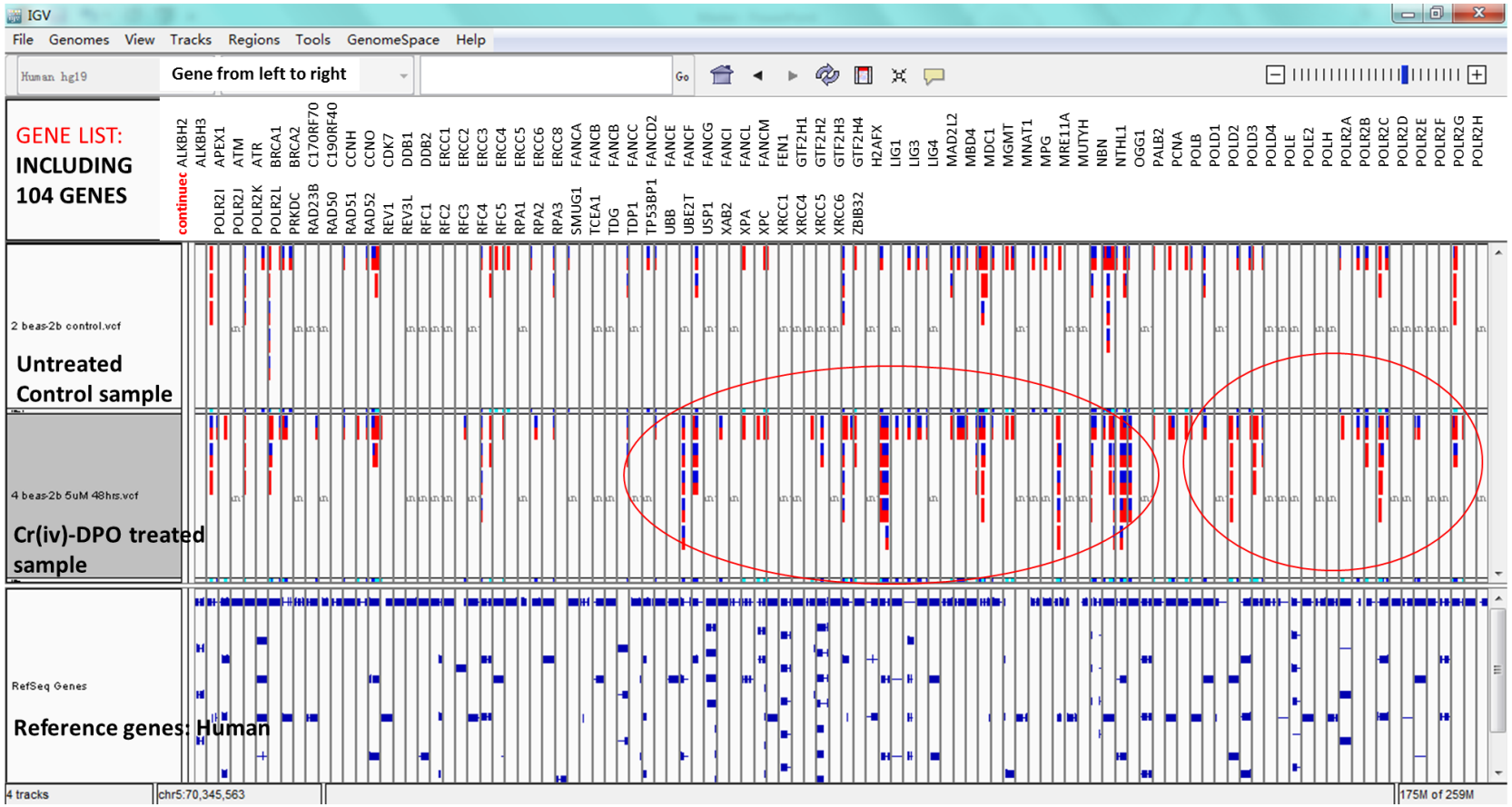

Figure 16. Gene sequence variants of control sample (sample#2) and Cr(IV)-DPO-treated sample (sample#4) of DNA repair with reference to human genome library

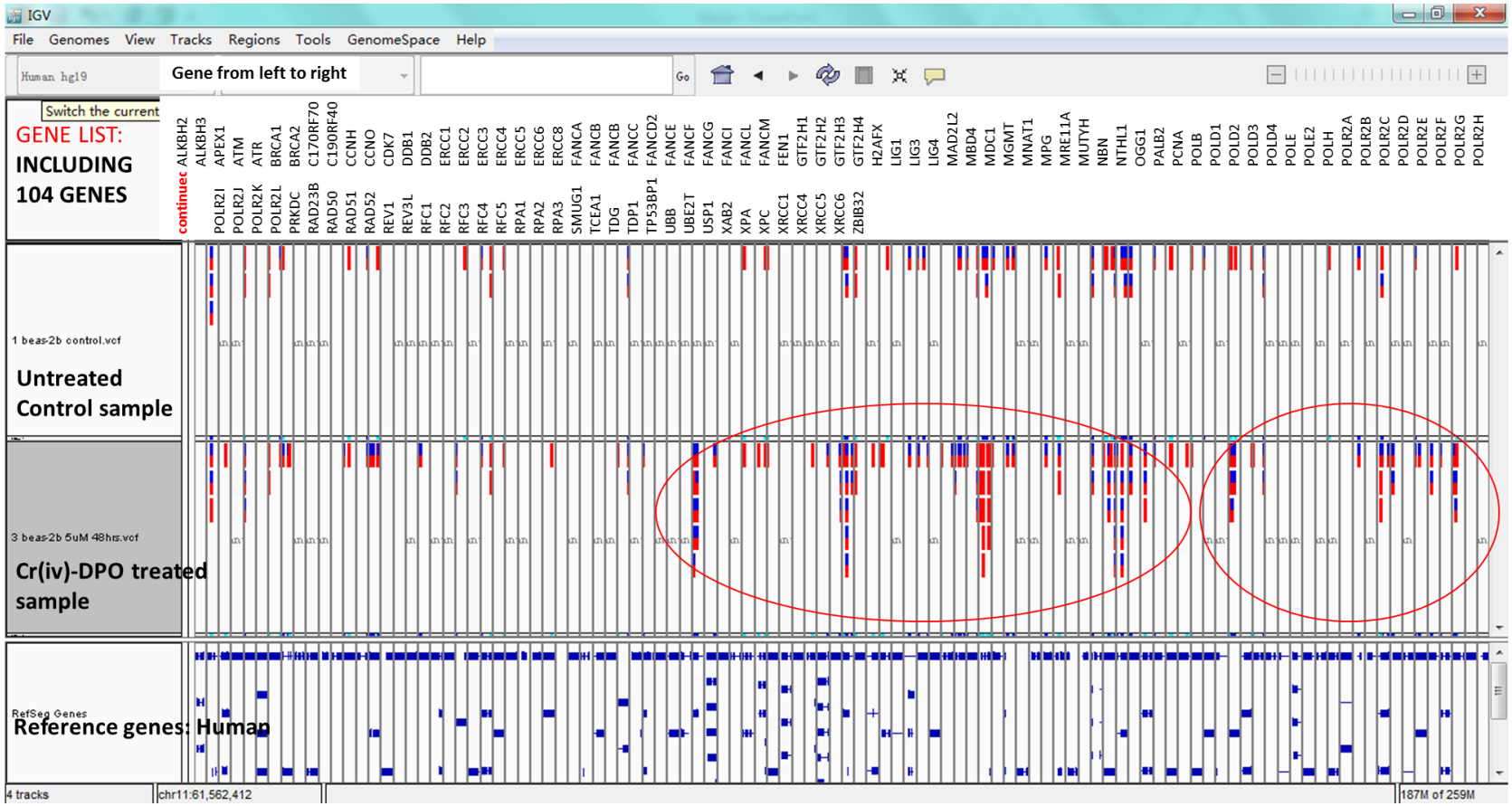

Figure 17. Gene sequence variants of control sample (sample#1) and Cr(IV)-DPO-treated sample (sample#3) of DNA repair with reference to human genome library

Figure 16, lists the DNA repair genes, and shows the variations between the control sample (sample#2) and the Cr(IV)-treated sample (sample#4). Figure 17 lists the DNA repair gene variations between variants of the control sample (sample#1) and variants of the Cr(IV)-treated sample (sample#3). Two control samples and two treated samples were sequenced to check the variants in duplicate. Similarly, the blue color shows the length of inserts is small than expected and the red color shows the length of inserts is larger than expected based on the hg19 library. Each gene in the DNA repair related gene list of 104 genes was checked by localizing the position of each variant. Because many variants in the control samples were also detected, the variants of treated samples and control samples were compared with each other to eliminate the same variants which were not caused by 5 μM Cr(IV)-DPO treatment but by natural mutations during sub-culture processes or by other factors. Notably, some of the variant differences were neglected in analysis because their coverage were too low to be significant.

Table 10 lists significant variants from 13 genes that are not present in control samples relative to Cr(IV)-treated samples, or the variants are too low in the control samples that they are neglected. On the other hand, the variants in treated samples are high enough to be considered significant.

Table 10. Variants between the treated (5 μM-48 hr treatment) and untreated control samples of the DNA repair genes

Position	Reference	Variant	Allele Call	Coverage
	1. ***ALKBH3*** Genomic Location: chr11:43,902,357-43,941,825			
43,919,026	A	C	Homozygous	13
43,919,038	A	G	Homozygous	17
43,919,053	C	T	Homozygous	21
Table 10 continued				
43,919,054	A	G	Homozygous	21
43,919,092	G	A	Homozygous	24
43,919,109	C	T	Homozygous	23
43,919,110	A	G	Homozygous	23
43,919,114	A	G	Homozygous	24
43,919,146	T	C	Homozygous	25
43,919,159	G	A	Homozygous	26
43,919,203	A	C	Homozygous	23
43,919,236	C	T	Homozygous	19
43,919,254	G	A	Homozygous	18
	2. ***BRCA2*** Genomic Location: chr13:32,889,617-32,973,809			
32,890,667	A	T	Heterozygous	13
32,890,669	T	A	Heterozygous	13
32,890,669	T	G	Heterozygous	13
	3. ***DDB1*** Genomic Location: chr11:61,066,919-61,100,684			
61,067,254	T	C	Heterozygous	15
	4. ***FANCC*** Genomic Location: chr9:97,861,336-98,079,991			
98,054,972	T	C	Homozygous	15
98,054,996	T	G	Homozygous	28
98,055,355	T	G	Homozygous	21
	5. ***GTF2H3*** Genomic Location: chr12:124,118,286-124,147,151			
124,146,392	C	A	Heterozygous	19
124,146,569	A	G	Heterozygous	59
124,146,597	A	G	Heterozygous	37
	6. ***MAD2L2*** Genomic Location: chr1:11,734,537-11,751,678			
11,740,535	G	T	Heterozygous	10
	7. ***MNAT1*** Genomic Location: chr14:61,201,459-61,435,398			
61,246,911	A	G	Homozygous	17
61,246,995	A	G	Homozygous	16
61,247,016	T	C	Homozygous	14
61,247,067	T	C	Homozygous	14
	8. ***PCNA*** Genomic Location: chr20:5,095,599-5,107,268			
5,096,009	CTGAAAGACAGGAAGA TGGTTAATTACTGAGG AGTATGTATCACATAT GACTACCTACAAAACA AGGTTCAAATTTATTA TCTTAC	-	Homozygous	43

Table 10 continued

Position	Reference	Variant	Allele Call	Coverage
5,099,324	CTACCAAAAGAAAGCA GATGCTTTTGAGAAAT ACTGACACAGAGTTTT GATTTTCTGTAGCTTC GTGACTCGGTAAAAA GGTACGACTTAC	-	Homozygous	36
5,100,447	T	C	Heterozygous	22
	9. ***POLB*** Genomic Location: chr8:42,195,972-42,229,326			
42,199,770	-	C	Homozygous	16
42,199,773	G	A	Homozygous	32
42,199,759	T	C	Homozygous	22
42,199,972	T	A	Homozygous	37
	10. ***POLD4*** Genomic Location: chr11:67,118,236-67,121,067			
67,119,282	C	T	Heterozygous	29
POLR2I	chr19:36,604,611-36,606,206			
36,605,616	CTGTGGGGAGGGGGAG GTGCCAGGGGTTAGTTC TGGAGCCATTCCTCG CCCGCCTTCTAACATCAC CCGCTCCCTCCGCCTCAC	-	Homozygous	39
	11. ***PRKDC*** Genomic Location: chr8:48,685,669-48,872,743			
48,805,817	-	G	Homozygous	16
	12. ***REV1*** Genomic Location: chr2:100,016,938-100,106,480			
100,058,870	C	T	Homozygous	17
	13. ***RPA1*** Genomic Location: chr17:1,733,273-1,802,848			
1,800,932	T	C	Heterozygous	28
1,800,949	C	G	Heterozygous	32
1,800,950	G	A	Heterozygous	32
1,801,189	C	T	Heterozygous	21

Although there were very few variants (43 variants), compared to the whole variants detected by the cDNA sequencing, we still concluded that DNA molecules were mutated when BEAS-2B cells were treated with 5 μM Cr(IV)-DPO for 48 hr because 13 genes were found mutated (in Table 10). Among these 43 mutation positions listed in the table, the number of mutated T (thymine) is 13 (30.2%), the number of mutated G (Guanine) is 6 (14.0%); the number of mutated C (Cytosine) is 8 (18.6%), the number of mutated A (Adenine) is 11 (25.6%), the number of deleted sequence is 3 (7.0%) and the number of

inserted sequence is 2 (4.7%). These results show that, instead of the guanine (G), thymine (A) seemed to be the most mutated bases under the influence of Cr(IV)-DPO. Furthermore, the number of base alternation to T is 8 (18.6%), the number of base alternation to G is 12 (27.9%), the number of base alternation to C is 10 (23.3%), and the number of base alternation to A is 8 (18.6%).

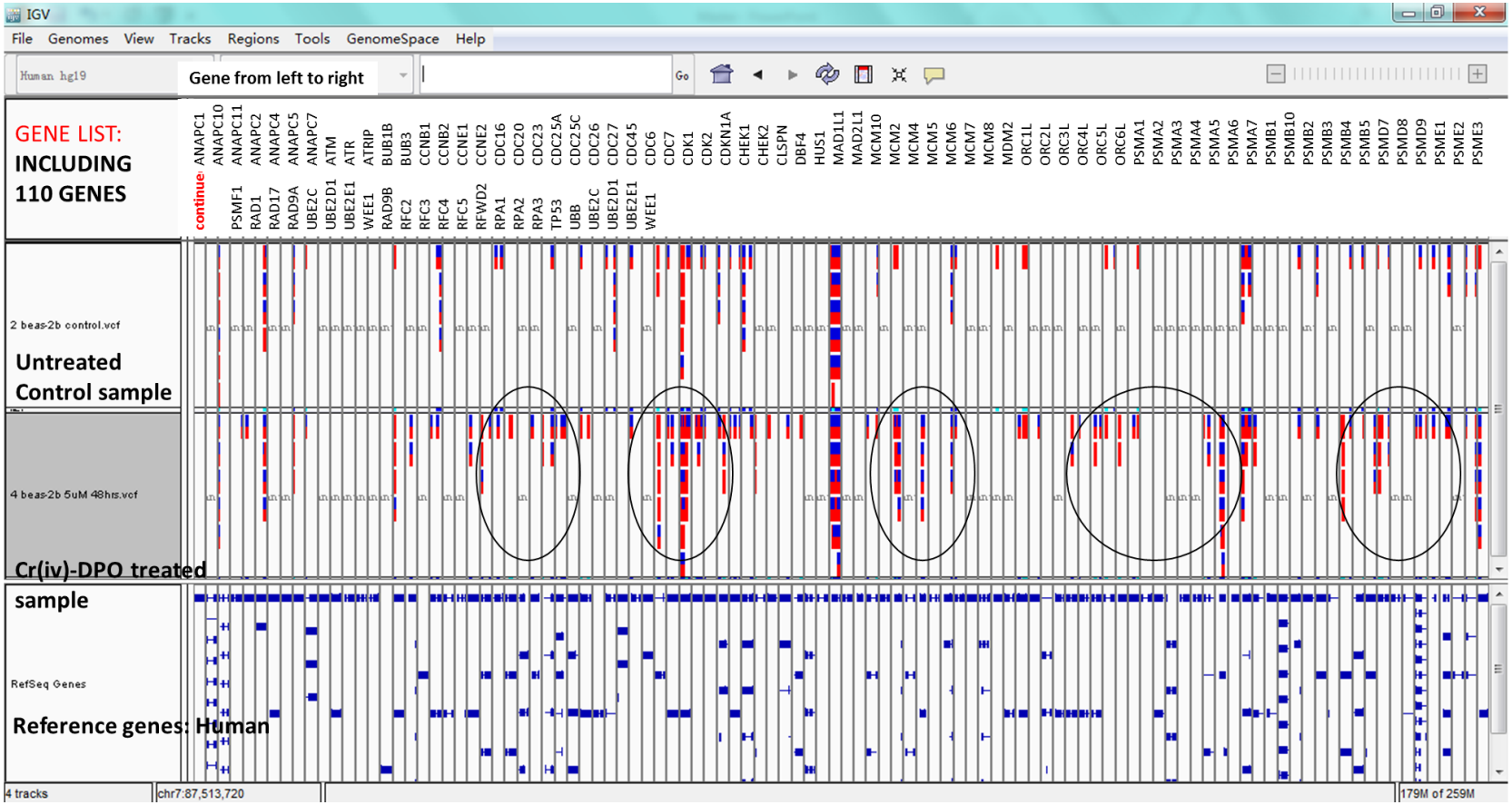

Figure 18. Gene sequence variants of control sample (sample#2) and Cr(IV)-DPO-treated sample (sample#4) of cell cycle checkpoints with reference to human genome library

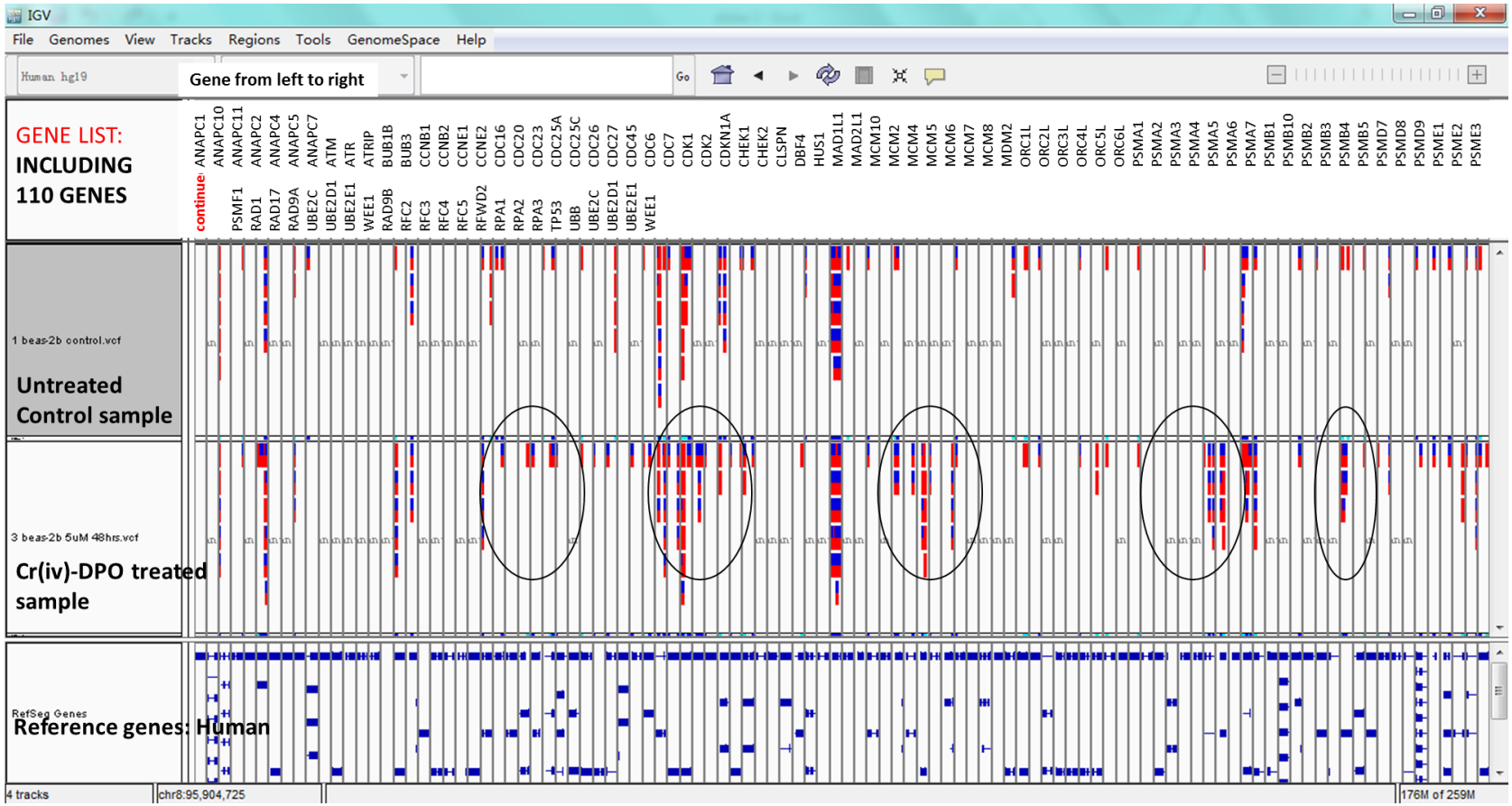

Figure 19. Gene sequence variants of control sample (sample#1) and Cr(IV)-DPO-treated sample (sample#3) of cell cycle checkpoints with reference to human genome library

Figure 18 shows the cellular cycle checkpoint gene list of variants from control sample (sample#2) and variants of treated sample (sample#4). Figure 19 displays cellular cycle checkpoint gene list of variants from control sample (sample#1) and variants of treated sample (sample#3). Two control samples and two treated samples were sequenced to check the variants in duplicates. The blue color shows the length of inserts is small than expected and the red color shows the length of inserts is larger than expected. Each gene in the DNA repair related gene list (110 genes) was checked by localizing the position of each variant. Because, as the Figure shows, many variants in the control samples were also detected, the variants of treated samples and control samples were compared with each other to eliminate the same variants which were not caused by 5 μM Cr(IV)-DPO treatment but by natural mutations during sub-culture processes or by other factors. Some of the variant differences were neglected because their coverage were too low to be significant.

Table 11 lists significant variants of 14 genes that control samples didn't contain but the treated samples did or the variants in control samples were too low that they were neglected but in treated samples were high enough to be considered significant.

Table 11. Variants between the treated (5 μM-48 hr treatment) and untreated control samples of the cell cycle checkpoints genes

Position	Reference	Variant	Allele Call	Coverage
1. ***ANAPC11*** chr17:79,847,780-79,856,544				
79,848,556	G	A	Heterozygous	21
79,848,556	G	T	Heterozygous	21
79,848,557	T	A	Heterozygous	25
79,848,559	-	AGCGT	Heterozygous	14
79,848,559	-	CAAAT	Heterozygous	14
79,848,558	C	A	Absent	14
79,848,558	C	T	Absent	14
79,848,559	T	G	Heterozygous	23
79,848,561	T	G	Homozygous	28

Table 11 continued

Position	Reference	Variant	Allele Call	Coverage
79,848,563	A	T	Homozygous	29
79,848,554	T	G	Heterozygous	16
79,848,698	T	C	Heterozygous	20
79,847,209	G	A	Heterozygous	37
79,847,210	G	A	Heterozygous	37
79,848,701	A	G	Heterozygous	20
79,848,702	G	A	Heterozygous	14
79,848,702	T	A	Heterozygous	14
79,848,703	G	A	Heterozygous	12
2. ***ANAPC5*** chr12:121,746,048-121,792,012				
121,785,688	T	G	Heterozygous	13
121,785,689	G	A	Heterozygous	13
121,785,690	T	G	Homozygous	12
121,785,691	A	C	Heterozygous	13
3. ***CDKN1A*** chr6:36,644,237-36,655,116				
36,654,209	G	A	Heterozygous	15
36,654,213	G	A	Heterozygous	15
4. ***MCM4*** chr8:48,872,763-48,890,719				
48,874,241	G	C	Homozygous	18
48,874,246	T	C	Heterozygous	14
48,874,248	-	AC	Heterozygous	11
48,874,247	G	C	Heterozygous	11
48,874,248	T	C	Heterozygous	14
48,874,249	C	T	Heterozygous	14
48,874,610	T	C	Heterozygous	14
48,874,778	T	A	Heterozygous	14
48,874,785	G	A	Heterozygous	20
48,874,786	C	T	Heterozygous	20
48,874,784	T	-	Heterozygous	10
48,874,783	AT	GA	Heterozygous	10
48,874,789	T	A	Heterozygous	15
48,874,850	T	A	Heterozygous	14
48,874,851	G	C	Heterozygous	14
48,874,854	T	A	Heterozygous	17
48,874,854	T	C	Heterozygous	17
48,874,856	-	GCAG	Heterozygous	16
48,874,855	T	G	Heterozygous	16
48,874,862	T	C	Heterozygous	19
48,874,860	T	A	Homozygous	15
48,874,861	G	C	Homozygous	15
48,874,862	T	G	Homozygous	15
48,874,863	A	G	Homozygous	15
48,874,967	G	T	Heterozygous	14
48,874,968	T	A	Heterozygous	14
48,874,969	G	T	Homozygous	27
48,874,970	A	T	Heterozygous	28

Table 11 continued

Position	Reference	Variant	Allele Call	Coverage
48,874,971	G	T	Heterozygous	28
48,874,974	A	T	Homozygous	25
48,874,978	G	T	Homozygous	19
48,874,983	A	G	Homozygous	18
48,875,420	G	A	Heterozygous	19
48,875,420	G	T	Heterozygous	19
48,875,425	C	G	Homozygous	15
48,875,426	A	T	Homozygous	16
48,875,427	A	T	Heterozygous	15
48,875,501	C	G	Heterozygous	12
48,875,314	C	A	Heterozygous	12
48,875,314	C	G	Heterozygous	12
48,875,316	-	AAAGAAA	Heterozygous	14
48,875,315	C	A	Heterozygous	14
48,875,320	A	T	Homozygous	18
48,875,321	A	C	Homozygous	19
48,875,431	C	A	Heterozygous	15
48,875,431	C	G	Heterozygous	15
48,875,602	T	A	Homozygous	16
48,875,604	A	G	Homozygous	16
48,875,605	G	T	Homozygous	16
48,875,606	A	T	Homozygous	16
48,875,610	T	A	Heterozygous	13
48,875,610	T	C	Heterozygous	13
48,879,919	C	A	Heterozygous	12
48,879,920	T	A	Heterozygous	12
48,879,921	T	G	Heterozygous	13
48,879,924	-	GAT	Heterozygous	13
48,879,923	A	T	Heterozygous	13
5. ***PSMA7*** chr20:60,711,783-60,718,514				
60,712,416	T	A	Heterozygous	27
60,712,414	G	T	Heterozygous	21
60,712,407	A	T	Heterozygous	12
60,712,413	T	G	Heterozygous	19
60,713,219	A	G	Heterozygous	18
60,713,219	A	T	Heterozygous	18
60,713,220	A	G	Heterozygous	18
60,712,016	A	G	Heterozygous	14
60,712,016	A	T	Heterozygous	14
60,712,017	A	G	Heterozygous	14
60,712,411	G	C	Homozygous	14
60,712,412	G	A	Homozygous	14
60,713,222	CTT	ACC	Homozygous	17
60,713,349	A	T	Homozygous	25
60,713,351	A	T	Homozygous	22
60,713,352	A	C	Homozygous	25
60,713,368	T	C	Heterozygous	11

Table 11 continued

Position	Reference	Variant	Allele Call	Coverage
60,713,370	A	G	Heterozygous	11
60,713,371	C	A	Heterozygous	11
60,713,373	T	G	Heterozygous	10
60,714,116	-	GAC	Heterozygous	15
60,714,115	T	C	Heterozygous	15
60,714,116	T	A	Heterozygous	19
60,714,124	A	C	Homozygous	30
60,714,126	C	T	Homozygous	30
60,714,128	C	G	Homozygous	35
60,714,129	A	G	Homozygous	35
60,714,256	A	-	Heterozygous	36
60,714,256	-	GCTTC	Heterozygous	36
60,714,259	A	T	Heterozygous	34
60,714,271	A	G	Heterozygous	13
60,714,830	C	T	Heterozygous	23
60,714,976	G	C	Heterozygous	21
60,714,970	A	C	Heterozygous	19
60,714,970	A	G	Heterozygous	19
60,714,971	A	C	Heterozygous	19
60,714,983	T	A	Heterozygous	12
60,714,985	-	CCGCA	Heterozygous	8
60,716,004	T	G	Heterozygous	25
60,716,005	A	C	Heterozygous	21
60,716,006	A	G	Heterozygous	21
60,716,006	A	T	Heterozygous	21
60,716,008	T	G	Heterozygous	13
60,716,010	A	C	Heterozygous	12
60,718,252	C	T	Heterozygous	13
60,718,253	C	T	Heterozygous	14
60,718,260	T	C	Heterozygous	21
	6. ***PSMB4*** chr1:151,372,041-151,374,412			
151,373,065	G	C	Homozygous	18
151,374,107	G	T	Heterozygous	14
151,374,108	T	G	Heterozygous	14
	7. ***PSMD9*** chr12:122,326,637-122,355,771			
122,341,014	G	C	Heterozygous	9
122,341,017	-	AC	Heterozygous	8
122,341,018	G	A	Heterozygous	7
122,353,851	G	C	Heterozygous	7
122,353,853	A	G	Heterozygous	6
122,353,854	A	C	Heterozygous	6
122,353,856	G	A	Heterozygous	6
122,353,857	T	C	Heterozygous	6
122,353,860	C	-	Heterozygous	6
122,353,862	G	A	Heterozygous	6
122,353,865	T	C	Heterozygous	6

Table 11 continued

Position	Reference	Variant	Allele Call	Coverage
	8. ***PSME1*** chr14:24,605,378-24,608,176			
24,606,348	A	C	Homozygous	7
24,606,349	C	A	Homozygous	9
24,606,344	A	G	Homozygous	10
24,606,345	C	T	Homozygous	12
24,606,416	T	A	Homozygous	8
24,606,417	A	G	Heterozygous	9
24,606,526	C	A	Heterozygous	10
24,606,527	C	A	Heterozygous	10
24,606,641	G	A	Heterozygous	10
24,606,642	C	G	Heterozygous	9
24,606,652	A	T	Heterozygous	8
24,607,680	C	G	Heterozygous	8
24,606,639	AGGCAAGCTGGGAAGACCTGG GAGAAGGGATCCAACTATGGGG GTAATCAACCTTAGTCCTGACTC TCATGAGCTCCTCTCTTTCTGC	-	Homozygous	32
24,607,325	AGGTGAGAGCGCTGCCCCACTT CCCTGCTCTTTTCTAGTCCATG CTTCCTTCCACTTTCCCCCTTGCT TTTTTTCCCT	-	Homozygous	52
24,607,402	T	C	Heterozygous	11
24,607,473	GTGAGTGACCACCCATGTG CACACTGTTTTTGTTTT GGGAGACCTCCTTCTTCTA CTCCATACACACTTCTCCT TCCACAG	-	Homozygous	37
24,607,682	-	TGT	Heterozygous	10
24,607,681	A	T	Heterozygous	10
24,607,771	-	C	Heterozygous	7
	9. ***PSME3*** chr17:40,985,159-40,995,777			
40,990,229	C	T	Heterozygous	8
40,990,237	G	C	Heterozygous	7
40,993,945	TAAT	-	Heterozygous	20
	10. ***PSMF1*** chr20:1,093,906-1,148,426			
1,106,143	G	A	Heterozygous	16
1,099,329	A	G	Homozygous	8
1,099,523	T	G	Homozygous	11
1,106,143	G	A	Heterozygous	7
1,106,295	-	AA	Heterozygous	7
1,106,296	G	A	Heterozygous	7
1,106,297	A	T	Heterozygous	7
1,106,299	T	G	Homozygous	7

Table 11 continued

Position	Reference	Variant	Allele Call	Coverage
11. ***RFC4*** chr3:186,507,682-186,524,484				
186,508,044	CCTATAATAAAAAAAACTT TTGGTATGATGACTTAATAT TCCTTTCCCCAAAGTTAGTA AGCTGACTTTA	-	Homozygous	28
186,510,400	CTGTGGAAGATGAGAAAAA CCAAGTTGGTGTCTAAAGAA AGAATTTCCCCAAAAGAA CTCATTTTTATCAAGAACAAA TCAAGATTTGATGGAGGAAAA ATTAATGTAGCCTTGAAAATC CTAAATTTCCTTTCCCTAAT TGGGTTATGAAAATAAGGCTG CCTAGCATCTGTCTTCAGGG CAATATACATAC	-	Homozygous	40
186,512,436	A	C	Heterozygous	8
186,512,439	T	C	Heterozygous	9
186,512,443	T	C	Heterozygous	11
186,512,444	T	C	Heterozygous	11
186,524,264	-	AA	Heterozygous	7
12. ***TP53*** chr17:7,571,720-7,590,868				
7,579,548	G	A	Heterozygous	17
13. ***UBE2E1*** chr3:23,847,384-23,933,131				
23,929,045	G	C	Homozygous	11
23,929,048	TT	-	Heterozygous	11
23,929,047	AT	CC	Heterozygous	11
23,929,051	T	A	Heterozygous	13
23,929,054	A	G	Homozygous	14
23,929,193	A	T	Homozygous	11
14. ***WEE1*** chr11:9,595,228-9,611,313				
9,597,641	G	T	Heterozygous	12
9,597,643	A	C	Heterozygous	13
9,597,644	A	T	Heterozygous	12
9,597,647	C	G	Heterozygous	11
9,597,648	G	A	Heterozygous	11

The variants in Table 11, although very few (191 variants) compared to the whole variants detected by the sequencing analysis, still can indicate that the DNA molecules were mutated when the BEAS-2B cells were treated with 5 μM Cr(IV)-DPO for 48 hr. Among these 191 mutation positions listed in Table 11, when conducting the statistical analysis, the number of mutated T (thymine) is 48 (25.1%), the number of mutated G (Guanine) is

41 (21.5%), the number of mutated C (Cytosine) is 17 (14.1%), the number of mutated A (Adenine) is 51 (26.7%), the number of deleted sequence is 10 (5.2%), and the number of inserted sequence is 14 (7.3%). These results show that, instead of the guanine (G), adenine (A) appeared to be the most mutated bases under the influence of Cr(IV)-DPO. Still, these observations seem to contradict the prevailing assumption that G is the most easily oxidized base by chromium complex. Furthermore, the number of base alternation to T is 39 (20.4%), the number of base alternation to G is 42 (22.0%), the number of base alternation to C is 40 (20.9%), and the number of base alternation to A is 46 (24.1%). The analysis implies that the most of the mutated bases belonging to these 14 mutated cell cycle checkpoint genes tend to become adenine under the effects of 5 μM Cr(IV)-DPO treatment for 48 hr.

In addition, because chromium complex has the potential to cause lung cancer,[2] the genes related to lung cancer development (oncogenes), were also checked in the method stated above. Firstly, 41 published oncogenes of lung cancer[39] were checked to identity the variants in control and treated samples by referring human genome. These oncogenes include: *ALDH1A1* Chr9: 75,515,578~75,695,358 (9q21.13); *CALR* Chr19:13,049,392~ 13,055,304(19p13.2); *CCNE1* Chr19:30,302,805~30,315,215 (19q12); *CDC25B* Chr20: 3,767,578 ~3,786,762 (20p13); *CDC42* Chr1: 22,379,120~22,419,437 (1p36.12); *CSF2* Chr5: 131,409,483~31,411,859 (5q31.1); *DPF3* Chr14: 73,086,004~73,360,809 (14q24.2); *EEF1A2* Chr20:62,119,366~62,130,505 (20q13.33); *EEF1G* Chr11: 62,327,073~ 62,342,401 (11q12.3); *EFABP* Chr8: 82,192,598~82,197,012 (8q21.13); *EIF5A* Chr17: 7,210,318~7,215,782 (17p13.1); *FGR* Chr1: 27,938,575~27,961,788 (1p36.11); *GSTP1* Chr11: 67,351,066~67,354,131(11q13.2); *GTM4* Chr1:110,198,698~110,208,123

(1p13.3); *HAP1* Chr17:39,873,994~39,890,898 (17q21.2); *HP* Chr16: 72,088,491~ 72,094,955 (16q22.2); *HSPB1* Chr7: 75,931,861~75,933,614 (7q11.23); *IGFBP-3* Chr7: 45,951,844~45,961,473 (7p12.3); *JTK9* Chr20: 30,639,991~30,689,659 (20q11.21); *KCIP-1* Chr8:101,928,753~101,965,623(8q22.3); *KIF11* Chr10: 94,352,825~94,415,152 (10q23.33); *KRT17* Chr17:39,775,689~39,781,094 (17q21.2); *KRT18* Chr12: 53,342,655 ~53,346,685 (12q13.13); *KRT19* Chr17: 39,679,869 ~39,684,641 (17q21.2); *KRT8* Chr12: 53,290,971~53,343,738 (12q13.13); *LGALS1* Chr22: 38,071,613~ 38,075,813(22q13.1); *MAP4* Chr3: 47,892,180~48,130,769 (3p21.31); *MCM3* Chr6: 52,128,807~52,149,679 (6p12.2); *MDM2* Chr12: 69,201,956~69,239,214 (12q15); *MMP7* Chr11: 102,391,239~ 102,401,484 (11q22.2); *NFKB1* Chr4: 103,422,486 ~103,538,459 (4q24); *P4HB* Chr17: 79,801,034~79,818,570 (17q25.3); *PGK1* ChrX: 77,320,685~77,384,793 (Xq21.1); *PRDX1* Chr1: 45,976,707~45,988,719 (1p34.1); *PSMB6* Chr17: 4,699,439~4,701,790 (17p13.2); *RAC1* Chr7: 6,414,126~6,443,608 (7p22.1); *RHOA* Chr3: 49,396,578~ 49,450,431 (3p21.31); *S100A2* Chr1: 153,533,584 ~153,540,366 (1q21.3); *TAGLN* Chr11: 117,070,037~117,075,508 (11q23.3); *TUBB* Chr6: 30,687,978~30,693,203 (6p21.33); *ZBTB17* Chr1: 16,268,364~16,302,627 (1p36.13).

Sequencing data analysis demonstrated that the sequence of these 41 oncogenes had several variants in either control or Cr(IV)-DPO-treated samples. However the number of the variants in Cr(IV)-treated samples was higher than that of the control samples. Noticeably, even the same variants which existed both in control and Cr(IV)-treated samples, had an apparent higher coverage in the treated samples. But despite their higher coverage, the same variants were neglected in this comparison analysis. The number of variations

between variants of controls samples and variants of treated samples was 560. This number of variants represented the number of DNA mutation positions when BEAS-2B cells were treated with 5 μM Cr(IV)-DPO for 48 hrs. However, more than 2/3 of the 560 variants were not statistically significant to be mutation positions because of their low coverage (<10). Too low coverage failed to prove data reliability and reproducibility. Thus, only 169 of the 560 variants with a coverage larger than 10 were taken into consideration. Statistical analysis revealed that these 169 significant variants belonged to 11 genes (*CALR, P4HB, KRT17, GSTP1, LGALS1, KRT8, NFKB1, S100A2, RHOA, RAC1*, and *PSMB6*). Detailed mutation positions of the 11 genes are listed in the Table 12.

Table 12. Variants between the treated (5 μM, 48 hr treatment) and untreated control samples of the 41 oncogenes of lung cancer

Gene Symbol; Gene location; Ensembl cytogenetic band				
Position	**Reference**	**Variant**	**Allele Call**	**Coverage**
1. ***CALR***; Chr19: 13,049,392~13,055,304; 19p13.2				
13,050,052	A	T	Heterozygous	14
13,050,053	A	C	Heterozygous	14
13,050,240	-	GAGGA GAAAG ATAA	Heterozygous	10
13,050,239	C	A	Heterozygous	10
13,050,448	G	C	Heterozygous	16
13,050,449	A	C	Heterozygous	15
13,050,449	A	T	Heterozygous	15
13,050,450	G	C	Heterozygous	14
13,050,452	G	A	Heterozygous	14
13,050,452	G	C	Heterozygous	14
13,050,454	-	AT	Heterozygous	13
13,050,457	C	G	Heterozygous	14
13,050,457	C	T	Heterozygous	14
13,050,458	T	C	Heterozygous	14
13,050,458	T	G	Heterozygous	14
13,050,053	A	T	Heterozygous	14
13,050,055	-	C	Heterozygous	14
13,050,054	G	A	Heterozygous	14
13,050,862	C	G	Heterozygous	13

Table 12 continued

Position	Reference	Variant	Allele Call	Coverage
13,050,862	C	T	Heterozygous	13
13,050,865	A	T	Homozygous	12
13,050,965	T	A	Homozygous	11
13,050,967	-	TTTACA	Heterozygous	11
13,050,967	-	TTTA CACA	Heterozygous	11
13,051,265	AGGTTGGTGTTTG GGCAGGGGCTCTGCTCTCCA CATTGGAGGGTGTGGAAG ACATCTGGGCCAACTCTGA TCTCTTCATCTACCCCCC	-	Homozygous	32
13,051,265	AGGTTGGTGTTTGGG CAGGGGCTCTGCTCT CCACATTGGAGGGTG TGGAAGACATCTGGG CCAACTCTGATCTCTT CATCTACCCCCC	-	Homozygous	43
	2. ***P4HB***; Chr17: 79,801,034~79,818,570; 17q25.3			
79,803,016	G	T	Heterozygous	10
79,805,107	T	G	Heterozygous	11
79,805,108	T	G	Heterozygous	12
79,813,158	-	GAA	Homozygous	55
79,813,158	TG	GA	Heterozygous	55
79,813,176	C	A	Heterozygous	27
79,813,315	A	G	Heterozygous	21
79,813,316	G	C	Heterozygous	21
79,817,056	G	C	Homozygous	45
79,813,004	T	C	Heterozygous	10
79,813,005	G	T	Heterozygous	10
79,803,870	G	T	Homozygous	10
79,803,873	G	T	Heterozygous	10
79,803,875	G	C	Heterozygous	10
79,804,822	C	T	Homozygous	23
79,804,952	T	C	Heterozygous	14
79,803,736	G	A	Heterozygous	10
79,803,738	A	C	Heterozygous	13
79,804,953	G	T	Heterozygous	15
79,805,105	C	G	Heterozygous	15
79,805,107	G	T	Heterozygous	15
79,805,108	G	T	Heterozygous	15
79,805,235	A	G	Heterozygous	21
79,805,096	T	A	Homozygous	12
79,805,097	G	A	Homozygous	12
79,805,098	G	A	Homozygous	12
79,805,099	G	A	Homozygous	12

Table 12 continued

Position	Reference	Variant	Allele Call	Coverage
79,805,100	G	A	Homozygous	12
79,805,101	G	T	Homozygous	12
79,813,003	-	TT	Heterozygous	10
79,813,002	G	T	Heterozygous	10
79,813,005	T	G	Heterozygous	12
79,813,017	C	A	Homozygous	49
79,813,011	-	TT	Heterozygous	19
79,813,010	C	T	Heterozygous	19
79,813,317	T	A	Heterozygous	19
79,813,324	T	A	Heterozygous	49
79,813,158	GA	TG	Heterozygous	80
79,813,176	A	C	Heterozygous	35
79,813,304	A	C	Heterozygous	13
79,813,305	A	T	Heterozygous	14
79,813,306	G	A	Heterozygous	17
79,813,308	C	T	Heterozygous	26
79,813,312	A	T	Heterozygous	29
79,817,042	G	A	Heterozygous	18
79,817,051	C	T	Heterozygous	60
79,817,053	A	C	Homozygous	70
79,817,272	G	A	Heterozygous	48
79,818,191	C	A	Heterozygous	11
79,817,056	C	G	Homozygous	85
79,817,270	G	C	Heterozygous	45
	3. ***KRT17***; Chr17: 39,775,689~39,781,094; 17q21.2			
39,778,790	AG	-	Heterozygous	10
39,778,789	T	C	Heterozygous	10
39,777,147	C	A	Heterozygous	12
39,777,149	C	G	Heterozygous	12
39,777,151	T	C	Heterozygous	11
39,775,941	C	G	Heterozygous	23
39,775,943	G	T	Heterozygous	15
39,775,945	A	T	Heterozygous	15
39,775,947	G	T	Heterozygous	16
39,775,948	A	T	Heterozygous	14
39,776,811	CTGAAAGAAAAAAA AAAACAGAGAGGAA ATTAGATGTGGGTCT GAGAGCCCCACCCCT GCCAAGAGACCCCCA GCCCTGACCCCAGGC GCCCCCACTCAC	-	Homozygous	48
39,777,150	A	G	Heterozygous	10
39,777,153	A	T	Heterozygous	12
39,777,348	A	T	Heterozygous	22
39,777,351	C	-	Homozygous	14

Table 12 continued

Position	Reference	Variant	Allele Call	Coverage
39,777,354	G	A	Homozygous	13
39,777,358	C	A	Heterozygous	12
39,777,369	G	A	Heterozygous	11
39,777,369	G	C	Heterozygous	11
39,777,370	G	T	Heterozygous	11
39,778,591	G	C	Heterozygous	17
39,778,767	C	G	Homozygous	43
39,777,826	G	C	Heterozygous	11
39,777,844	C	T	Homozygous	31
39,778,768	C	T	Homozygous	33
39,778,770	T	C	Heterozygous	32
39,778,773	G	A	Heterozygous	28
39,778,775	-	GTC	Heterozygous	25
39,778,775	A	G	Heterozygous	24
39,778,587	T	A	Homozygous	11
39,779,177	-	CAG	Heterozygous	11
39,779,176	T	G	Heterozygous	11
39,779,179	C	G	Heterozygous	14
39,779,182	A	G	Heterozygous	14
39,779,193	A	C	Homozygous	29
39,779,194	G	T	Homozygous	29
39,779,196	A	T	Homozygous	38
39,779,200	-	AA	Heterozygous	70
39,779,199	C	A	Heterozygous	70
39,780,329	C	T	Homozygous	38
4. ***GSTP1***; Chr11: 67,351,066~67,354,131; 11q13.2				
67,353,567	T	C	Heterozygous	11
67,353,570	G	A	Heterozygous	11
67,353,570	G	C	Heterozygous	11
67,353,571	G	C	Heterozygous	12
67,353,571	G	T	Heterozygous	12
67,353,573	-	ATCT ACAC CAACT	Heterozygous	14
67,353,851	G	T	Heterozygous	11
67,353,856	G	C	Heterozygous	13
67,352,718	C	T	Heterozygous	11
67,352,719	A	G	Heterozygous	12
67,353,851	G	T	Homozygous	11
67,353,853	C	A	Homozygous	13
67,353,854	C	T	Heterozygous	14
67,353,857	-	TGGG AGAC	Homozygous	14
5. ***LGALS1***; Chr22: 38,071,613~38,075,813; 22q13.1				
38,073,073	G	C	Heterozygous	13
38,073,075	G	T	Heterozygous	12

Table 12 continued

Position	Reference	Variant	Allele Call	Coverage
38,074,486	C	A	Homozygous	10
38,074,487	C	G	Heterozygous	10
38,074,665	G	T	Homozygous	10
6. ***KRT8***; Chr12: 53,290,971~53,343,738; 12q13.13				
53,298,838	A	T	Heterozygous	19
53,343,036	T	C	Heterozygous	16
53,291,342	G	A	Heterozygous	14
53,291,348	A	C	Heterozygous	13
53,344,692	C	A	Heterozygous	11
53,298,775	A	T	Heterozygous	135
7. ***NFKB1***; Chr4: 103,422,486~103,538,459; 4q24				
103,488,139	CCCTCAGG	-	Heterozygous	11
103,488,138	G	G	Heterozygous	11
103,488,293	G	C	Heterozygous	12
103,488,295	A	T	Heterozygous	12
103,488,296	A	C	Heterozygous	12
103,488,298	T	C	Homozygous	11
8. ***S100A2***; Chr1: 153,533,584~153,540,366; 1q21.3				
153,534,027	C	T	Heterozygous	17
9. ***RHOA***; Chr3: 49,396,578~49,450,431; 3p21.31				
49,412,850	A	C	Homozygous	11
49,412,851	T	C	Homozygous	12
49,412,852	G	A	Heterozygous	12
49,412,852	G	C	Heterozygous	12
49,412,854	-	C	Heterozygous	13
49,412,853	A	C	Heterozygous	13
49,412,858	T	C	Homozygous	16
49,412,859	A	C	Homozygous	16
49,412,860	T	A	Homozygous	16
49,412,865	-	T	Homozygous	17
49,399,922	A	C	Heterozygous	10
49,399,922	A	T	Heterozygous	10
49,412,849	T	C	Heterozygous	11
49,413,027	G	C	Heterozygous	12
49,413,028	A	C	Heterozygous	12
49,413,029	A	G	Heterozygous	11
49,413,030	A	G	Heterozygous	10
10. ***RAC1***; Chr7: 6,414,126~6,443,608; 7p22.1				
6,442,169	A	C	Heterozygous	13
6,442,155	C	A	Heterozygous	20

Table 12 continued

Position	Reference	Variant	Allele Call	Coverage
	11. ***PSMB6***; Chr17: 4,699,439~4,701,790; 17p13.2			
4,701,448	GGTGAGAGCTTAGGCT TCTGGGCCTATGAGCT TCAACCCCAACTACCCA AGCCAGGCCAGCATTCCT CATTCCTTGCAGTGATCC CGGCATCTGAATCTGAACCC AGCTTTCTTCTTTTATC CACA	-	Homozygous	35

Although there were very few variants, compared to the whole variants detected by sequencing (Table 12), it still leads to the conclusion that DNA molecules in BEAS-2B cells were mutated when the cells were treated with 5 μM Cr(IV)-DPO for 48 hrs. Among the 168 mutation positions listed in Table 12, the number of mutated T (Thymine) is 23 (13.7%), the number of mutated G (Guanine) is 53 (31.5%); the number of mutated C (Cytosine) is 33 (19.6%), the number of mutated A (Adenine) is 38 (22.6%), the number of deleted sequence is 6 (3.6%) and the number of inserted sequence is 15 (8.9%). These results show that, in these genes, guanine (G) is the most frequent mutated position under the influence of Cr(IV)-DPO. Furthermore, the number of base alternation to T is 46 (27.4%), the number of base alternation to G is 24 (14.3%), the number of base alternation to C is 44 (26.2%), and the number of base alternation to A is 33 (19.6%).

CHAPTER IV: DISCUSSION

The aim of the work was to address the mutations caused by the putative chromium carcinogen, Cr(IV)-DPO, which could mimic the real mutations caused by chromium(VI). In order to find exact experimental conditions for this mutation study, cellular morphology, cell survival assay, and the fate of apoptotic and DNA repair genes were evaluated. Both cell morphology and survival experiments helped to select 5 μM concentration as the optimal dose with a treatment time of 48 hr. Under these conditions, cells exhibited severe stress yet they were not dying at an accelerated rate. Likewise, gene expression experiments revealed that both apoptotic and DNA repair genes were unable to protect the cells from oxidative stress caused by the chromium compound.

Usually, various mutations happen spontaneously in cells everyday but can be repaired by the DNA repair genes through various signaling pathways. But once the mutations are not repaired accurately due to some specific internal or external factors, mutations and severe consequences to gene expressions can occur. Scheme 8 (courtesy to The Pennsylvania State University online-course) shows a schematic diagram of several point mutations and the consequences. As can be seen from Scheme 8, a purine to purine or pyrimidine to pyrimidine change is transition mutation type, and a purine to pyrimidine or a pyrimidine to purine change is transversion mutation type. As Scheme 8 shows, the gene expressions can be terminated by a single nucleotide mutation, and the insertion and deletion mutations usually cause disastrous consequences, since it is often seen that all the sequence following the mutation positions will be utterly changed.

Scheme 8. General examples of mutations in DNA and the consequences in gene expressions

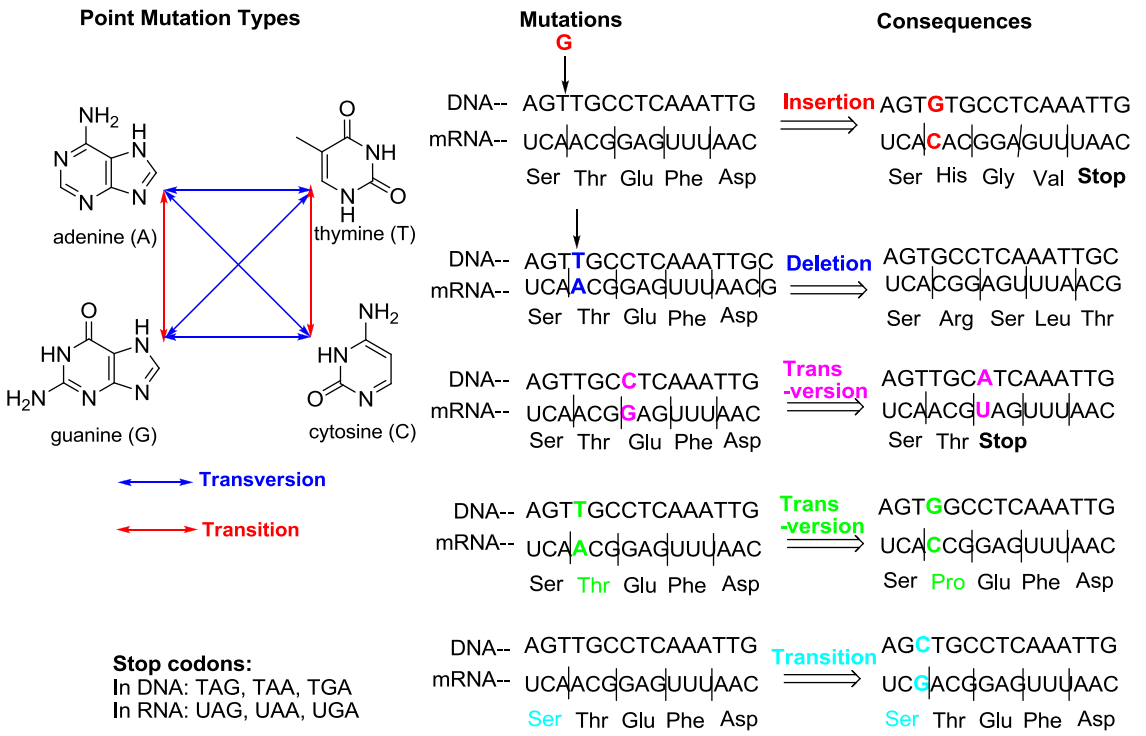

The primary origin of mutation is the creation of Apurinic/apyrimidinic (AP) sites. These sites are the noncoding DNA lesions that are generated via hydrolysis of the N-glycosyl bond, leading to base release from the deoxyribose of the DNA backbone. Spontaneous AP sites exist in cells with large quantities while the DNA-damaging chemicals, for example Cr(IV)-DPO, promote the base release that are orders of magnitude larger than natural AP sites formation. As mentioned in the background introduction chapter, it is known that DNA oxidation by chromium compounds leads to base cleavage, resulting in AP sites. Since the oxidized base destabilize the N-glycosyl linkage, suggesting that more bases are prone to be released to produce more AP sites. In healthy cells, the AP sites lesions usually can be efficiently repaired in several steps by activating the base excision repair pathway. But in the presence of the DNA-damaging chemical, such as Cr(IV)-DPO, the strand

opposite to the AP sites is more likely to be incorporated with the wrong nucleotides, resulting in the A:T to C:G or C:G to A:T mutations. These mutations were observed in the BEAS-2B cells treated with 5 μM for up to 48 hr, which are shown through cDNA sequencing data. But the genotoxicity of Cr(IV)-DPO is complicated by many other kind of DNA damage, including DNA double-strand scissions by releasing the sugar and phosphate-diester. The strand release of DNA backbone components is hypothesized to be one cause that cuts off the short DNA sequences, resulting in the loss of exact sequence information for the replication process. This hypothesis was demonstrated in the cDNA sequencing data. In the sequencing data of each sample, if there is a variant different as the reference, the human genome library (hg19), it is called and exported to be listed in the Excel form with detailed information. By analyzing all the variants both in the control samples and the 5 μM Cr(IV)-DPO-treated samples, we can get the statistical differences, which are shown in Table 13. These data are incorporated in Table 14. The columns in this table are designated as follows: S#1, first untreated control sample; S#2 the duplicate untreated control sample; S#3 first 5 μM, 48hr Cr(IV)-DPO-treated control sample; and S#4 the duplicate 5 μM, 48hr Cr(IV)-DPO-treated control sample. The term "count" signifies how many specific variants were observed; "percentage" indicates the percentage of each kind of variants; "X" (X represents A, C, G or T) informs that X was mutated to a different base; "INS" indicates a new short sequence of DNA was inserted; and "DEL X" signifies that one nucleotide or a short DNA sequence made up of several nucleotides was deleted.

Table 13. Statistical analysis on all variants in the cDNA sequences of four samples

All data	Count				Percentage			
Variants	S#1 Control_1	S#2 Control_2	S#3 Treated_1	S#4 Treated_2	S#1 Control_1	S#2 Control_2	S#3 Treated_1	S#4 Treated_2
T	8293	9542	13913	15174	25.95%	26.23%	25.97%	26.55%
G	6725	7639	11324	11980	21.05%	21.00%	21.14%	20.96%
C	6720	7768	11175	11744	21.03%	21.35%	20.86%	20.55%
A	8671	9839	14322	15403	27.13%	27.04%	26.73%	26.95%
DEL T	54	67	94	109	0.17%	0.18%	0.18%	0.19%
DEL G	92	71	148	146	0.29%	0.20%	0.28%	0.26%
DEL C	137	124	252	253	0.43%	0.34%	0.47%	0.44%
DEL A	93	114	177	174	0.29%	0.31%	0.33%	0.30%
INS	1171	1220	2174	2163	3.66%	3.35%	4.06%	3.79%
Sum	31956	36384	53579	57146	100.00%	100.00%	100.00%	100.00%

It should be noted that, in the Table 13, although in the control samples the number of variants is large, the number of variants in the Cr(IV)-DPO-treated samples is larger, suggesting that the Cr(IV)-DPO treatment on BEAS-2B cells indeed increase the frequency of mutations. Specifically, the treatment induces more A:T to G:C mutations than G:C to A:T mutations. We also note that there exists a large quantity of insertion mutations, suggesting the hypothesis that DNA strands were more prone to be broken and therefore were cut off with the Cr(IV)-DPO treatment. This hypothesis was also proven by the PCR assay where the double-strand break repair genes: *RAD51, XRCC6, RAD50, RAD21, RAD54L*, and *PRKDC* were over-expressed to try to repair the DNA double-strand break lesions. But the consequence of their activations were not efficient enough for some reasons to maintain the integrity of the DNA structures since the large quantities of insertion mutations were still observed. In addition, the deletion mutations are most often observed at the C positions, suggesting the possibility that, because of the Cr(IV)-DPO treatment, the cytosine bases (C) were cleaved to produce the abasic sites and the strand

opposite to those abasic sites was not incorporated with any base but, including the vicinity of the C, were skipped in replications.

Table 14. Statistical analysis of the variants remained after subtracting the overlapped variants of the Cr(IV)-DPO-treated samples from the control

	Subtract Overlaps between treated and control					
ALL data	count	percentage	count	percentage	count	percentage
Variants	S#4-S#2		S#3-S#1		Average Differences	
T	5632	27.13%	5620	25.99%	5626	26.56%
G	4341	20.91%	4599	21.27%	4470	21.09%
C	3976	19.15%	4455	20.60%	4216	19.88%
A	5564	26.80%	5651	26.13%	5608	26.47%
DEL T	42	0.20%	40	0.19%	41	0.19%
DEL G	75	0.36%	56	0.26%	66	0.31%
DEL C	129	0.62%	115	0.53%	122	0.58%
DEL A	60	0.29%	84	0.39%	72	0.34%
INS	943	4.54%	1003	4.64%	973	4.59%
sum	20762	100.00%	21623	100.00%	21193	100.00%

To further compare the differences between the untreated control samples and the Cr(IV)-treated samples, the overlapped variants caused by natural influence instead of the chemical inductions were subtracted from the treated samples. The statistical analysis after the data subtraction is shown in Table 14. The columns in this table are designated as follows: S#4-S#2, analysis after the overlapped variants existing in the control sample (S#2) were subtracted from the Cr(IV)-treated sample (S#4); S#3-S#1, analysis after the overlapped variants existing in the duplicate control sample (S#1) were subtracted from the duplicate Cr(IV)-treated sample (S#3); other terms are the same as in Table 13 and 14. When the mutation percentages of the group of A to C, A to T, and A to G and the group of C to A, C to T, and C to G were analyzed, the mutation percentage of A to G is found to be the most both in sample 3 and sample 4 (duplicate treated samples). It means that the double-strand DNAs in BEAS-2B cells after 5 μM, 48 hr treatment of Cr(IV)-DPO were mutated

in a large quantity of positions and the most frequent changes were A:T to G:C changes. Similar statistical calculations were done on the mutations from T to A, T to C, T to G, G to A, G to T, and G to C, the percentage mutation of T to C is found to be the most. This observation leads to a similar result that the double-strand DNAs in BEAS-2B cells after 5 μM, 48 hr treatment of Cr(IV)-DPO were mutated most preferably to be the T:A to C:G changes. Therefore, we can conclude that the chronic treatment (5 μM, 48 hr) with Cr(IV)-DPO on BEAS-2B cells induce A:T to C:G or T:A to G:C mutations of the DNAs.

Table 15. Statistical analysis of the variants in cDNA sequences with coverage more than 20 in all four samples

Coverage>20	Count				Percentage			
Variants	S#1 Control_1	S#2 Control_2	S#3 Treated_1	S#4 Treated_2	S#1 Control_1	S#2 Control_2	S#3 Treated_1	S#4 Treated_2
A	1863	2094	3046	3298	26.85%	27.36%	26.34%	26.57%
C	1405	1547	2354	2546	20.25%	20.21%	20.36%	20.51%
G	1400	1547	2393	2539	20.18%	20.21%	20.69%	20.45%
T	1797	1992	2926	3159	25.90%	26.03%	25.30%	25.45%
DEL A	56	63	110	118	0.81%	0.82%	0.95%	0.95%
DEL C	103	92	204	201	1.49%	1.20%	1.76%	1.62%
DEL G	64	49	107	100	0.92%	0.64%	0.93%	0.81%
DEL T	23	27	43	41	0.33%	0.35%	0.37%	0.33%
INS	227	243	381	411	3.27%	3.18%	3.30%	3.31%
Sum	6938	7654	11564	12413	100.00%	100.00%	100.00%	100.00%

Table 16. Statistical analysis of the variants (with coverage over 20) remaining after subtracting the overlapped variants of the Cr(IV)-DPO-treated samples from the control

	Subtract overlaps between the treated and control					
Coverage>20	S#4-S#2		S#3-S#1		Average	
Variants	count	percentage	count	percentage	count	percentage
A	1183	25.57%	1204	25.30%	1194	25.44%
C	949	20.51%	999	20.99%	974	20.75%
G	993	21.47%	992	20.85%	993	21.16%
T	1129	24.41%	1167	24.52%	1148	24.46%
DEL A	54	1.17%	55	1.16%	55	1.16%
DEL C	101	2.18%	109	2.29%	105	2.24%
DEL G	43	0.93%	51	1.07%	47	1.00%
DEL T	20	0.43%	14	0.29%	17	0.36%
INS	154	3.33%	168	3.53%	161	3.43%
Sum	4626	100.00%	4759	100.00%	4693	100.00%

To assure the reliability of the data, we tried to focus only on the variants with coverage over 20 in the four samples and performed similar statistical analysis (See Tables 15 and 16). Comparing the data in Table 16 with those in Table 14, we note that the number of variants with coverage over 20 is largely decreased compared to the total number of variants, but the quantity of variants in treated samples is still much higher than that in the control samples (around 5000 more variants). In addition, the A:T to C:G mutations are still occurring higher than the C:G to A:T mutations. Noticeably, the sequence deletions mutations at the C position are more favorable than the other three positions (A, G, and T), suggesting that when synthesizing the new DNA strand, the DNA polymerase is more prone to bypass the cytosine-abasic lesions by skipping due to the information loss of the sequence.

In the PCR assays, the genes, over-expressed in the BEAS-2B cells with the treatment of 5 μM Cr(IV)-DPO for 48 hr, were observed showing down-expression or no changes when the exposure time was elongated up to 72 hr. This observation exactly indicates the DNA repair genes in BEAS-2B cells become dysfunctional or inactive as the exposure time increases. When the DNA repair genes were over-expressed, the cells were actively defending against all kinds of DNA damage. And when they are down-expressed or inactive, the DNA repair system was mutated or inhibited and therefore failed to efficiently repair the DNA damage. Consequently, without any corrections, DNA mutations occurred in daughter cells with a much higher frequency. It is intriguing to find that the DNA repair genes PCR results are consistent to the cDNA sequencing results. Specifically, in BEAS-2B cells, 13 out of 104 DNA repair genes were observed significantly mutated after the

treatment with 5 μM Cr(IV)-DPO for 48 hr. They are *ALKBH3, BRCA2, DDB1, FANCC, GTF2H3, MAD2L2, MNAT1, PCNA, POLB, POLD4, PRKDC, REV1*, and *RPA1*. Specially, *DDB1, POLB, REV1, PRKDC*, and *PCNA* are important genes regulating cellular proliferations. Their mutations lead to carcinogenesis which have been observed in many cancer cells.[40-44]

DBB1, down-expressed in PCR data, was observed a thymine (T) mutation (T to C) at the position of Chr11:61,067,254 in the sequencing data. Any mutation in DDB1 is fatal since DDB1 is a gene encoding ddb1 protein which binds to ddb2 to form a UV-damaged DNA-binding protein complex. This protein complex is required for DNA nucleotide excision repair (BER) since it recognizes the UV-induced DNA damage and recruits proteins for activating the BER pathway.[45]

POLB, over-expressed in PCR data, is a gene encoding the DNA polymerase protein which functions as an enzyme to catalyze the gap-filling DNA synthesis. POLB is very important to cells because it regulate one nucleotide to the 3' end of the arising single-nucleotide gap to be added.[46] If *POLB* is activated, it means that the strand opposite to the DNA gaps caused by Cr(IV)-DPO oxidation were bypassed by filling in with a random nucleotide in the absence of a template as the reference. And if *POLB* is mutated, the strands are more prone to be filled with the wrong nucleotides, which causes incorrect information to be copied, leading to further mutations in the new newly synthesized DNAs. In experiments described in this thesis, when treating the BEAS-2B cells with 5 μM Cr(IV)-DPO for 48 hr, the gene *POLB* in the cells was found to be mutated at the 4 positions in the sequencing analysis: one cytosine (C) was inserted at the position of Chr8: 42,199,770, one guanine(G)

was mutated to be one adenine (A) at the position of Chr8: 42,199,773, one guanine (G) was mutated to be one adenine (A) at the position of Chr8: 42,199,759, and one thymine (T) was mutated to be one adenine (A) at the position of Chr8: 42,199,972.

REV1 is active when DNA mutations are induced by physical and chemical agents. It is a gene encoding rev1 protein which plays a crucial role in protein-protein interactions. For example, in DNA repair process, rev1 recruits DNA polymerases involved in translesion synthesis (TLS) of damaged DNA. Rev1-like terminal deoxycytidyl transferase is also encoded by the *REV1* gene. This transferase transfers a dCMP residue from dCTP to the 3'-end of a DNA primer in the DNA repair process, leading to the successful bypass of abasic lesions by inserting an unspecific nucleotide opposite the lesion.[47] Thus, mutation in REV1 will introduce more mutations because incorrect DNA information is introduced and successfully copied to daughter cells with much higher chances. Consequently, the cells with mutated REV1 are prone to undergo apoptosis or tumorigenesis. Compared to the control, in the sequencing data, the BEAS-2B cells with the treatment of 5 μM Cr(IV)-DPO for 48 hr indeed showed mutation in the REV1 gene at the position of Chr2: 100,058,870, where the cytosine (C) was mutated to be thymine (T).

PRKDC, over-expressed in BEAS-2B cells with 5 μM, 48 hr-Cr(IV)-DPO treatment but down-expressed in BEAS-2B cells with 5 μM, 72 hr-Cr(IV)-DPO treatment, is a gene encoding a DNA-dependent protein kinase (DNA-PK). DNA-PK is a nuclear protein serine/ threonine kinase whose function is sensing the DNA damage. It means that when DNA is damaged, DNA-PK is activated through phosphorylation by ATM/ATR. And only when DNA-PK binds to DNA can it play the catalytic role in the ligation step of the non-

homologous end joining (NHEJ) pathway, recombination and telomere stabilization.[48] Thus, any mutation of *PRKDC* may directly lead to the DNA repair system becoming inactive since some of the DNA lesions may not be recognized. In sequencing analysis data, it was observed mutated at the position of Chr8: 48,805,817 by inserting a guanine (G), corresponding to its disordered expressions in PCR assays since the expression was not constant when the treatment exposure time is elongated.

PCNA, found in the cell nucleus, is a gene encoding a protein which acts as a co-factor of DNA polymerase delta to help increase the processing of DNA leading strand synthesis during DNA replication. It means that once the DNA is damaged, this protein encoded by *PCNA* gene is ubiquitinated and involved in the RAD6-dependent DNA-repair pathway, making *PCNA* indispensable to the DNA repair.[49, 50] In the BEAS-2B cells treated with 5 μM Cr(IV)-DPO for 48 hr, *PCNA* was observed to be mutated at three positions: one is at Chr20: 5,096,009 where a short DNA sequence (DNACTGAAAGACAGGAAGATG GTTAATTACTGAGGAGTATGTATCACATATGACTACCTACAAAACAAGGTTC AAATTTATTATCTTAC) was deleted; the second is at Chr20: 5,099,324 where another short sequence (CTACCAAAAGAAAGCAGATGCTTTTGAGAAATACTGACACAG AGTTTTGATTTTCTGTAGCTTCGTGACTCGGTAAAAAGGTACGACTTAC) was deleted; and the third one is at Chr20: 5,100,447 where a thymine (T) was mutated to be a cytosine (C). These mutations indicate that the Cr(IV)-DPO treatment leads to DNA information becoming lost, which severely influences the DNA repair genes expression and tends to cause more mutations in the daughter cells, eventually leading to carcinogenic cells formation.

Table 17. Statistical analysis of the variants resulting from mutated genes (including apoptosis, DNA repair, cell cycle checkpoints genes, and lung-cancer oncogenes) in cDNA sequences with coverage more than 10 in all four samples

	Count	Percentage	Count	Percentage	Count	Percentage	Count	Percentage
Variants	Cellular apoptosis genes (13/129)		DNA repair genes (13/104)		Cell cycle checkpoints genes (14/110)		related oncogenes (11/41)	
T	43	23.4%	13	30.2%	48	25.1%	23	13.7%
G	41	22.3%	6	14.0%	41	21.5%	53	31.6%
C	37	20.1%	8	18.6%	27	14.1%	33	19.6%
A	46	25.0%	11	25.6%	51	26.7%	38	22.6%
INS	10	5.4%	2	4.7%	14	7.3%	15	8.9%
DEL	7	3.8%	3	7.0%	10	5.2%	6	3.6%
Sum	184	100.0%	43	100.0%	191	100.0%	168	100.0%

To find out whether the mutations induced by Cr(IV)-DPO treatment at the key genes are more favorable to happen at the A, C, G, or T sites, we have conducted statistical analysis on the mutated genes including 13 cellular apoptosis genes (13 out of the total 129 genes are mutated), 13 DNA repair genes (13 out of the total 104 genes are mutated), 14 cell cycle checkpoints genes (14 out of the total 110 genes are mutated), and 11 lung cancer related oncogenes (13 out of the total 41 genes are mutated). The results are shown in Table 17. As can be seen from Table 17, generally no preference in T, G, C or A mutations is found. But it is still clear to see that the A:T to C:G mutations are more preferred except the 11 oncogenes where mutated G is dominant. This observation suggests that with the treatment of Cr(IV)-DPO for up to 48 hr, the A and T bases of DNAs are most likely to be cleaved and incorporated with a C or G bases on the opposite strand.

All the statistical analysis conducted based on the results analyzed by the Ion System™ analyzer method (Ion Torrent™, Life technologies) was also conducted by the GATK method (©Broad Institute 2012), and the results are consistent with each other.

In summary, more variants were observed in Cr(IV)-DPO-treated BEAS-2B cells suggesting that the DNAs were oxidized or severely damaged by Cr(IV)-DPO treatment. Given a longer period of exposure, cells are likely to transform to cancer cells when the mutations are accumulated to certain extent, resulting in uncontrolled proliferation of faulty cells. In contrast to some literature reported before, the sequencing results from experiments have shown that G is not the most frequent mutation positions. But this observation does not refute the previous observation carried out in our lab that guanine is not the most favored cleaved base by conducting the experiments with sequence specific oligomers because the test tube reaction system lacked the various enzymes to repair any damages caused by the chromium oxidations promptly. Also, those earlier experiments were done with Cr(V)-compounds which might have different mutation profile. The contradiction can also be explained by the possibility that in different cellular milieu, the DNA repair system responds differently.

CHAPTER V: CONCLUSION

The ability of a Cr(IV) compound, a very strong oxidizing agent, to mutate DNA leading to the production of faulty cells was explored. Two normal human cell lines: human umbilical vein endothelial cells (HUVEC) and the human lung bronchial epithelial cells (BEAS-2B) were exposed to Cr(IV)-DPO compound. BEAS-2B cells were selected as a model because chromium is reported to cause lung cancer. Based on the morphological assay which showed that HUVECs were undergoing death when treated with Cr(IV)-DPO, the apoptosis gene expressions array on HUVECs was carried out to efficiently find out the specific genes involved in this death processes. Considering the fact that in cultured cells the DNA repair signaling pathways plays a crucial role in defending against any DNA damage caused by chemicals, DNA repair gene expressions on BEAS-2B cells were also carried on. When the exposure time was extended from 48 hr to 72 hr, the most of the activated or over-expressed DNA repair genes turned to be inactivated or down-expressed. This observation leads us to propose the hypothesis that many key genes in BEAS-2B cells were mutated under longer time treatment with the 5 μM Cr(IV)-DPO. In addition, the DNA repair gene expression profiling assays on BEAS-2B cells with different exposure time give us the clues of the complexities of DNA lesions caused by Cr(IV) since various DNA repair pathways were found to be activated after the Cr(IV)-DPO exposure. The time-dependent gene expression profiles were also helpful in monitoring the tumorigenesis processing of the BEAS-2B cells.

The cDNA sequencing experiments carried on both untreated control BEAS-2B cell samples and 5 μM-48hr treated BEAS-2B cell samples showed significant mutation

information on specific genes. In addition, by analyzing the sequencing data focusing only on oncogenes of lung cancer, we concluded that the guanine was the most vulnerable base to be mutated. But overall, the A:T to C:G mutations are more dominant. The most frequent mutations happen at the adenine instead of the guanine positions. All these data taken together, provided insights to explain the observed phenomena of the morphological and viability assay that gene expressions are altered and DNA mutations occurred in key genes, which are responsible for cellular proliferation.

This set of sequencing data was useful since it highlighted some critical but mutated genes in the DNA repair signaling pathway, cellular apoptosis pathway, and cellular checkpoints of BEAS-2B cells treated with Cr(IV)-DPO. Specifically, 13 out of the 129 apoptotic genes were discovered to be mutated, 13 out of the 104 DNA repair genes were demonstrated to be mutated, and 14 out of the 110 cell cycle checkpoints genes were observed to be mutated. The mutations in these key genes introduced more mutations or DNA lesions when the disordered DNA repair system tried to fix the lesions caused by Cr(IV)-DPO. And when the wrong gene information was copied constantly to the daughter cells, carcinogenic cells formed. We also observed that 11 out of 41 oncogenes of lung cancer were also found mutated in several positions in Cr(IV)-DPO-treated BEAS-2B cells, which means that Cr(IV) might indeed cause BEAS-2B to become carcinogenic given a longer exposure of time. In conclusion, this thesis explained the genotoxicity of a Cr(IV) compound to human normal cells at the gene level.

REFERENCES

1. Fishbein L. Sources, transport and alterations of metal compounds: an overview. I. Arsenic, beryllium, cadmium, chromium, and nickel. Environmental Health Perspectives 1981;40: 43.

2. Wilbur S, Abadin H, Fay M, et al. Toxicological profile for chromium 2012.

3. Mertz W. Chromium in human nutrition: a review. The Journal of Nutrition 1993;123(4): 626-33.

4. Liu X, Conner H, Kobayashi T, et al. Cigarette smoke extract induces DNA damage but not apoptosis in human bronchial epithelial cells. American Journal of Respiratory Cell and Molecular Biology 2005;33(2): 121-29.

5. Zhang J, Li S. Cancer mortality in a Chinese population exposed to hexavalent chromium in water. Journal of Occupational and Environmental Medicine 1997;39(4): 315-19.

6. Sedman RM, Beaumont J, McDonald TA, Reynolds S, Krowech G, Howd R. Review of the evidence regarding the carcinogenicity of hexavalent chromium in drinking water. Journal of Environmental Science and Health Part C 2006;24(1): 155-82.

7. Mikalsen A, Alexander J, Andersen RA, Daae H-L. Reduction of hexavalent chromium in a reconstituted system of cytochrome P-450 and cytochrome b5. Chemico-Biological Interactions 1989;71(2): 213-21.

8. Connett PH, Wetterhahn KE. Metabolism of the carcinogen chromate by cellular constituents. Inorganic Elements in Biochemistry: Springer, 1983:93-124.

9. Voitkun V, Zhitkovich A, Costa M. Complexing of amino acids to DNA by chromate in intact cells. Environmental Health Perspectives 1994;102(Suppl 3): 251.

10. O'Brien TJ, Fornsaglio JL, Ceryak S, Patierno SR. Effects of hexavalent chromium on the survival and cell cycle distribution of DNA repair-deficient S. cerevisiae. DNA Repair 2002;1(8): 617-27.

11. Kunkel TA, Bebenek K. DNA Replication Fidelity 1. Annual Review of Biochemistry 2000;69(1): 497-529.

12. Stearns DM, Courtney KD, Giangrande PH, Phieffer LS, Wetterhahn KE. Chromium (VI) reduction by ascorbate: role of reactive intermediates in DNA damage in vitro. Environmental Health Perspectives 1994;102(Suppl 3): 21.

13. Bose RN, Moghaddas S, Gelerinter E. Long-lived chromium (IV) and chromium (V) metabolites in the chromium (VI)-glutathione reaction: NMR, ESR, HPLC, and kinetic characterization. Inorganic Chemistry 1992;31(11): 1987-94.

14. Bose RN, Fonkeng BS, Moghaddas S, Stroup D. Mechanisms of DNA damage by chromium (V) carcinogens. Nucleic Acids Research 1998;26(7): 1588-96.

15. Bose RN, Moghaddas S, Mazzer PA, Dudones LP, Joudah L, Stroup D. Oxidative damage of DNA by chromium (V) complexes: relative importance of base versus sugar oxidation. Nucleic Acids Research 1999;27(10): 2219-26.

16. Moghaddas S, Gelerinter E, Bose RN. Mechanisms of formation and decomposition of hypervalent chromium metabolites in the glutathione-chromium (VI) reaction. Journal of Inorganic Biochemistry 1995;57(2): 135-46.

17. Hussain SP, Hofseth LJ, Harris CC. Radical causes of cancer. Nature Reviews Cancer 2003;3(4): 276-85.

18. Valko M, Izakovic M, Mazur M, Rhodes CJ, Telser J. Role of oxygen radicals in DNA damage and cancer incidence. Molecular and cellular biochemistry 2004;266(1-2): 37-56.

19. Breen AP, Murphy JA. Reactions of oxyl radicals with DNA. Free Radical Biology and Medicine 1995;18(6): 1033-77.

20. Cadet J, Delatour T, Douki T, et al. Hydroxyl radicals and DNA base damage. Mutation Research/Fundamental and Molecular Mechanisms of Mutagenesis 1999;424(1): 9-21.

21. O'Connor TR, Boiteux S, Laval J. Ring-opened 7-methylguanine residues in DNA are a block to in vitro DNA synthesis. Nucleic Acids Research 1988;16(13): 5879-94.

22. Basu AK, Loechler EL, Leadon SA, Essigmann JM. Genetic effects of thymine glycol: site-specific mutagenesis and molecular modeling studies. Proceedings of the National Academy of Sciences 1989;86(20): 7677-81.

23. Hatahet Z, Kow YW, Purmal AA, Cunningham RP, Wallace SS. New substrates for old enzymes. 5-hydroxy-2'-deoxycytidine and 5-hydroxy-2'-deoxyuridine are substrates for Escherichia coli endonuclease III and formamidopyrimidine DNA N-glycosylase, while 5-hydroxy-2'-deoxyuridine is a substrate for uracil DNA N-glycosylase. Journal of Biological Chemistry 1994;269(29): 18814-20.

24. Wang D, Kreutzer DA, Essigmann JM. Mutagenicity and repair of oxidative DNA damage: insights from studies using defined lesions. Mutation Research/Fundamental and Molecular Mechanisms of Mutagenesis 1998;400(1): 99-115.

25. Bose RN, Fonkeng B, Barr-David G, et al. Redox potentials of chromium (V)/(IV),-(V)/(III), and-(IV)/(III) complexes with 2-ethyl-2-hydroxybutanoato (2-/1-) ligands. Journal of the American Chemical Society 1996;118(30): 7139-44.

26. Costa M, Klein CB. Toxicity and carcinogenicity of chromium compounds in humans. CRC Critical Reviews in Toxicology 2006;36(2): 155-63.

27. Hodges N, Adam B, Lee A, Cross H, Chipman J. Induction of DNA-strand breaks in human peripheral blood lymphocytes and A549 lung cells by sodium dichromate: association with 8-oxo-2-deoxyguanosine formation and inter-individual variability. Mutagenesis 2001;16(6): 467-74.

28. Pritchard DE, Singh J, Carlisle DL, Patierno SR. Cyclosporin A inhibits chromium (VI)-induced apoptosis and mitochondrial cytochrome c release and restores clonogenic survival in CHO cells. Carcinogenesis 2000;21(11): 2027-33.

29. Sun H, Clancy HA, Kluz T, Zavadil J, Costa M. Comparison of gene expression profiles in chromate transformed BEAS-2B cells. PLOS ONE 2011;6(3): e17982.

30. Ye J, Shi X. Gene expression profile in response to chromium-induced cell stress in A549 cells. Molecular Mechanisms of Metal Toxicity and Carcinogenesis: Springer, 2001:189-97.

31. Sun H, Clancy HA, Kluz T, Zavadil J, Costa M. Comparison of gene expression profiles in chromate transformed BEAS-2B cells. PLOS ONE 2011;6(3): e17982

32. Hofseth LJ, Khan MA, Ambrose M, et al. The adaptive imbalance in base excision–repair enzymes generates microsatellite instability in chronic inflammation. Journal of Clinical Investigation 2003;112(12): 1887-94.

33. Glassner BJ, Rasmussen LJ, Najarian MT, Posnick LM, Samson LD. Generation of a strong mutator phenotype in yeast by imbalanced base excision repair. Proceedings of the National Academy of Sciences 1998;95(17): 9997-10002.

34. Arakawa, Hirohumi, et al. Chromium (VI) induces both bulky DNA adducts and oxidative DNA damage at adenines and guanines in the p53 gene of human lung cells. Carcinogenesis 2012;33(10): 1993-2000.

35. Reynolds M, Peterson E, Quievryn G, Zhitkovich A. Human nucleotide excision repair efficiently removes chromium-DNA phosphate adducts and protects cells against chromate toxicity. Journal of Biological Chemistry 2004;279(29): 30419-24.

36. Hartwig A. Carcinogenicity of metal compounds: possible role of DNA repair inhibition. Toxicology Letters 1998;102: 235-39.

37. Marin R, Ahuja Y, Bose RN. Potentially deadly carcinogenic chromium redox cycle involving peroxochromium (IV) and glutathione. Journal of the American Chemical Society 2010;132(31): 10617-19.

38. House D, Garner CS. The use of chromium (IV) diperoxo amines in the synthesis of chromium (III) amine complexes. Some monoethylenediamine and monodiethylenetriamine complexes. Inorganic Chemistry 1966;5(5): 840-44.

39. Li R, Wang H, Bekele B, et al. Identification of putative oncogenes in lung adenocarcinoma by a comprehensive functional genomic approach. Oncogene 2006;25(18): 2628-35.

40. Hanawalt PC. Subpathways of nucleotide excision repair and their regulation. Oncogene 2002;21(58).

41. Yang ZQ, Streicher KL, Ray ME, Abrams J, Ethier SP. Multiple interacting oncogenes on the 8p11-p12 amplicon in human breast cancer. Cancer Research 2006;66(24): 11632-43.

42. Miremadi A, Oestergaard MZ, Pharoah PD, Caldas C. Cancer genetics of epigenetic genes. Human Molecular Genetics 2007;16(R1): R28-R49.

43. Donigan KA, Sun K-w, Nemec AA, et al. Human POLB gene is mutated in high percentage of colorectal tumors. Journal of Biological Chemistry 2012;287(28): 23830-39.

44. He X, Ye F, Zhang J, Cheng Q, Shen J, Chen H. REV1 genetic variants associated with the risk of cervical carcinoma. European Journal of Epidemiology 2008;23(6): 403-09.

45. Keeney S, Eker A, Brody T, et al. Correction of the DNA repair defect in xeroderma pigmentosum group E by injection of a DNA damage-binding protein. Proceedings of the National Academy of Sciences 1994;91(9): 4053-56.

46. Zienolddiny S, Campa D, Lind H, et al. Polymorphisms of DNA repair genes and risk of non-small cell lung cancer. Carcinogenesis 2006;27(3): 560-67.

47. Lin W, Xin H, Zhang Y, Wu X, Yuan F, Wang Z. The human REV1 gene codes for a DNA template-dependent dCMP transferase. Nucleic Acids Research 1999;27(22): 4468-75.

48. Falck J, Coates J, Jackson SP. Conserved modes of recruitment of ATM, ATR and DNA-PKcs to sites of DNA damage. Nature 2005;434(7033): 605-11.

49. Burkovics P, Hajdú I, Szukacsov V, Unk I, Haracska L. Role of PCNA-dependent stimulation of 3'-phosphodiesterase and 3' − 5' exonuclease activities of human Ape2 in repair of oxidative DNA damage. Nucleic Acids Research 2009;37(13): 4247-55.

50. Gary R, Ludwig DL, Cornelius HL, MacInnes MA, Park MS. The DNA repair endonuclease XPG binds to proliferating cell nuclear antigen (PCNA) and shares sequence elements with the PCNA-binding regions of FEN-1 and cyclin-dependent kinase inhibitor p21. Journal of Biological Chemistry 1997;272(39): 24522-29.

51. Akasaka S, Yamamoto K. Hydrogen peroxide induces G: C to TA and G: C to C: G transversions in the supF gene of Escherichia coli. Molecular and General Genetics MGG 1994;243(5): 500-05.

52. McBride TJ, Preston BD, Loeb LA. Mutagenic spectrum resulting from DNA damage by oxygen radicals. Biochemistry 1991;30(1): 207-13.

53. Snow ET. Effects of chromium on DNA replication in vitro. Environmental Health Perspectives 1994;102(Suppl 3): 41.